Calhoun: The NPS Institutional Archive

DSpace Repository

Theses and Dissertations 1. Thesis and Dissertation Collection, all items

1985-12

Experimental investigation of turbulent heat transfer in straight and curved rectangular ducts.

Galyo, George Gregory

http://hdl.handle.net/10945/21328

This publication is a work of the U.S. Government as defined in Title 17, United States Code, Section 101. Copyright protection is not available for this work in the United States.

Downloaded from NPS Archive: Calhoun

Calhoun is the Naval Postgraduate School's public access digital repository for research materials and institutional publications created by the NPS community. Calhoun is named for Professor of Mathematics Guy K. Calhoun, NPS's first appointed -- and published -- scholarly author.

Dudley Knox Library / Naval Postgraduate School
411 Dyer Road / 1 University Circle
Monterey, California USA 93943

http://www.nps.edu/library

DUDLEY KNOX LIBRARY
NAVAL POSTGRADUATE SCHOOL
MONTEREY, CALIFORNIA 93943-5002

NAVAL POSTGRADUATE SCHOOL

Monterey, California

THESIS

EXPERIMENTAL INVESTIGATION OF TURBULENT HEAT TRANSFER IN STRAIGHT AND CURVED RECTANGULAR DUCTS

by

George Gregory Galyo

December 1985

Thesis Advisor: M. D. Kelleher

Approved for public release; distribution is unlimited

T226336

URITY CLASSIFICATION OF THIS PAGE

REPORT DOCUMENTATION PAGE

REPORT SECURITY CLASSIFICATION UNCLASSIFIED	1b. RESTRICTIVE MARKINGS
SECURITY CLASSIFICATION AUTHORITY	3 DISTRIBUTION / AVAILABILITY OF REPORT Approved for public release; distribution is unlimited
DECLASSIFICATION / DOWNGRADING SCHEDULE	
ERFORMING ORGANIZATION REPORT NUMBER(S)	5 MONITORING ORGANIZATION REPORT NUMBER(S)

NAME OF PERFORMING ORGANIZATION Naval Postgraduate School	6b OFFICE SYMBOL *(If applicable)* 69	7a. NAME OF MONITORING ORGANIZATION Naval Postgraduate School
ADDRESS *(City, State, and ZIP Code)* Monterey, California 93943-5100		7b. ADDRESS *(City, State, and ZIP Code)* Monterey, California 93943-5100
NAME OF FUNDING / SPONSORING ORGANIZATION	8b. OFFICE SYMBOL *(If applicable)*	9. PROCUREMENT INSTRUMENT IDENTIFICATION NUMBER

ADDRESS *(City, State, and ZIP Code)*

10 SOURCE OF FUNDING NUMBERS

PROGRAM ELEMENT NO	PROJECT NO	TASK NO	WORK UNIT ACCESSION NO

TITLE *(Include Security Classification)*
EXPERIMENTAL INVESTIGATION OF TURBULENT HEAT TRANSFER IN STRAIGHT AND CURVED RECTANGULAR DUCTS

PERSONAL AUTHOR(S)
George Gregory Galyo

TYPE OF REPORT Master's Thesis	13b TIME COVERED FROM ________ TO ________	14 DATE OF REPORT *(Year, Month, Day)* 1985 December	15 PAGE COUNT 110

SUPPLEMENTARY NOTATION

COSATI CODES		
FIELD	GROUP	SUB-GROUP

18 SUBJECT TERMS *(Continue on reverse if necessary and identify by block number)*
Taylor-Gortler Vortices, Dean Number, Heat Transfer, Turbulent Flow, Rectangular Curved Channel, Rectangular Straight Channel, Secondary Flow, Concave, Convex

ABSTRACT *(Continue on reverse if necessary and identify by block number)*

An experimental apparatus has been constructed and tested to examine the convective heat transfer in straight and curved ducts of rectangular cross-section. The channel can be configured with both walls independently heated at a constant heat flux, or one wall at a constant heat flux and the opposite wall adiabatic. Local and average Nusselt numbers can be calculated, and used to evaluate the effect of curvature on heat transfer.

Experiments were conducted at steady state for turbulent flow with one wall heated at a constant flux and the opposite wall adiabatic. The heat transfer characteristics of the straight and curved sections, on both the inner and outer walls, were compared. The heat transfer rate of the concave curved wall proved to be enhanced over both the convex curved wall and both straight sections.

DISTRIBUTION / AVAILABILITY OF ABSTRACT ☒ UNCLASSIFIED/UNLIMITED ☐ SAME AS RPT ☐ DTIC USERS	21. ABSTRACT SECURITY CLASSIFICATION UNCLASSIFIED	
NAME OF RESPONSIBLE INDIVIDUAL Matthew D. Kelleher	22b TELEPHONE *(Include Area Code)* (408) 646-2530	22c. OFFICE SYMBOL 69Kk

D FORM 1473, 84 MAR

83 APR edition may be used until exhausted
All other editions are obsolete

SECURITY CLASSIFICATION OF THIS PAGE

Approved for public release; distribution is unlimited

Experimental Investigation of Turbulent Heat Transfer in Straight and Curved Rectangular Ducts

by

George Gregory Galyo
Lieutenant, United States Navy
B.S., United States Naval Academy, 1980

Submitted in partial fulfillment of the
requirements for the degree of

MASTER OF SCIENCE IN MECHANICAL ENGINEERING

from the

NAVAL POSTGRADUATE SCHOOL
December 1985

ABSTRACT

An experimental apparatus has been constructed and tested to examine the convective heat transfer in straight and curved ducts of rectangular cross-section. The channel can be configured with both walls independently heated at a constant heat flux, or one wall at a constant heat flux and the opposite wall adiabatic. Local and average Nusselt numbers can be calculated, and used to evaluate the effect of curvature on heat transfer.

Experiments were conducted at steady state for turbulent flow with one wall heated at a constant heat flux and the opposite wall adiabatic. The heat transfer characteristics of the straight and curved sections, on both the inner and outer walls, were compared. The heat transfer rate of the concave curved wall proved to be enhanced over both the convex curved wall and both straight sections.

TABLE OF CONTENTS

I. INTRODUCTION 13

    A. TAYLOR-GORTLER VORTICES 13

    B. HISTORY 15

II. INTENT OF STUDY 22

III. EXPERIMENTAL SETUP 25

    A. DESCRIPTION OF THE APPARATUS 25

    B. DETAILS OF THE CONSTRUCTION 29

    C. INSTRUMENTATION 43

IV. EXPERIMENTAL PROCEDURES 51

V. PRESENTATION OF DATA 55

    A. DATA REDUCTION 55

    B. RESULTS 57

VI. DISCUSSION AND CONCLUSIONS 69

VII. RECOMMENDATIONS 79

APPENDIX A: COMPUTER PROGRAM 81

APPENDIX B: SAMPLE CALCULATIONS 91

    1. SAMPLE CALCULATION DATA 92

    2. TEMPERATURE CALCULATIONS 95

    3. POWER CALCULATIONS 96

    4. MASS FLOW RATE CALCULATIONS 97

    5. REYNOLDS NUMBER CALCULATIONS 99

    6. HEAT CONVECTED TO AIR CALCULATION 99

  7. AVERAGE HEAT TRANSFER COEFFICIENT CALCULATION 99

  8. AVERAGE NUSSELT NUMBER CALCULATION 99

  9. DEAN NUMBER CALCULATION 100

APPENDIX C: EXPERIMENTAL UNCERTAINTY 101

LIST OF REFERENCES 106

INITIAL DISTRIBUTION LIST 109

LIST OF TABLES

I. SUMMARY OF STRAIGHT OUTER WALL TEST RESULTS 58
II. SUMMARY OF STRAIGHT INNER WALL TEST RESULTS 59
III. SUMMARY OF CURVED CONCAVE WALL TEST RESULTS 60
IV. SUMMARY OF CURVED CONVEX WALL TEST RESULTS 61

LIST OF FIGURES

1. Schematic of Taylor-Gortler Vortices in a Curved Channel 14
2. Schematic of Taylor Vortices between Cylinders . . . 17
3. Schematic Cross-sectional View of Channel 26
4. Schematic of Rectangular Channel 27
5. Thermocouple Placement in Copper Plates 30
6. Photograph of Milled Thermocouple Slots 32
7. Photograph of Thermocouple Placement Holes 32
8. Photograph of Both Inner Plates Showing Slot Pattern 33
9. Photograph of Both Outer Plates Showing Slot Pattern 33
10. Photograph of Epoxied Thermocouples in Outer Curved Plate 34
11. Photograph of Epoxied Thermocouples in Outer Straight Plate 35
12. Photograph of Convex Surface of Copper Plate 36
13. Photograph of Completed Heated Test Section 36
14. Photograph of Channel Frame 38
15. Photograph of Bottom View of Inner Straight Test Section 38
16. Photograph of Inner Straight Wall at Copper-Plexiglas Joint 39
17. Photograph of Inner Curved Wall at Copper-Plexiglas Joint 39
18. Photograph of Outer Frame and Lexan Wall Showing Straight Test Section 40

19. Photograph of Outer Curved Test Section 41

20. Power Measurement Circuit 45

21. Photograph of Data Acquisition System 47

22. Photograph of Flow Measuring Apparatus 48

23. Photograph of Spencer Turbo Compressor 49

24. Photograph of Test Channel 50

25. Present Straight vs. Curved Section Results 62

26. Present Concave vs. Convex Section Results 63

27. Present Straight Outer vs. Inner Section Results 64

28. Present Concave vs. Straight Outer Section Results 65

29. Present Convex vs. Straight Inner Section Results 66

30. Comparison of Present Data with Daughety and Wilson, Curved Section 71

31. Comparison of Present Data with Daughety and Wilson, Straight Section 72

32. Comparison of Present Data with Daughety and Corrected Wilson, Curved Section 73

33. Comparison of Present Data with Daughety and Corrected Wilson, Straight Section 74

34. Comparison of Present Data with Dittus-Boelter, Kays and Leung, for Turbulent Flow, Straight Section 76

35. Comparison of Present Data with Brinich and Graham, and Kreith, for Turbulent Flows, Curved Section 78

36. Energy Balance in Test Section 91

LIST OF SYMBOLS

Symbol	Meaning	Units
A	cross-sectional area of the orifice	m^2
A_c	cross-sectional area of the channel	m^2
A_{pipe}	cross-sectional area of the pipe	m^2
A_{PL}	area of the heated wall	m^2
C_{pair}	specific heat of air at constant pressure	J/KgK
Dc	channel height	m
De	Dean number	
D_{hd}	hydraulic diameter	m
D_{orf}	diameter of the orifice	m
D_{pipe}	diameter of the pipe	m
F_{wo-wi}	radiation shape factor	
g_c		$\frac{Kg\ m}{N\ sec^2}$
$\overline{h}$	average heat transfer coefficient	W/m^2C
K	flow coefficient	
K_{air}	thermal conductivity of air	W/mC
K_{ins}	thermal conductivity of insulation	W/mC
$\dot{m}$	mass flow rate of air	Kg/sec
Nu	local Nusselt number	
$\overline{Nu}$	average Nusselt number	
Pr	Prandtl number	
P_{atm}	atmospheric pressure	N/m^2

Symbol	Meaning	Units
P_1	pressure upstream of orifice	N/m^2
P_{wet}	wetted perimeter of channel	m
Q_{air}	heat convected to air	W
Q_{li}	heat lost through inner wall	W
Q_{lo}	heat lost through outer wall	W
Q_p	power supplied	W
Q_r	heat transferred by radiation	W
R	gas constant for air	Nm/Kg K
Re_d	Reynolds number based on channel height	
Re_{hd}	Reynolds number based on hydraulic diameter	
Re_{pipe}	Reynolds number based on pipe diameter	
Ri	radius of curvature of inner convex wall	m
R_{PR}	electrical resistance of precision resistor	Ω
R_R	total radiation resistance	m^{-2}
Ta	Taylor number	
T_{blk}	bulk temperature of flow	C
T_{in}	average flow inlet temperature	C
$T_{ins,i1}$	temperature between Plexiglas and first layer of inner insulation	C
$T_{ins,i2}$	temperature between first and second layers of inner insulation	C
$T_{ins,i3}$	temperature between second and third layers of inner insulation	C
$T_{ins,o1}$	temperature between Lexan and first layer of outer insulation	C
$T_{ins,o2}$	temperature between first and second layers of outer insulation	C

Symbol	Meaning	Units
$T_{ins,o3}$	temperature between second and third layers of outer insulation	C
T_{orf}	temperature of air flowing downstream of orifice	C
T_{out}	average flow outlet temperature	C
T_{wi}	average temperature of inner wall	C
T_{wo}	average temperature of outer wall	C
V_{PR}	voltage across precision resistor	V
V_H	voltage across the wall heater	V
W_{id}	width of channel	m
Y	expansion factor	
β	ratio or orifice diameter to pipe diameter	
ε_{cu}	emissivity of copper plate	
γ	ratio of specific heats of air	
μ_{air}	dynamic viscosity of air	Kg/m sec
ρ_{air}	density of air	Kg/m^3
σ	Stefan-Boltzmann constant	W/m^2K^4
ΔP	pressure drop across the orifice	N/m^2
ΔT	mean temperature difference	C
ΔX_{ins}	thickness of insulation layer	m

ACKNOWLEDGEMENT

The author wishes to express his deep appreciation to Professor Matthew D. Kelleher for his insight and guidance throughout all phases of this project. His experience and assistance made the work on this thesis a valuable learning experience. Also, a special thanks to Dr. Amarawansa Wanniarachchi for his assistance in developing and writing the computer program used to gather and reduce the data. In addition, Mr. Charles Crow deserves a special thanks for all his work and effort in the construction of the experimental channel.

Finally, the author wishes to thanks his wife Susan and daughter Michelle for all their sacrifices and encouragement during this course of study.

I. INTRODUCTION

A. TAYLOR-GORTLER VORTICES

Since the early part of the twentieth century, considerable research has shown that the fully developed laminar flow along a concave wall does not remain two-dimensional [Refs. 1, 2, 3]. The flow instead forms a system of spiral vortices, of counter rotating pairs, whose axes are aligned in the principle flow direction. This phenomenon is the result of the variations in the centrifugal forces acting on the fluid particles, and is known as Taylor-Gortler vortices. Figure 1 illustrates the type of fluid motion just described.

In a channel that is curved in the streamwise direction, those fluid particles located in the center of the flow cross-section are subject to higher centrifugal forces than those fluid particles traveling along the channel's outer boundary wall. As a result, the fluid in the center of the channel moves outwardly toward the concave boundary. As the process continues, the fluid particles near the boundary wall, move in a spanwise direction, and finally radially inward replacing the outwardly moving particles. These particles then come under the same centrifugal force and the process repeats itself. The resulting cyclic motion causes the formation of the counter rotating Taylor-Gortler

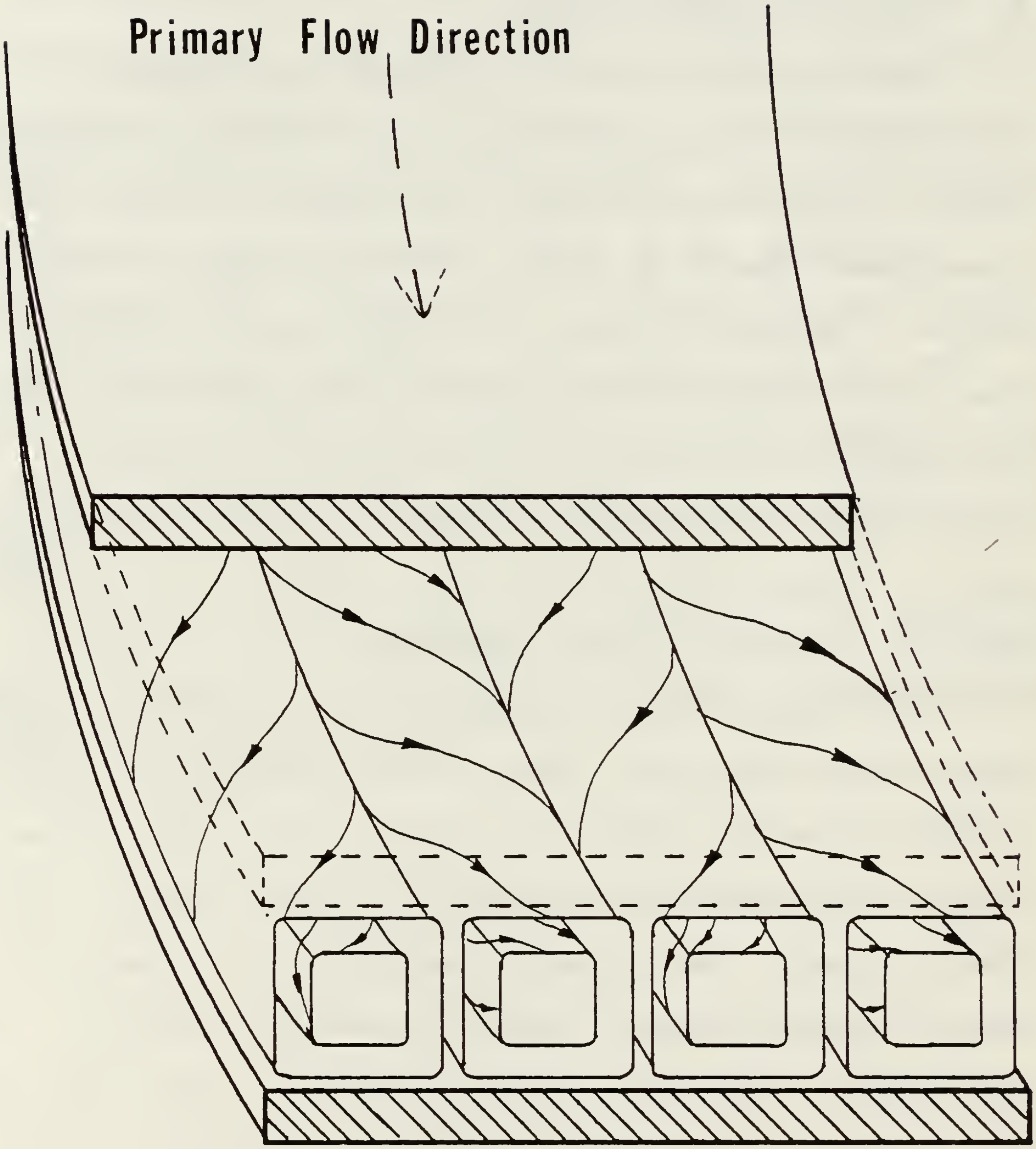

Figure 1. Schematic of Taylor-Gortler Vortices in a Curved Channel.

vortices, considered to be primarily a laminar flow phenomenon.

It has been observed [Ref. 4] that the heat transfer rate from flow along a concave curved wall is greater than that for flow along a straight wall, a phenomenon attributed to the additional mixing provided by the secondary motion of the Taylor-Gortler vortices.

There are many possible applications that could result from a more thorough understanding of Taylor-Gortler vortices and their effect on heat transfer and fluid flow characteristics. Two such applications could lead to improved heat exchanger designs and improved turbine blade cooling [Refs. 5, 6, 7].

B. HISTORY

The stability of an inviscid fluid flowing past a curved boundary, was first considered by Lord Rayleigh in 1916 [Ref. 8]. By assuming that the fluid was non-viscous, he determined that for the motion to remain stable, its circulation must increase with increasing radius. G. I. Taylor, in 1923, [Refs. 1, 9], continued this study with an extensive analytical and experimental study of viscous fluids. His investigations focused on the flow between two cylinders, in which the inner cylinder rotated while the outer cylinder remained stationary. Taylor ascertained that such flows become unstable when the value of a dimensionless parameter exceeded a critical value of 41.3.

The parameter, known as the Taylor number is defined as:

$$Ta = Re\sqrt{d/Ri}$$

where 'd' is the width of the gap, assumed small when compared to 'Ri', the radius of the inner cylinder, and 'Re' is the Reynolds number based on the peripheral velocity of the inner cylinder. Taylor determined that for those cases in which the value of the Taylor number exceeded the critical value, a secondary motion developed and the Taylor vortices formed. Figure 2 illustrates this fluid motion.

Instability of a similar nature is also observed when a viscous fluid flows in a curved channel due to a pressure gradient acting along the channel wall. This problem was first considered analytically by W. R. Dean [Ref. 10] in 1928, for a channel formed by two concentric cylinders, where the radius of the inner cylinder was large in comparison to the spacing between the inner and outer cylinder walls. Dean concluded that there would be an initiation of flow instability, and the formation of vortices, when a dimensionless parameter, the Dean number, exceeded a value of 36. The Dean number is defined as:

$$De = Re\sqrt{\frac{d}{Ri}}$$

where 'd' represents the channel half-width, 'Ri' is the inner cylinder radius, and 'Re' is the Reynolds number based

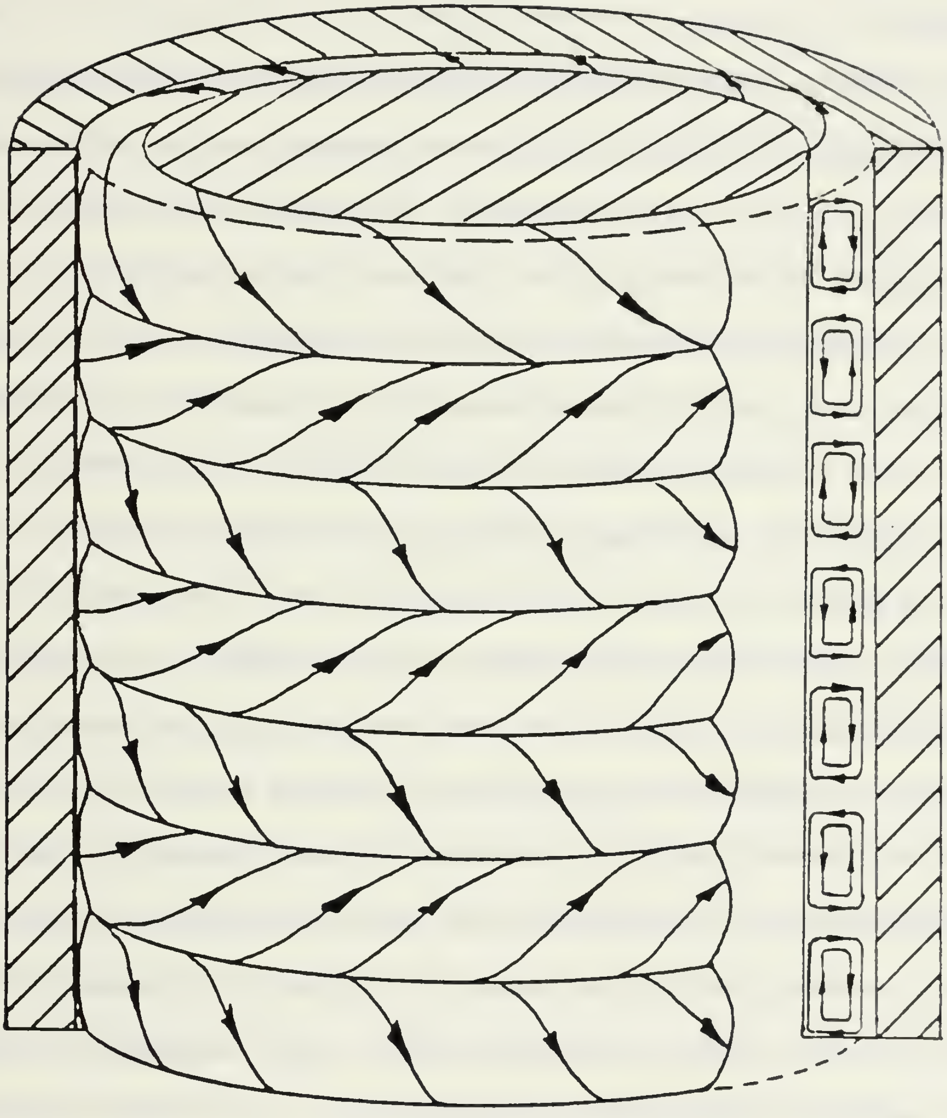

Figure 2. Schematic of Taylor Vortices between Cylinders.

on the mean velocity of the undisturbed flow and the channel half-width 'd'. The analytical work of Dean was later verified by W. H. Reid [Ref. 11], using an approximate solution.

In 1940, H. Gortler [Ref. 2] studied the stability of laminar boundary layer profiles on curved walls under the influence of small disturbances. He found that these disturbances were similar to the vortices studied by G. I. Taylor. Using approximate numerical calculations, Gortler concluded that the disturbances of vortices were produced only on the concave boundary walls and that the overall flow profile appeared to remain laminar in nature. These results were verified, with an exact solution, by G. Hammerlin, and reported by H. Schlichting [Ref. 12] in 1955. A. M. O. Smith completed an even more extensive numerical analysis that further substantiated these findings [Ref. 3]. The results of these numerical solutions have recently been demonstrated with the use of hot wire anemometry, laser doppler systems, and flow visualizations techniques, [Refs. 13, 14]; and in 1976, Y. Aihara [Ref. 15] conducted a non-linear analysis of Gortler Vortices.

As interest began to develop concerning the effects of the secondary flows associated with the Taylor-Gortler vortices, many studies were published concerning the influences of these vortices on heat transfer in the laminar and turbulent flow regimes. In 1955, F. Kreith [Ref. 16], studied the influence of heat transfer with respect to the curvature of the boundary wall for fully turbulent flows. He concluded that the heat transfer from the heated concave boundary wall was considerably higher than that transferred from the convex boundary wall of the same curvature and under similar turbulent conditions.

In 1965, L. Persen [Ref. 17], considered the special cases of very high and very low Prandtl number fluids and related the increase in heat transfer from a curved wall to the presence of the Taylor-Gortler vortices.

There has been only a limited amount of published literature dealing with the flow and heat transfer in curved channels of rectangular cross-section and large aspect ratios, where the aspect ratio is equal to the spanwise distance of the channel divided by the channel height. Much of what has been published involves the development of numerical approximations and solutions for heat and mass transfer in curved ducts of various geometries. K. Cheng and M. Akiyama [Ref. 18] developed a numerical solution for forced convection heat transfer with laminar flows in curved channels of rectangular cross-section, but only for small aspect ratios.

In 1976, A. A. Shibani and M. N. Ozisik [Ref. 19], using matched asymptotic expansion techniques for a wide range of

Prandtl numbers, solved the heat transfer problem between straight parallel plates with turbulent flow, for the case of uniform wall temperature.

Other experimental and analytical studies that are worth citing with regard to this present study are Y. Mori [Ref. 20], who obtained results for hydrodynamically fully developed flows with constant wall heat flux in curved channels of square cross-section. W. M. Kays and E. Y. Leung [Ref. 21] reported solutions for turbulent flow heat transfer in a concentric circular tube annulus with a fully developed velocity profile and constant heat rate per unit length, for a fluid of Prandtl number 0.7. P. F. Brinich and R. W. Graham [Ref. 22] reported results for turbulent flows in a rectangular curved channel with an aspect ratio of 6, for the inner wall heated, the outer wall heated, and both walls heated.

In 1973, at the Naval Postgraduate School, R. J. Mckee [Ref. 23] confirmed the presence of Taylor-Gortler vortices in a curved rectangular channel of aspect ratio 40. M. Durao [Ref. 24] modified R. J. Mckee's channel and modeled it as infinite parallel plates with the outer wall heated and inner wall adiabatic. M. Durao and J. Ballard [Refs. 24, 25] investigated the effects of Taylor-Gortler vortices on the heat transfer in a straight and curved test section for laminar flows. R. Holihan, Jr. [Ref. 26] reported results for laminar and transition flows. S. Daughety [Ref. 27] reported results for turbulent flows and J. Wilson [Ref. 28] reported results for transition and turbulent flows. Each time Mckee's apparatus was used it was modified slightly using prior recommendations to improve on the accuracy of the results.

II. INTENT OF STUDY

The purpose of this investigation was to build an improved curved rectangular duct of large aspect ratio which could be configured with a variety of boundary conditions, and yield more accurate data then previously attained. By combining new ideas and experimental equipment with past experiences and recommendations of R. Mckee and others previously mentioned [Refs. 23, 24, 25, 26, 27, 28], the effect of streamwise curvature on the heat transfer rate in a curved rectangular channel could be studied in greater detail while providing a smaller uncertainty in the results.

Some of the improvements incorporated in the new channel include: the ability to heat one or both walls over a wide range of constant heat fluxes; the ability to heat both walls at different constant heat fluxes; the use of more calibrated thermocouples which will allow greater precision in reading surface and air stream temperatures, combined with a better arrangement which will allow the calculation of the local heat transfer coefficient and Nusselt number; a longer transition region at the outlet which will allow for more mixing and a more accurate outlet temperature measurement. The use of an outer and inner section allowed both wall surfaces to be specially constructed with smooth transitions between wall and heater surfaces in both straight and curved test sections, preventing unexpected tripping from laminar to turbulent flow. Finally, by constructing the channel with materials having low thermal conductivities and avoiding any heat sinks along the channel walls, heat losses could be minimized.

Taylor-Gortler vortices are known to enhance heat transfer in curved channels for transition and turbulent flows. This enhancement in the transfer of heat has been attributed to the secondary flow velocity components of the Taylor-Gortler vortices. These secondary components transport the heated fluid from the outer concave wall, inward toward the opposite wall of the channel, displacing the cooler fluid particles and causing them to move toward the heated concave wall. It was expected that similar results would be observed in this study.

This investigation was conducted using a single channel with a rectangular cross-section and constant aspect ratio, again defining aspect ratio as the spanwise distance divided by the channel height. The channel incorporates a straight and a curved test section. Each test section consists of opposing walls which can be independently heated. The results obtained in each test section at approximately the same flow rates were compared in an effort to determine the effects of the Taylor-Gortler vortices on the heat transfer rate. Also, the results of both the straight and curved outer sections were compared to the results of Daughety [Ref. 27], and Wilson [Ref. 28] to compare the new channel to the old one.

The straight section results of this study were compared to the Dittus-Boelter correlation using hydraulic diameter [Ref. 29], and the results of Kays and Leung for turbulent and transition flow in annular passages [Ref. 21].

The curved section results of this study were compared with the results of Brinich and Graham [Ref. 22] for turbulent flow in a rectangular curved channel, and with Kreith [Ref. 16] for turbulent flows in concave and convex curved channels.

III. EXPERIMENTAL SETUP

A. DESCRIPTION OF THE APPARATUS

To meet the objectives of this investigation, a channel of rectangular cross-section and constant aspect ratio was constructed. The rectangular channel has four electrically heated wall sections, composed of a rubber heater bonded to a thin copper plate. All four heated wall sections are 30.48 centimeters long and 25.4 centimeters wide, with a heated area of 774.2 square centimeters. The rectangular channel is 0.635 centimeters high and 25.4 centimeters wide resulting in an aspect ratio of 40. The cross-sectional area of the channel is 16.13 square centimeters. The wetted perimeter is 52.07 centimeters, and the hydraulic diameter is 1.239 centimeters. Figure 3 shows a cross-sectional view presenting both the straight and curved sections of the channel.

The channel, shown in Figure 4, has a straight entrance region of 76.20 centimeters, which insures hydrodynamically fully developed flow prior to entering the straight heated test sections. The entrance region is followed by two parallel 30.48 centimeter straight heated test sections, which oppose each other, one in each wall. Following the straight heated test sections is a 15.32 centimeter straight

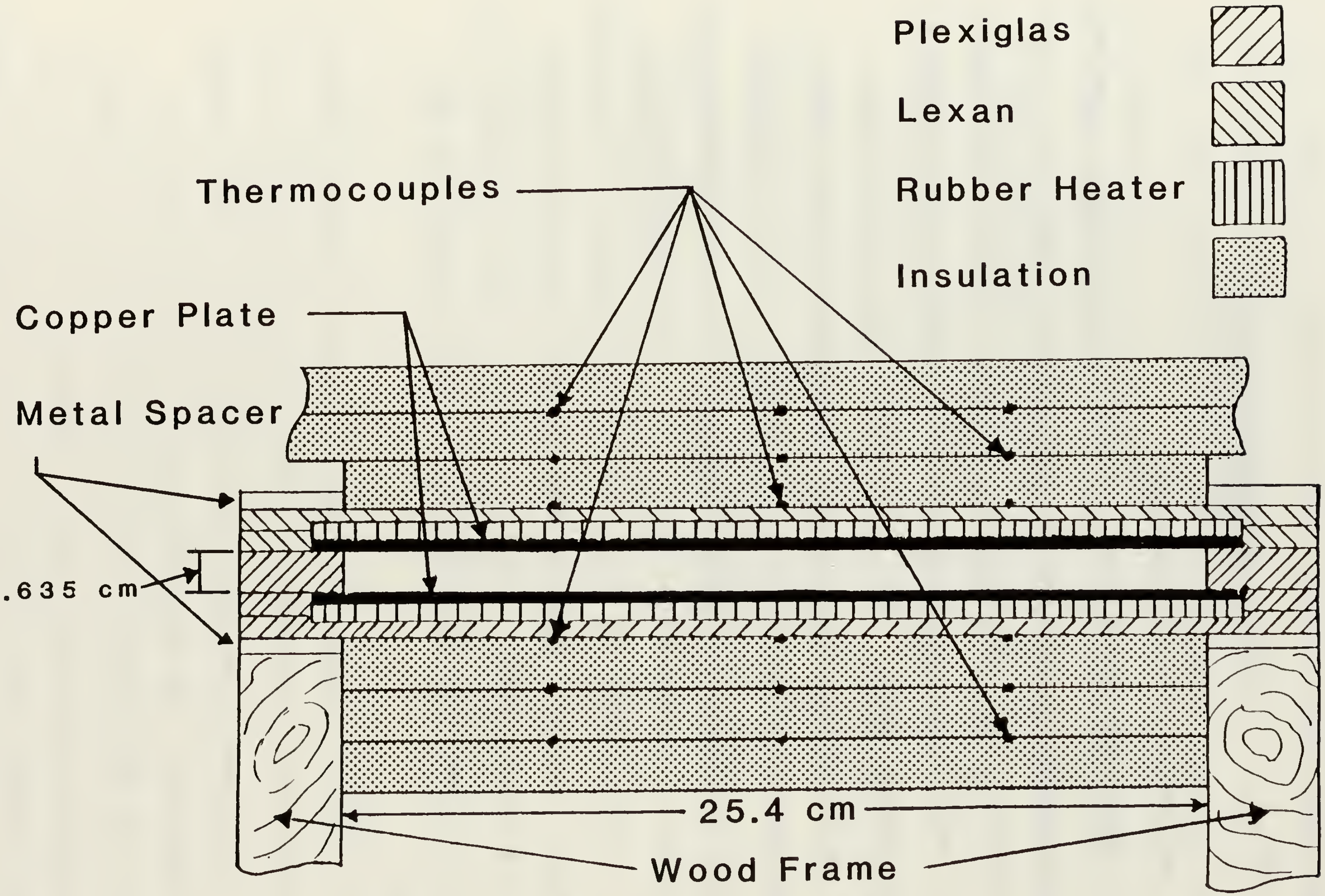

Figure 3. Schematic Cross-sectional View of Channel.

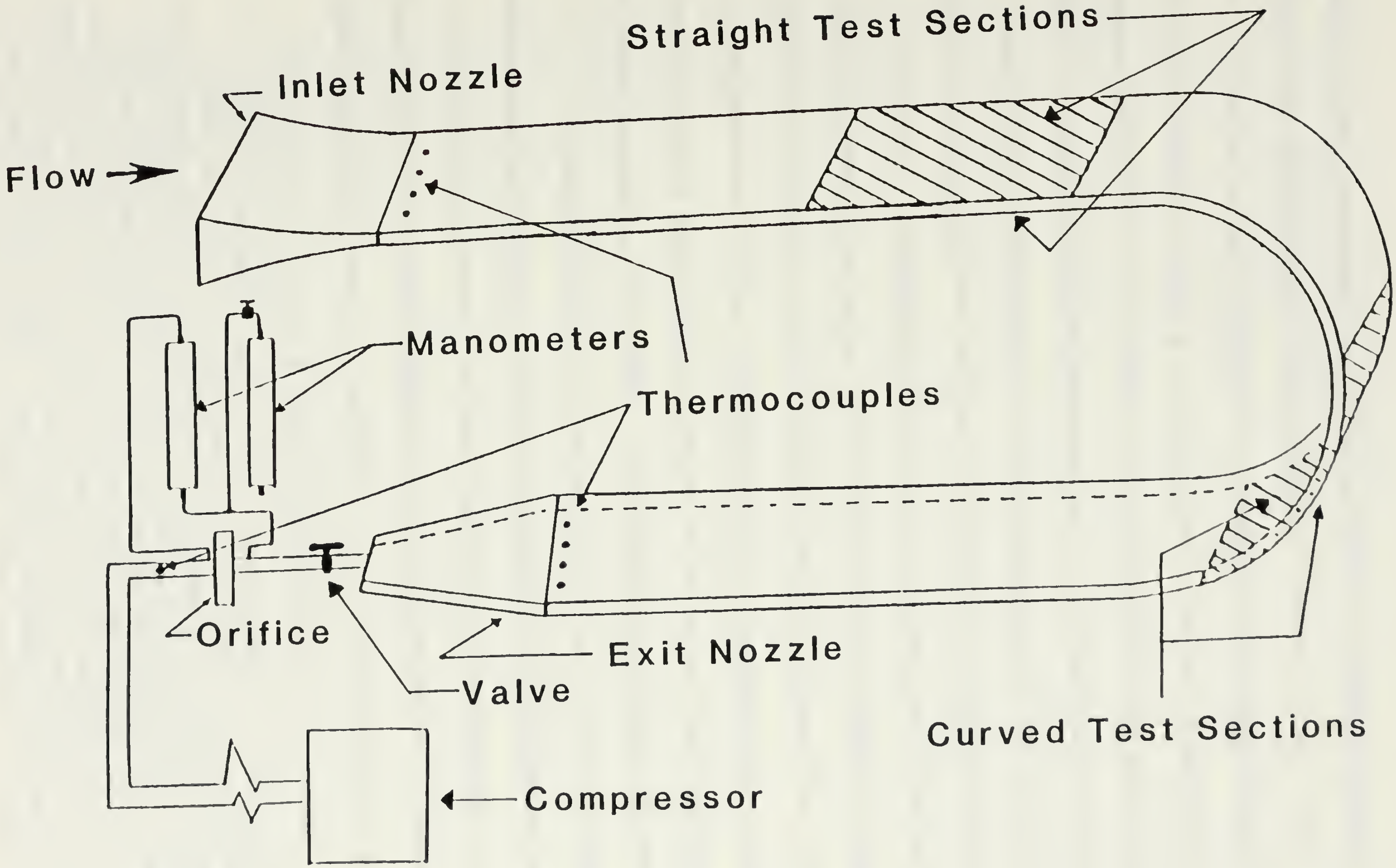

Figure 4. Schematic of Rectangular Channel.

exit region, that completes the straight test section. The straight test section is immediately followed by the curved test section which subtends a 180 degree arc, with the inner wall having a radius of curvature of 29.7 centimeters. The curved test section has a 52.63 centimeter unheated convex curved section prior to the curved heated sections. The two concentric curved heated sections, inner one convex and outer one concave, are 30.48 centimeters long and the outer heated wall subtends an arc of 58.8 degrees. The curved heated sections are followed by a 10.16 centimeter convex curved exit region which completes the curved test section. Finally, the channel is completed by a 92.0 centimeter straight exit region which allows sufficient mixing prior to reading the outlet temperature. The entire channel was then thermally insulated with a plastic foam material.

An entrance bell constructed of Plexiglas is connected to the inlet of the straight entrance section of the channel. It was designed and manufactured according to ASME nozzle standards, with an elliptical curved base on a major axis equal to 25.4 centimeters and a minor axis of 2.54 centimeters. A fiberglass filter was attached to the entrance nozzle to prevent foreign matter from entering the channel. An aluminum exhaust nozzle was attached to the exit of the channel and directed the flow from the channel into a two inch diameter pvc pipe. The piping contained a mass flow rate measuring section which could be fitted with standard ASME concentric orifices.

A total of one hundred and eighty-nine copper-constantan, 30 gauge thermocouples are located throughout the test apparatus. Only ninety-nine thermocouples are read at anyone time, through seventy-five data channels, to record the desired temperatures. Each heated wall section contains thirty thermocouples which are read individually and then averaged to give the wall section surface temperature. Four thermocouples span the width of the channel at the entrance and exit to give the average entrance and exit air temperatures. Three groups of five thermocouples are connected in parallel and inserted between each layer of insulation at each of the heated test sections. Each group of five thermocouples only uses one data channel, and these extra thermocouples comprise the difference between the number of thermocouples read and the data channels available. Finally, there is one thermcouple to measure the air temperature at the orifice.

B. DETAILS OF THE CONSTRUCTION

Each of the four heated wall sections was composed of a copper plate laminated to a wire wound silicone rubber heater. The rubber heater was made by Watlow Industries. There are thirty copper-constantan thermocouples placed between the copper plate and rubber heater. Figure 5 shows

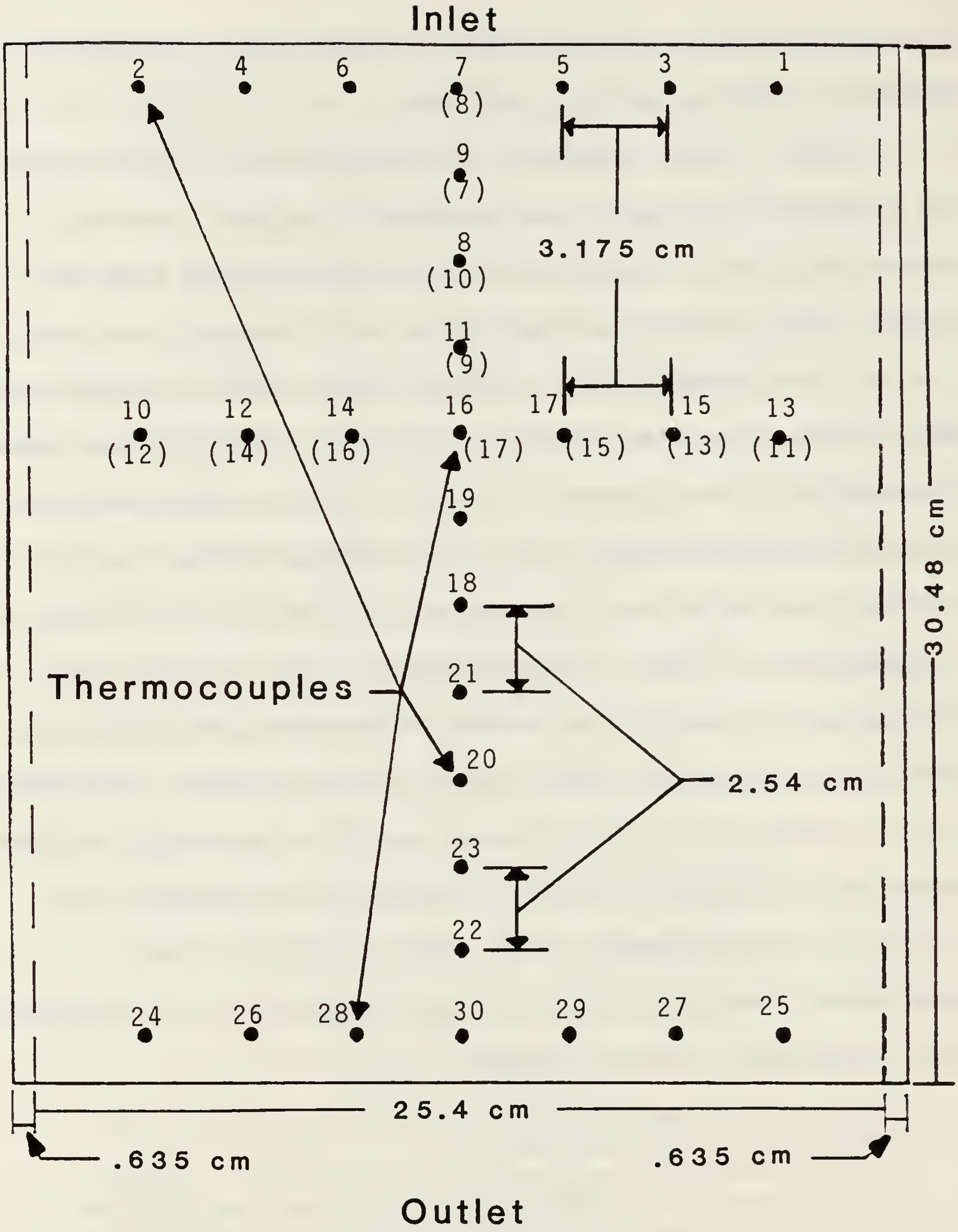

Legend: numbers above location marks are outer and inner thermocouple numbers, numbers in parentheses below location mark apply to inner plates only.

Figure 5. Thermocouple Placement in Copper Plates.

the placement of the thermocouples on the back of the copper plate. The copper plate is 30.48 centimeters long, 26.72 centimeters wide, and 0.155 centimeters thick, but only the middle 25.4 centimeters of copper plate width is heated and centered in the channel. The back of the copper plate has a pattern of slots milled 0.076 centimeters deep. The pattern of slots for the two inner plates is different from the pattern of slots for the two outer plates. See Figures 6, 7, 8, and 9. The calibrated thermocouples were numbered and expoxied into the slots, as shown in Figures 10 and 11. The rubber heater has the same length and width dimensions as the copper plate, but only heats the middle 25.4 centimeters of width. This results in a heated wall area of 774.2 square centimeters. The excess copper plate is sandwiched between the wall and the side spacer thereby helping to support the copper plate in the channel. Dow Corning 3140 RTV was used to adhere the rubber heater to the back of the copper plate, and complete the heated section. Figure 12 and 13 represent a completed test wall.

The channel was built on a carefully constructed wood frame with steel rails, that also was used to support the entire channel. The inner wall was composed of two 0.343 centimeter thick and 29.85 centimeter wide pieces of Plexiglas laminated together, that had spaces milled out for the heated copper sections. The inner wall was constructed

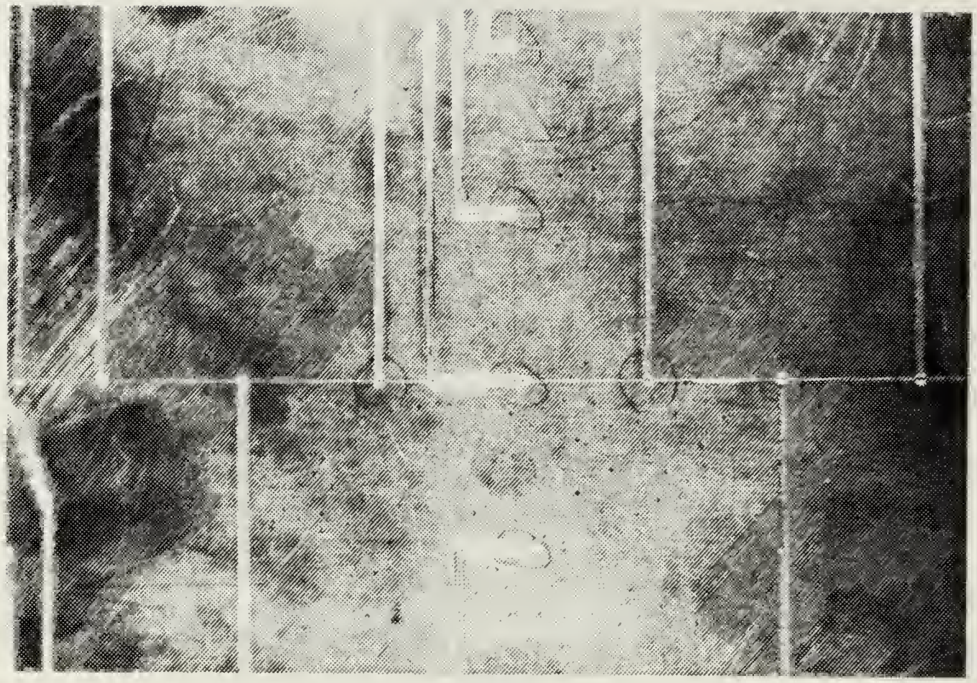

Figure 6. Photograph of Milled Thermocouple Slots.

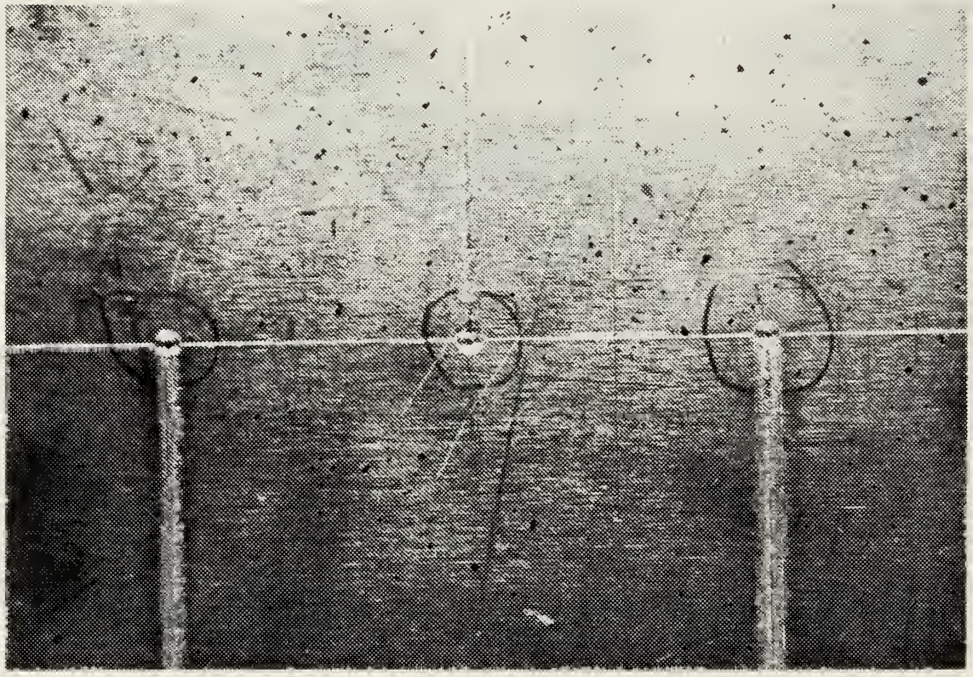

Figure 7. Photograph of Thermocouple Placement Holes.

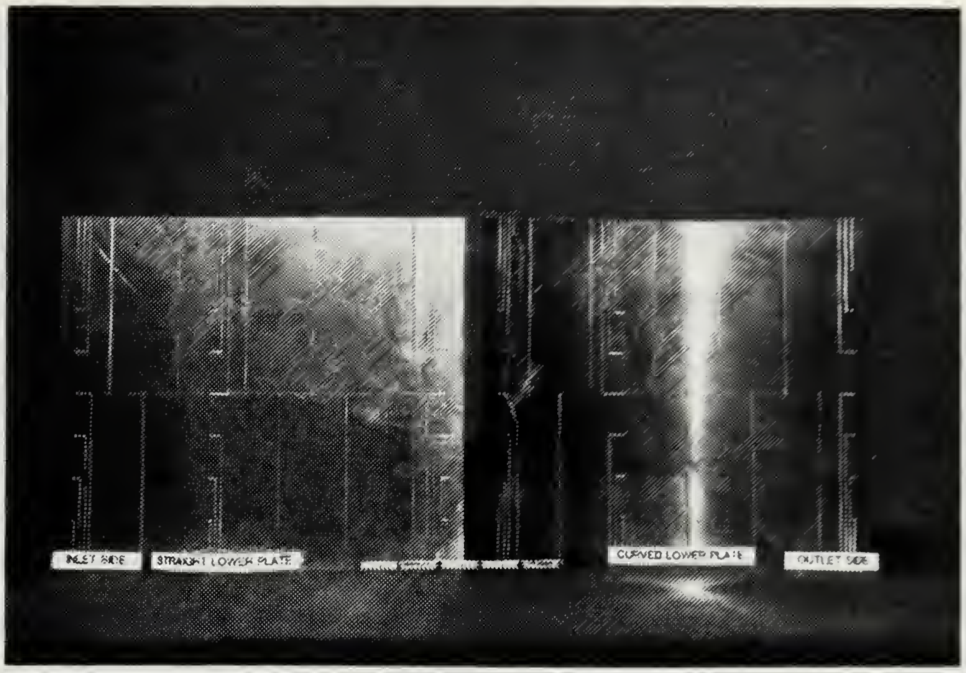

Figure 8. Photograph of Both Inner Plates Showing Thermocouple Slot Pattern.

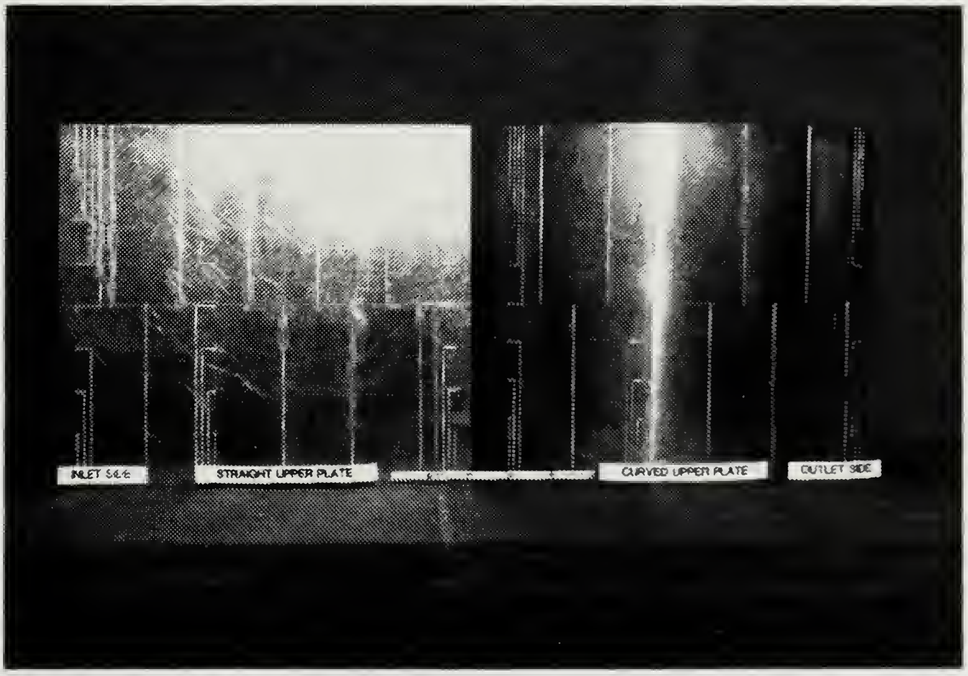

Figure 9. Photograph of Both Outer Plates Showing Thermocouple Slot Pattern.

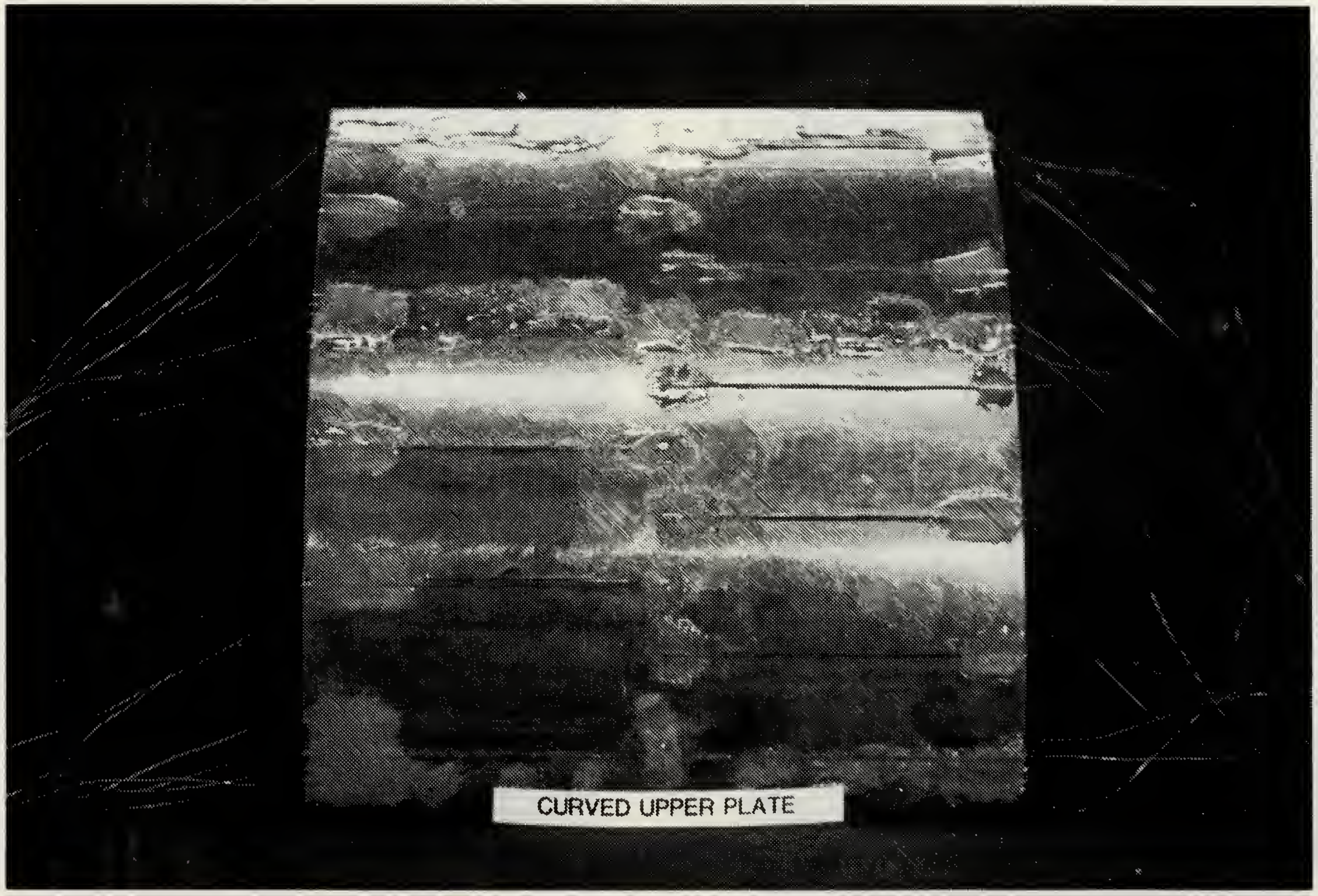

Figure 10. Photograph of Epoxied Thermocouples in Outer Curved Plate.

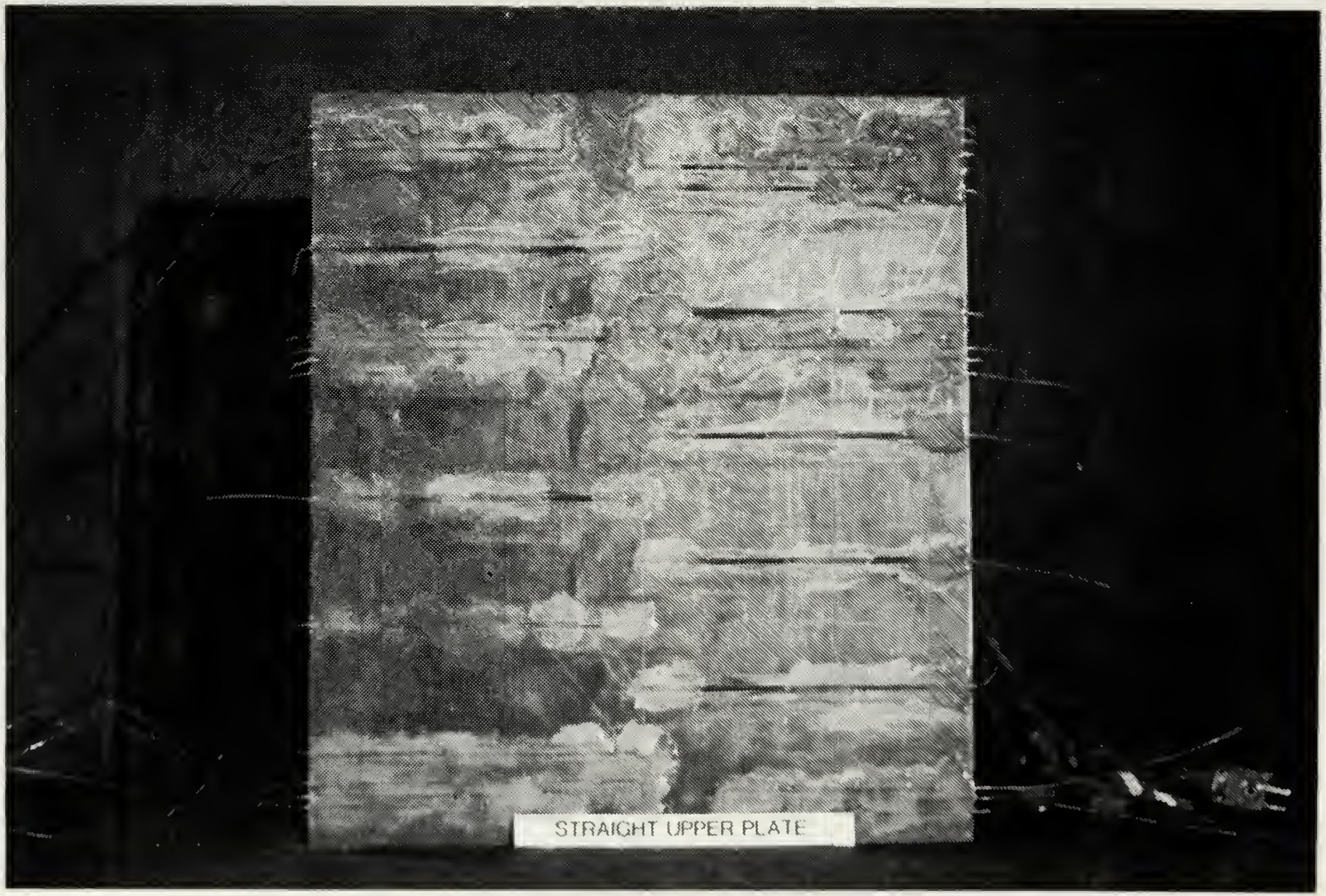

Figure 11. Photograph of Epoxied Thermocouples in Outer Straight Plate.

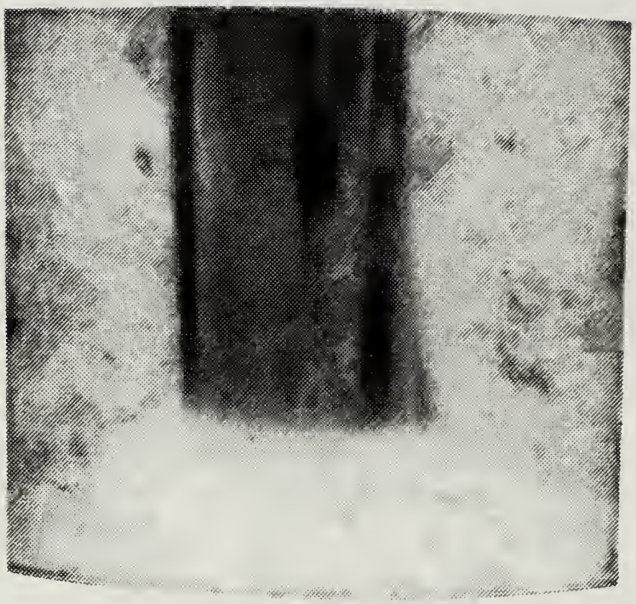

Figure 12. Photograph of Convex Surface of Copper Plate.

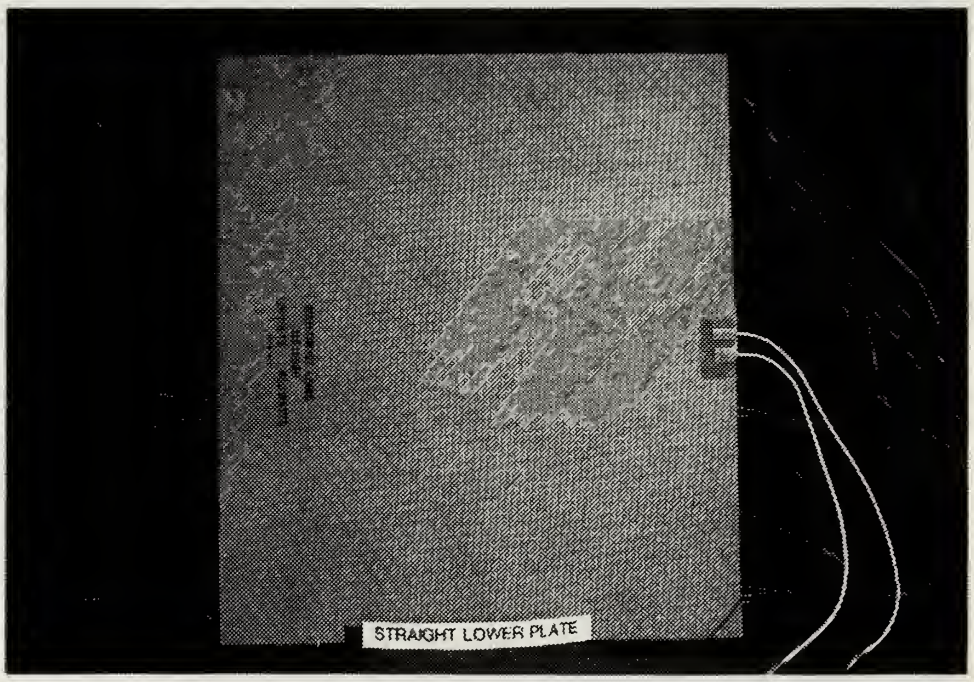

Figure 13. Photograph of Completed Heated Test Section.

by heating and forming the Plexiglas around the wood frame. The Plexiglas wall was secured to the frame by screws tapped into the steel rails. The heated copper sections were then fitted into the machined spaces and two 0.635 centimeter thick and 2.223 centimeter wide Plexiglas spacers, that served as the sides of the channel and support for the copper plates, were attached by screws to the inner wall and steel rails. The two spacers were 25.4 centimeters apart and formed the width of the channel. Additionally, five flat head screws spanning the width of the channel at the joints where the copper and Plexiglas met were used to secure the copper plates and maintain an even joint. The seams were then worked to a smooth transition by applying "Bondo" to the joints and sanding. See Figures 14, 15, 16, and 17.

The outer wall was constructed in a similar manner, but using 0.318 centimeter thick and 29.85 centimeter wide pieces of Lexan. Lexan was used on the outer wall because of its flexibility and ease of bending without heat, which would be required when attaching the outer wall to the inner wall and frame. Also, the outer wall was formed in an outer wood frame so that the transition joints of the outer wall could be worked smooth like the inner wall. See Figures 18 and 19. Both walls were constructed so that no seams or butt joints existed on the inside of the channel, except

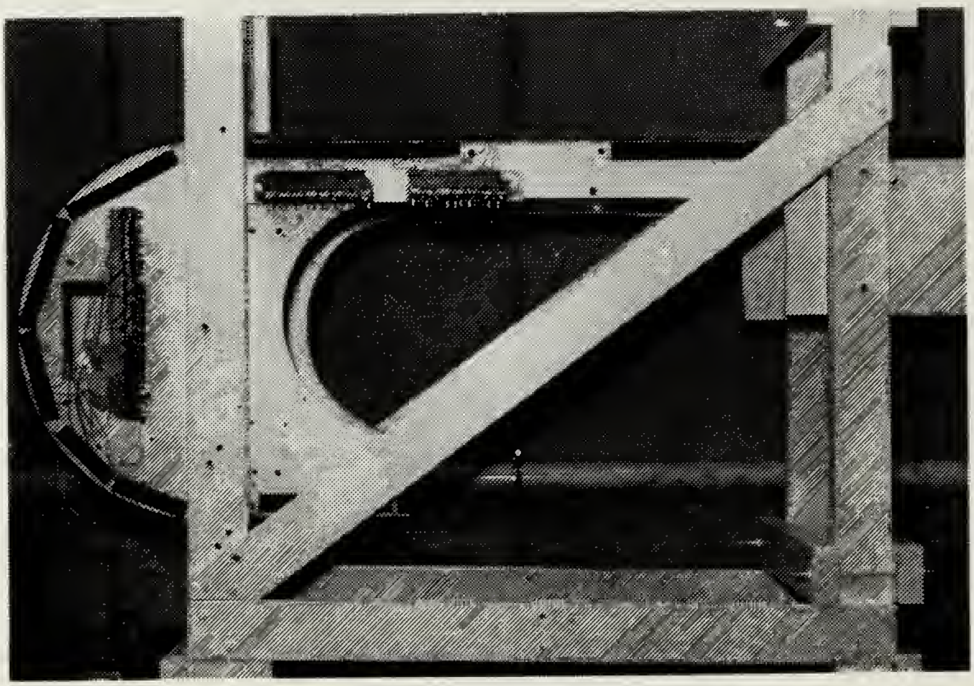

Figure 14. Photograph of Channel Frame.

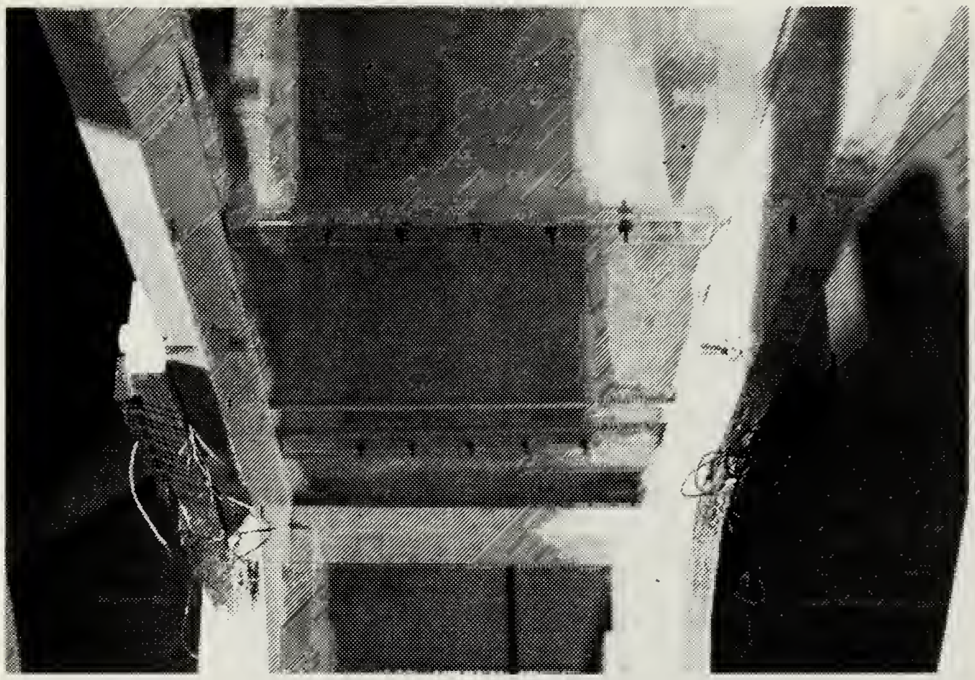

Figure 15. Photograph of Bottom View of Inner Straight Test Section.

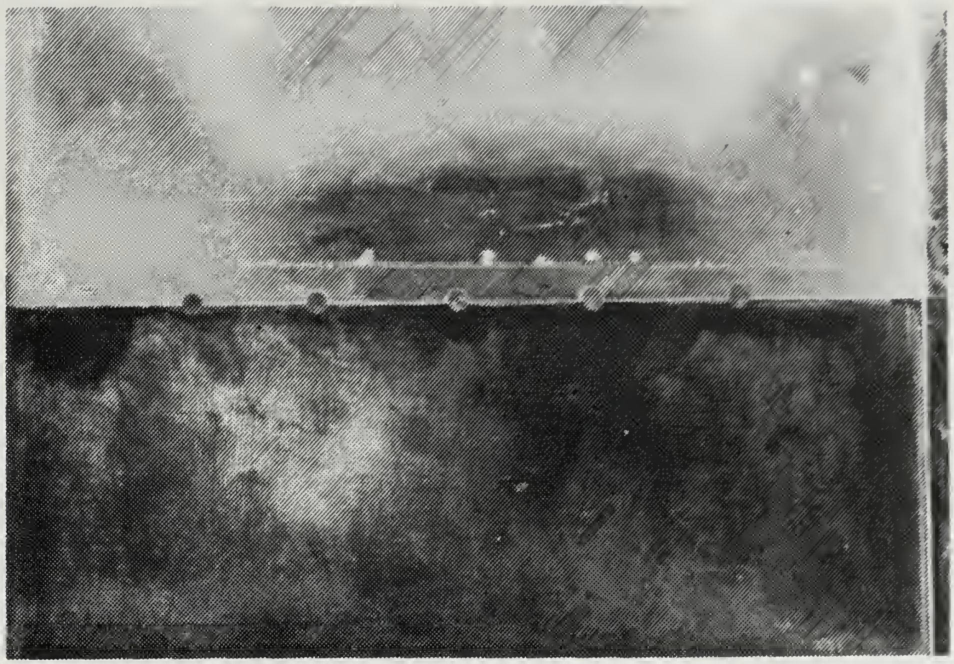

Figure 16. Photograph of Inner Straight Wall at Copper-Plexiglas Joint.

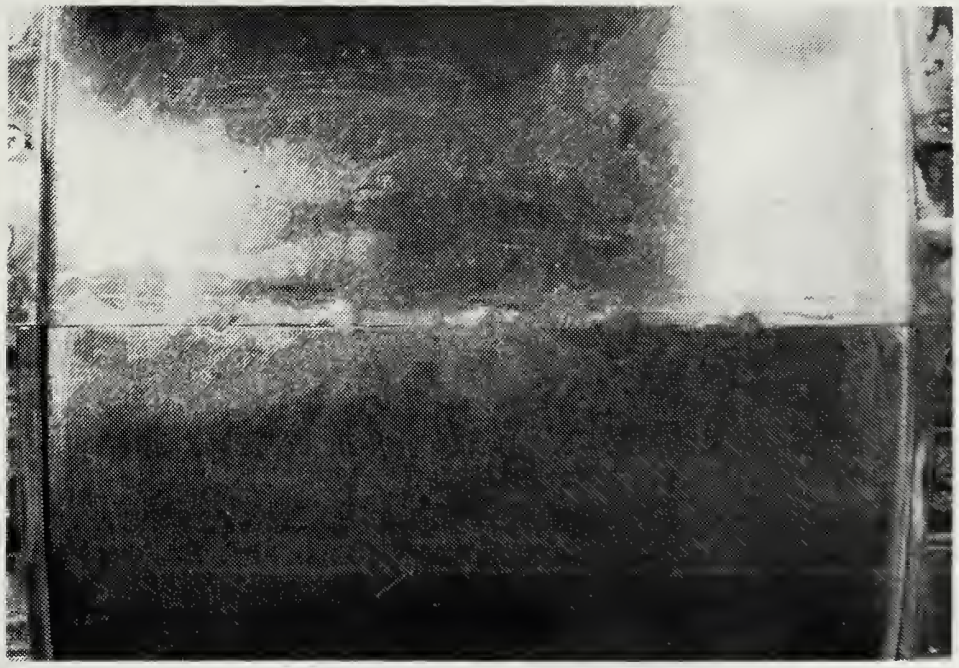

Figure 17. Photograph of Inner Curved Wall at Copper-Plexiglas Joint.

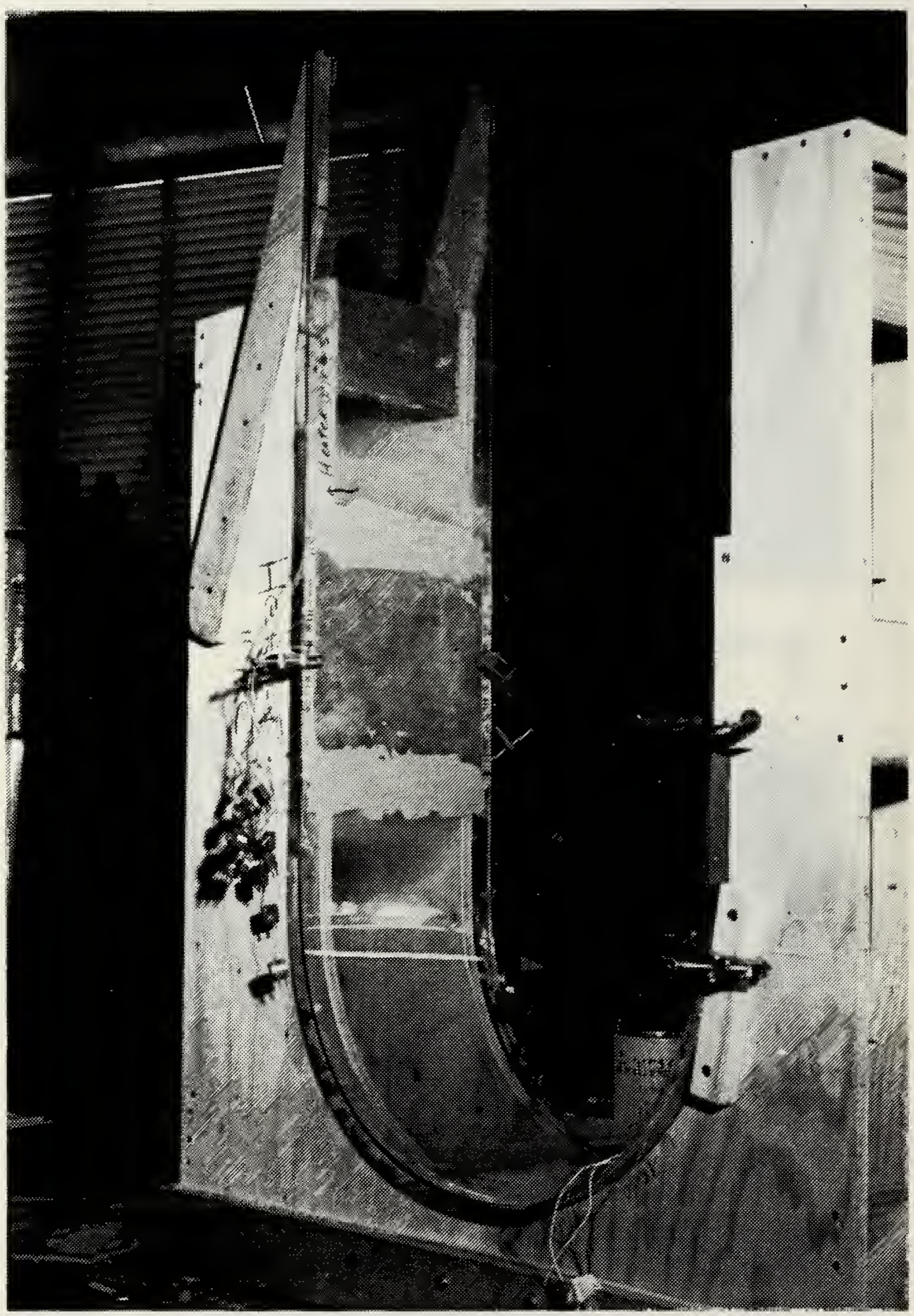

Figure 18. Photograph of Outer Frame and Lexan Wall Showing Straight Test Section.

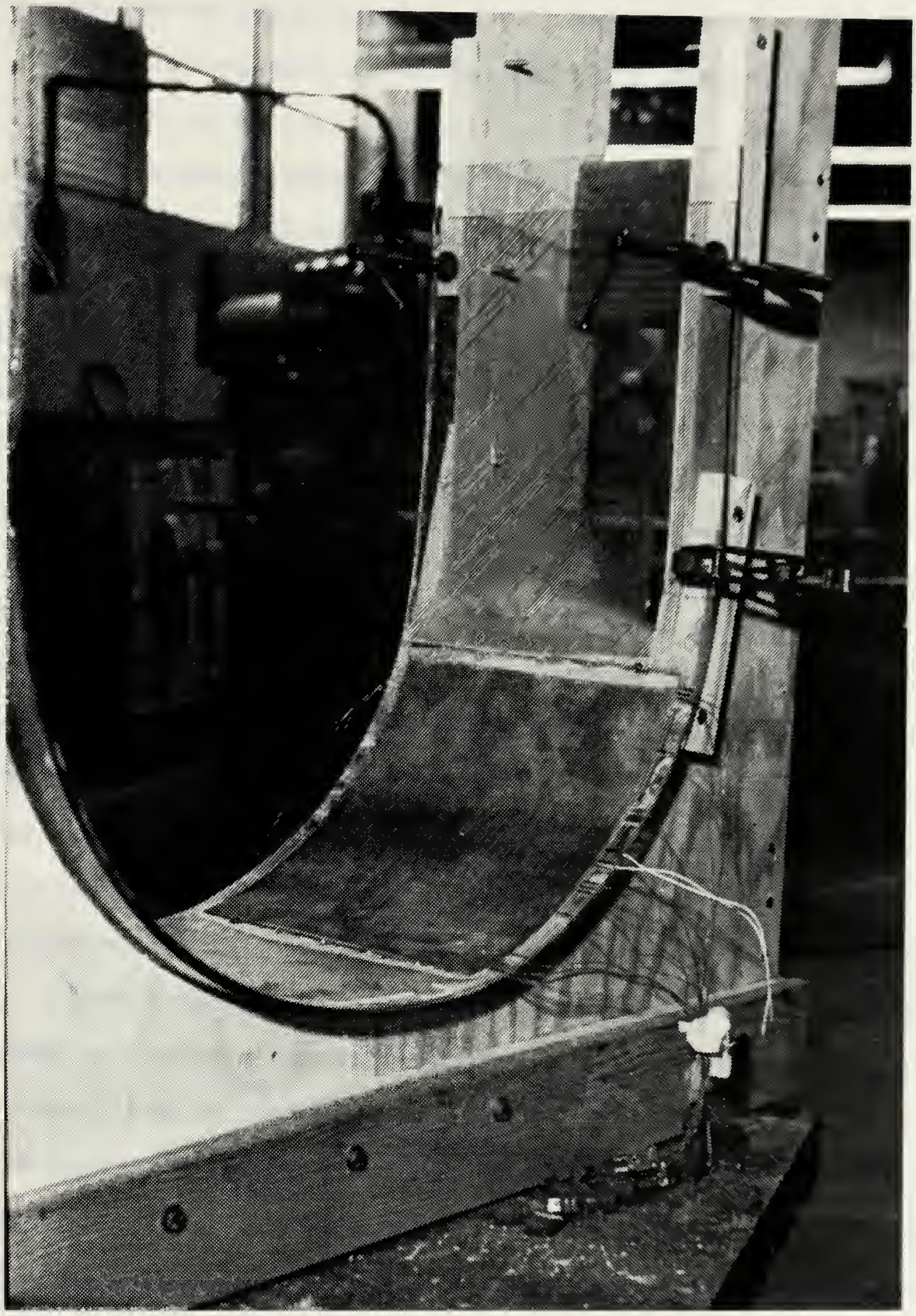

Figure 19. Photograph of Outer Curved Test Section.

where the heated copper section joined the Plexiglas and Lexan walls, and all eight of those joints had a smooth transition.

Once both walls were completed, the outer wall and support frame was positioned onto the inner wall and main frame. The outer wall was aligned onto the inner wall and the outer wall support frame removed. The outer wall was then bolted to the inner wall and frame with steel bars running the length of the channel used as a spacer to insure even compression. Once this was completed the inlet and outlet nozzles were attached to the channel.

The sides of the channel and all connections between the channel, the pvc piping, and the orifice were sealed with Macklanburg-Duncan Silicone Rubber Sealant Caulk to ensure there was no leakage of air into the channel or the piping which could effect the recorded temperatures or mass flow rate. The entire channel was thermally insulated with three layers of 1/2 inch Armstrong Armaflex 22 Sheet Insulation, a flexible foamed plastic material. By positioning thermocouples between these insulation layers, the heat lost through the insulation could be computed at each test section. The heat loss through insulation surrounding the rest of the channel due to the heated air flowing through the channel was a small fraction of the total power supplied to the heater. The insulation was held in place by the use of silver duct tape and velcro strips attached to the frame.

C. INSTRUMENTATION

The data acquisition system used for this experiment was a Hewlett Packard 3054A Automatic Data Acquisition/Control System consisting of a 3456A Digital Voltmeter, a 3497A Data Acquisition/Control Unit, and four input panels capable of reading any mix of eight voltages or copper-constantan thermocouples. Also used in conjunction with this data acquisition system, were a Hewlett Packard 9826 Computer and 2671A Printer. The program used to reduce the data is listed in Appendix A.

The copper-constantan thermocouples were calibrated against a platinum resistance thermometer using a ROSEMONT Commutating Bridge model 920A, and a ROSEMONT Constant Temperature Bath model 913A. All thermocouples were calibrated between 20 and 85 degrees Celsius, and a second order polynomial was curve fitted to correct each thermocouple.

The mass flow rate in the channel was measured with a thin plate orifice measuring device which was placed in the 2 inch pvc piping between the channel and the compressor. In this study an orifice with a diameter of 2.7318 centimeters was used to measure hydraulic Reynold's numbers above 5000. The orifice device was installed in accordance with ASME Power Test Code [Ref. 30], with 3/8 inch pressure taps placed on either side of the orifice at 1 and 1/2 diameters, and one thermocouple inserted in the two inch pvc piping down stream of the orifice to record the temperature of the air flowing through the orifice. Pressure measurements were taken with Meriam vertical manometers, one whose fluid was water with a 0 to 60 inch range, another using water with a 0 to 30 inch range, and a third whose fluid was mercury, calibrated to read inches of water with a range of 0 to 415 inches. Atmospheric pressure was measured with a Princo precision barometer. The pressure readings were used to calculate the mass flow rate of the working fluid as outlined in [Refs. 30, 31].

Power was supplied to the heated test section by using two Lambda Model LK345A FM 60 volt power supplies in series. The power supplies are rated at 6.0 amps. maximum at 40 degrees Celsius. Since the electrical resistance of the rubber heater is not constant, but varies slowly with temperature, a precision resistor was calibrated and connected in series with the heater to allow the calculation of the instantaneous power being supplied. Both the outer and inner heated test sections have their own circuitry and precision resistor. The value of the precision resistor for the outer test sections is 2.0173 ohms, and the value for the inner test sections is 2.0084 ohms. See Figure 20 for diagram of circuit used to measure instantaneous power.

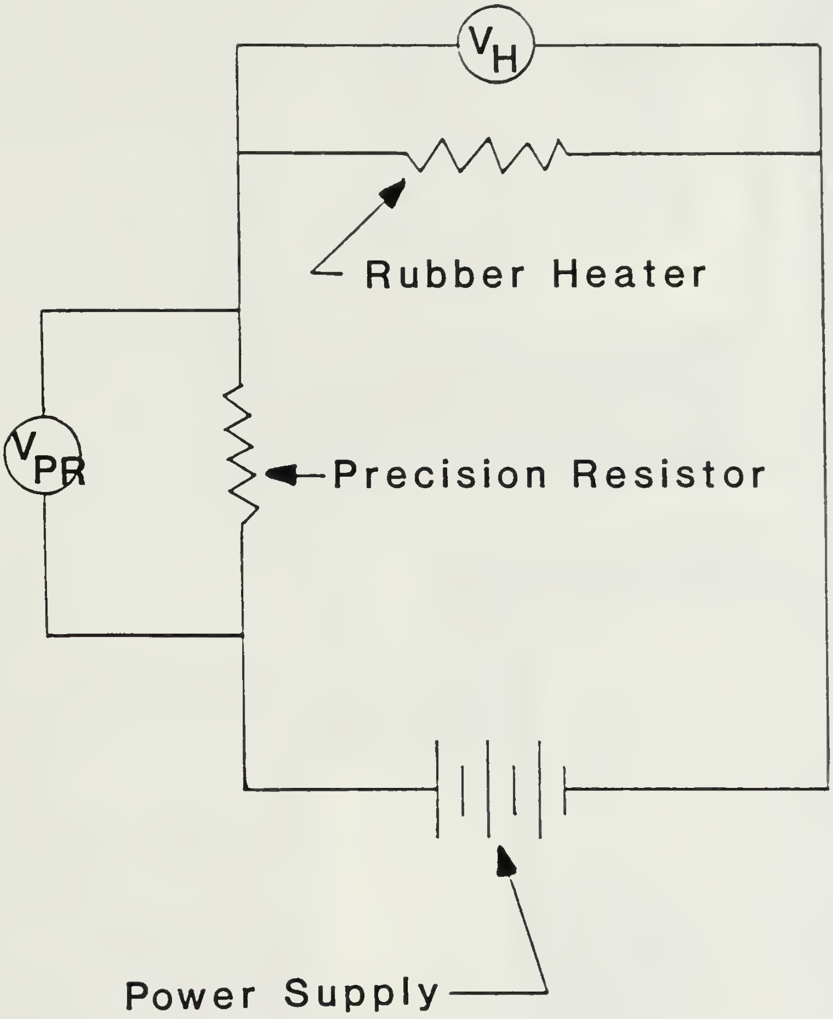

Figure 20. Power Measurement Circuit.

The working fluid was air at room temperature, which was drawn through the channel by an electrically driven Spencer Turbo Compressor, rated at 30 horsepower at 3500 rpm, and 550 cubic feet per minute at 70 degrees fahrenheit and one atmosphere. Photographs of the channel and associated test equipment are shown in Figures 21, 22, 23, and 24.

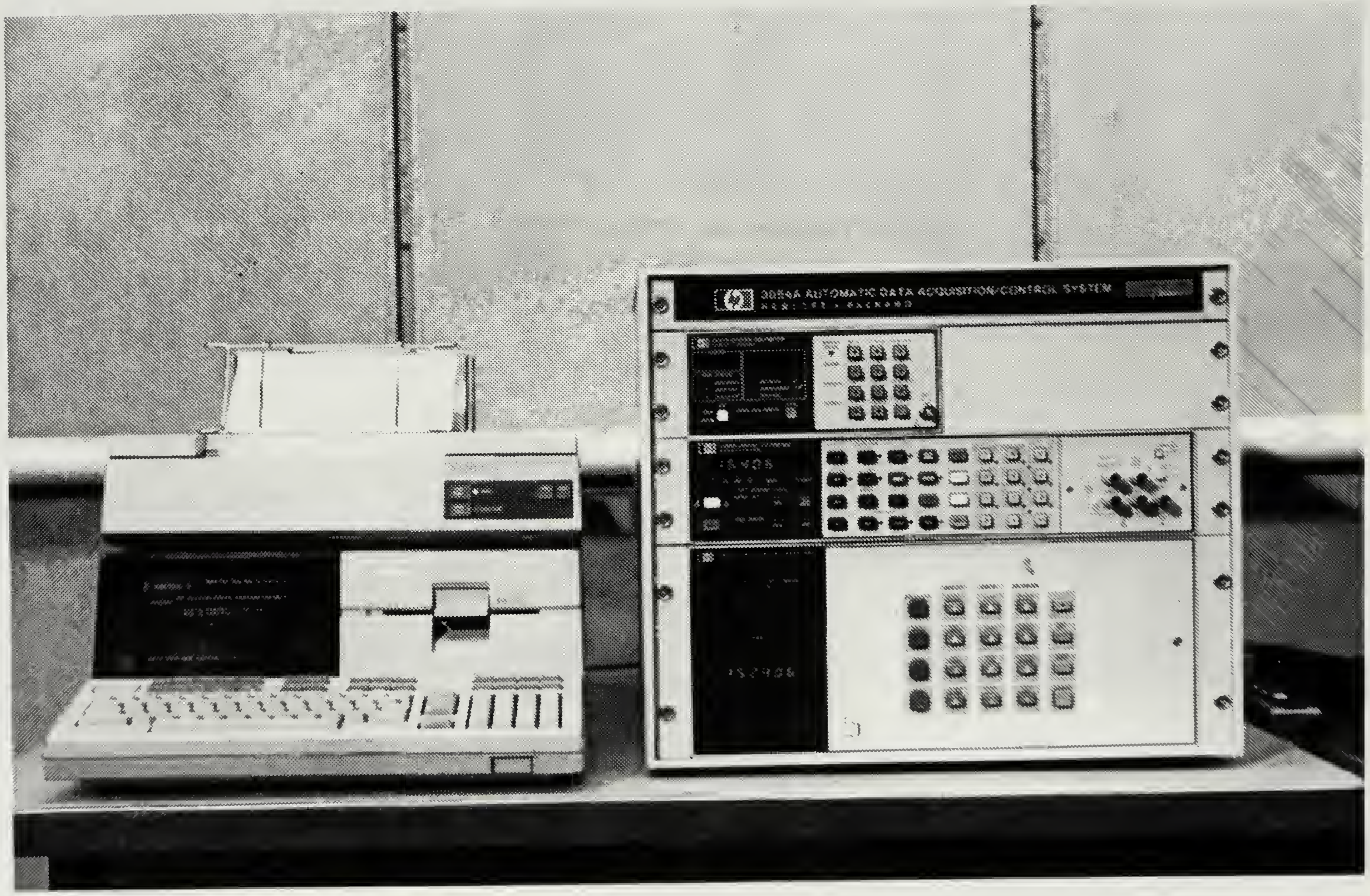

Figure 21. Photograph of Data Acquisition System.

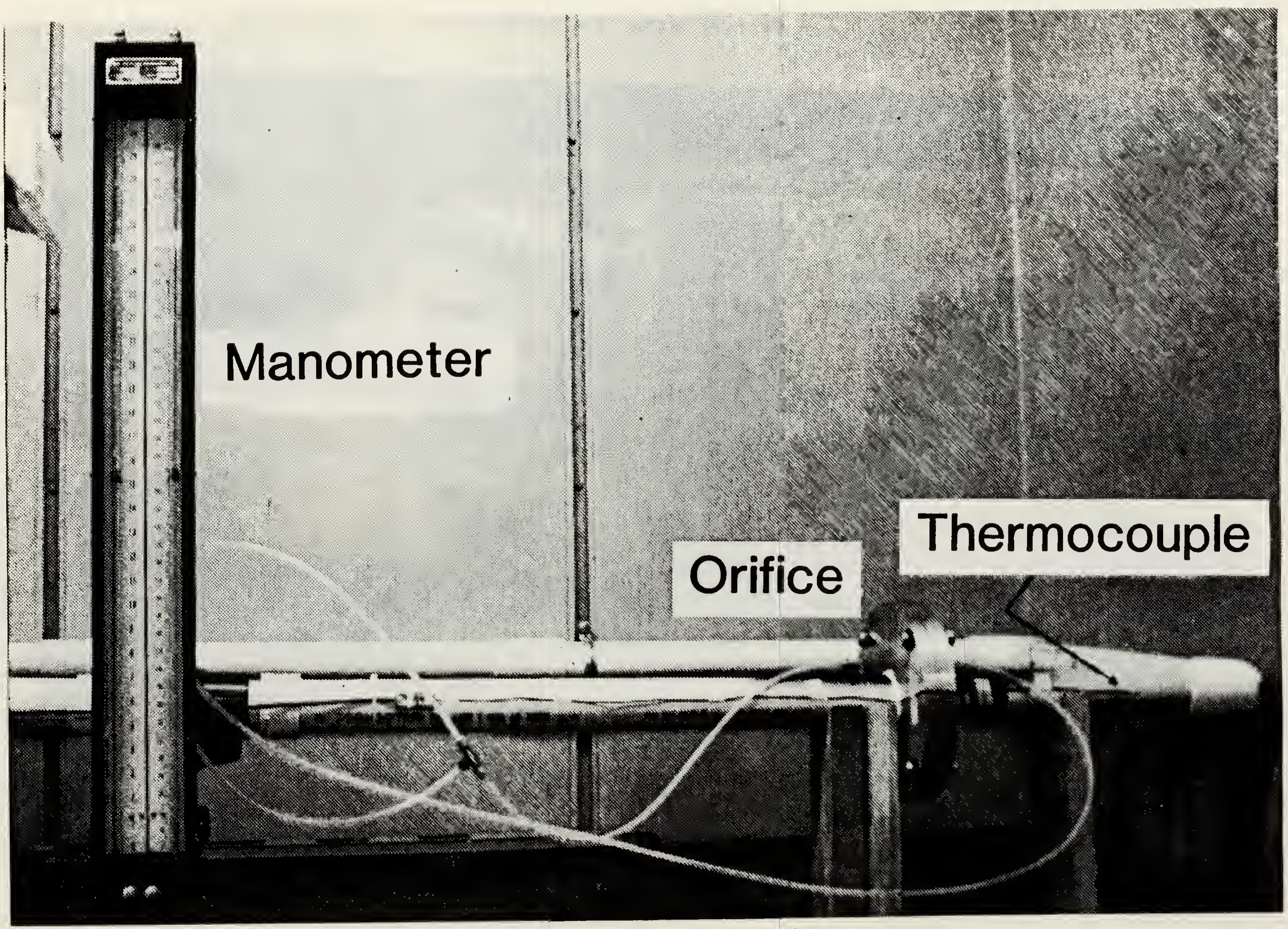

Figure 22. Photograph of Flow Measuring Apparatus.

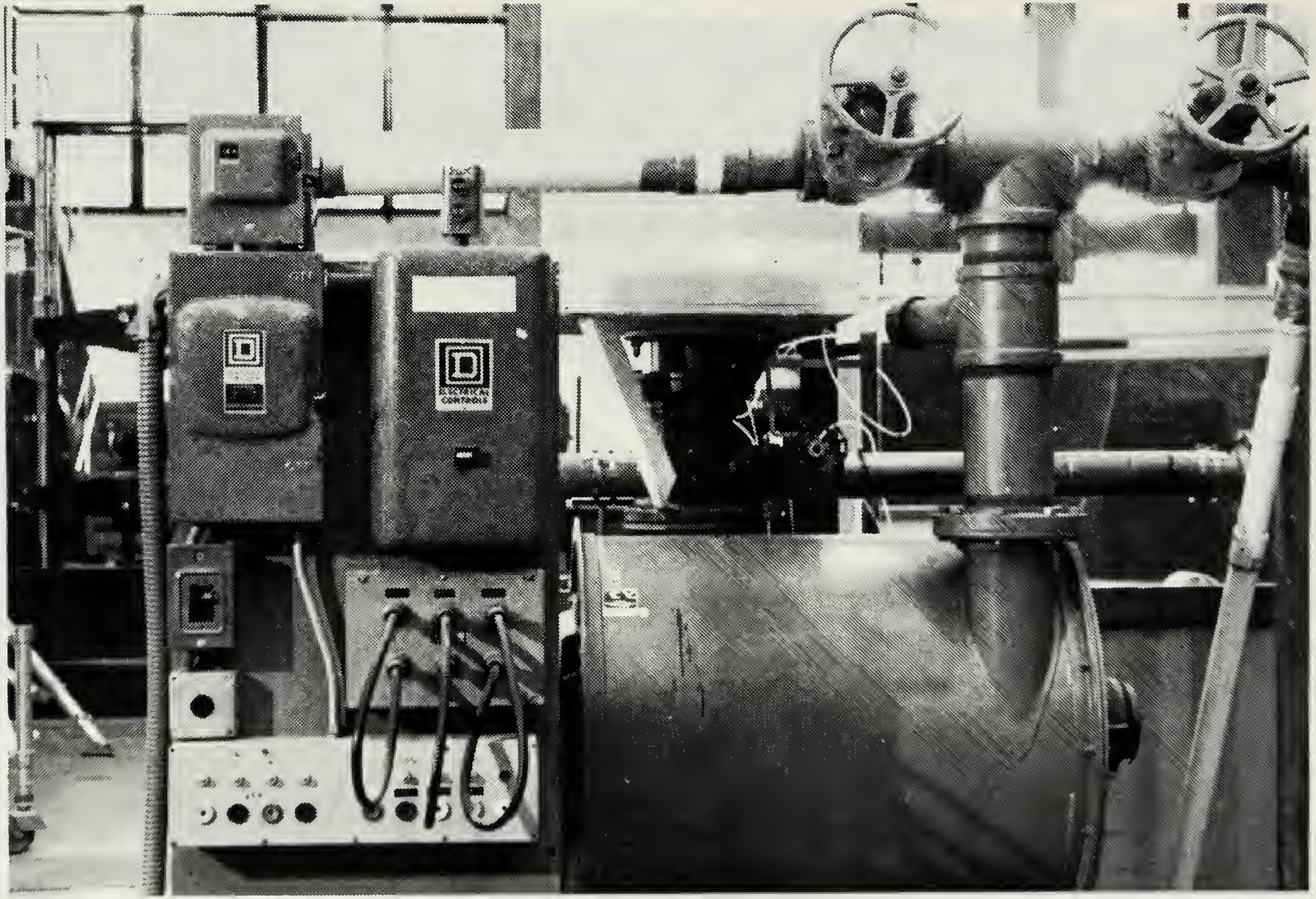

Figure 23. Photograph of Spencer Turbo Compressor.

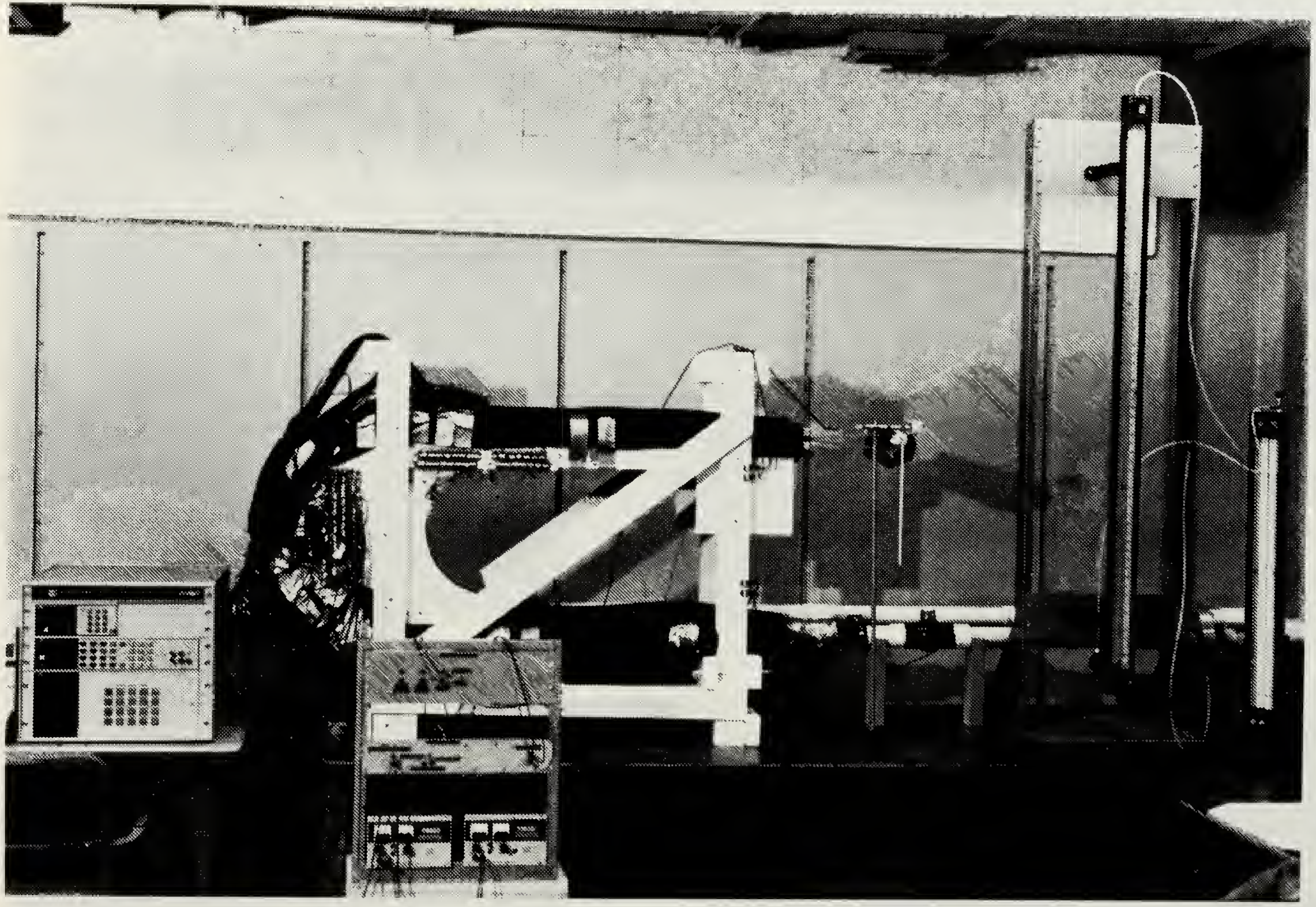

Figure 24. Photograph of Test Channel.

IV. EXPERIMENTAL PROCEDURES

The experimental procedures followed were the same for the straight and curved test sections. The procedure for starting up the experimental apparatus is as follows:

(1) turn on the computer and data acquisition system

(2) close globe valve at channel exit

(3) close valve to manometer reading P1

(4) set compressor blast gate to 1/8 open

(5) start turbo compressor

(6) open intake valve on compressor 1/4 to 1 turn

(7) open globe valve at channel

(8) open manometer valve slowly to ensure P1 does not exceed manometer scale

(9) turn on and adjust power supply to the heater

(10) use intake valve on compressor to control mass flow rate through the channel

It was necessary to determine the approximate voltage setting required to bring the heated wall to approximately 50 degrees Celsius. This heated wall temperature would ensure a large temperature difference between the inlet and outlet temperatures, and the heated and unheated wall temperatures, while not damaging the apparatus. The larger the temperature difference the smaller the uncertainty in the results. The required power setting was found by monitoring the heated plate temperature locally from the data acquisition system while the voltage to the heater was adjusted.

To compute the instantaneous power supplied to the heater the following relationship was used:

$$Q_P = \frac{V_H \, V_{PR}}{R_{PR}}$$

The precision resistor voltage and the heater voltage were read by the data acquisition system and the resistance of the precision resistor was a known constant. A diagram of the circuit used was shown in Figure 16.

The mass flow rate was monitored by the two manometers at the orifice. For each run, the atmospheric pressure, the pressure difference across the orifice, and the pressure upstream of the orifice were entered manually into the computer for the mass flow rate calculation. All other data was acquired by the data acquisition system directly from the experimental apparatus.

Once the apparatus was started properly, sufficient time was required to reach steady state prior to gathering data. Preliminary runs were performed to determine the time required for the test apparatus to reach steady state. For this experiment at least two hours were allowed for a cold test apparatus to reach steady state, and at least one hour if the apparatus was already running. After waiting the required time, data was taken at ten minute intervals to ensure that a steady state condition had been achieved. The criteria for steady state was based on three variables:

(1) the difference between inlet and outlet temperature
(2) the heated test section wall temperature
(3) the unaccounted heat loss in the system

When the first two of these quantities varied by less than two percent over a ten minute interval and the third was less than ten percent of the input power, it was considered that a steady state condition had been achieved.

Experiments were conducted at specific mass flow rates of air corresponding to Reynolds numbers between 7000 and 22000. The Reynolds number was based on the hydraulic diameter of the channel. For each mass flow rate, temperature and voltage data were taken automatically by the data acquisition system and immediately reduced and printed. The variables that were measured and used in this investigation were:

(1) the temperature of the air entering the channel (T_{in})
(2) the temperature of the air leaving the channel (T_{out})
(3) the temperature of the heated wall in the test section (T_{wo} or T_{wi})
(4) the temperature of the unheated wall in the test section (T_{wi} or T_{wo})
(5) the temperature between each layer of insulation at the test section (T_{ins})

(6) the temperature of the air at the orifice (T_{orf})

(7) the voltage across the precision resistor (V_{PR})

(8) the voltage across the rubber heater (V_H)

(9) the pressure upstream of the orifice (P1)

(10) the difference in the upstream and downstream pressure across the orifice (ΔP)

(11) the atmospheric pressure (P_{ATM})

The results obtained from the straight test sections served as a baseline for the comparison of the curved section results. An effort was made to match the mass flow rates for each test section as closely as possible.

V. PRESENTATION OF DATA

A. DATA REDUCTION

The constant heat flux surface for the heated wall of each test section was provided by the uniform electrical resistivity of the rubber heater. The insulated unheated wall was considered adiabatic since the heat losses through that wall were negligible. The straight portion of the channel upstream of the straight heated test section was of sufficient length to ensure that the air flow was hydrodynamically fully developed for the flow velocities of this experiment. The straight portion of the channel downstream of the curved section proved to be of sufficient length to ensure that the air flow exiting the channel was thoroughly mixed and that the measured outlet air temperature (T_{out}) was an average bulk temperature, as long as the hydraulic Reynolds number of the channel was less than 17000.

The analysis of the data required several quantities to be defined. The heat convected to the air was calculated using the equation:

$$Q_{air} = \dot{m}C_{pair}\ (T_{out} - T_{in})$$

where 'C_{pair}' is the specific heat of the air at constant pressure and '$\dot{m}$' is the mass flow rate of the air.

The average heat transfer coefficient between the heated wall and the flow of air in the channel was defined by the equation:

$$\bar{h} = \frac{Q_{air}}{A_{PL}\ \Delta T}$$

where 'Q_{air}' is defined above, 'A_{PL}' is the area of the heated copper plate in the test section, and 'ΔT' is the difference between the arithmetic average heated wall temperature (T_w) and the average bulk air temperature (T_{blk}). The average bulk air temperature is defined as the arithmetic mean of the entrance and exit air temperatures (T_{in}, T_{out}).

The average Nusselt number was then calculated using:

$$\overline{Nu}_{hd} = \frac{\bar{h}\ D_{hd}}{K_{air}}$$

In this equation 'D_{hd}' is the hydraulic diameter and 'K_{air}' is the thermal conductivity of the air.

The hydraulic Reynolds number was calculated for each test run as follows:

$$Re_{hd} = \frac{\dot{m}\ D_{hd}}{A_c\ \mu_{air}}$$

where again '$\dot{m}$' and 'D_{hd}' are the mass flow rate and hydraulic diameter of the channel, 'A_c' is the cross-sectional area of the channel, and 'μ_{air}' is the dynamic viscosity of the air.

For the curved sections the Dean number was defined as:

$$D_e = \frac{\dot{m}\, D_c/2}{A_c\, \mu_{air}} \sqrt{\frac{D_c/2}{Ri}} = \frac{Re_d}{2} \sqrt{\frac{D_c/2}{Ri}}$$

where 'Re_d' is the Reynolds number based on the channel height, 'D_c' is the channel height, and 'Ri' is the radius of curvature of the inner convex wall.

A sketch of the control volume and a set of sample calculations for one test run of the curved section are given in Appendix B. A sample calculation for the uncertainty analysis is given in Appendix C.

B. RESULTS

The data obtained from each experimental run was reduced by the computer program listed in Appendix A, utilizing the expressions described in Part A above. The major parameters resulting from this process are shown in Tables I through IV. Tables I and II contain the straight sections results and Tables III and IV contain the results of the curved sections. A plot of the average Nusselt number versus hydraulic Reynolds number is given in Figures 25, 26, 27, 28, and 29 for the comparison of the results. "Error" bands have been indicated as a result of the uncertainty analysis.

TABLE I

SUMMARY OF STRAIGHT OUTER WALL TEST RESULTS

Re_{hd}	Q_{air} (W)	$\overline{h}$ (W/mC)	ΔT (C)	$\overline{Nu}_{hd}$
7709	108.50	41.99	28.52	20.07
11953	135.26	61.57	25.49	29.51
15646	157.92	74.43	24.45	35.65
21455	217.53	87.42	27.36	41.95

Reynolds number and Nusselt number are based on hydraulic diameter. Results for Reynolds number of 21455 based on orifice air temperature instead of outlet air temperature.

TABLE II

SUMMARY OF STRAIGHT INNER WALL TEST RESULTS

Re_{hd}	Q_{air} (W)	$\overline{h}$ (W/mC)	ΔT (C)	$\overline{Nu}_{hd}$
7628	105.57	41.52	28.90	19.85
12169	138.36	59.50	27.42	28.50
15788	159.84	70.24	26.37	33.61
21312	204.42	81.82	27.84	39.17

Reynolds number and Nusselt number are based on hydraulic diameter. Results for Reynolds number of 21312 based on orifice air temperature instead of outlet air temperature.

TABLE III

SUMMARY OF CURVED CONCAVE WALL TEST RESULTS

Re_{hd}	De	Q_{air} (W)	$\bar{h}$ (W/mC)	T (C)	$\overline{Nu}_{hd}$
7782	206	115.88	52.43	25.51	25.00
11726	311	157.45	68.16	29.91	32.53
15813	419	158.17	83.13	22.34	39.78
21246	563	231.31	93.02	27.20	44.52

Reynolds number and Nusselt number are based on hydraulic diameter. Results for Reynolds number of 21246 based on orifice air temperature instead of outlet air temperature.

TABLE IV

SUMMARY OF CURVED CONVEX WALL TEST RESULTS

Re_{hd}	De	Q_{air} (W)	$\overline{h}$ (W/mC)	ΔT (C)	$\overline{Nu}_{hd}$
7757	206	82.37	38.33	24.47	18.37
12021	318	115.50	57.62	23.92	27.65
15908	421	142.54	68.57	24.34	32.94
21603	572	164.08	79.28	23.43	38.11

Reynolds number and Nusselt number are based on hydraulic diameter. Results for Reynolds number of 21603 based on orifice air temperature instead of outlet air temperature.

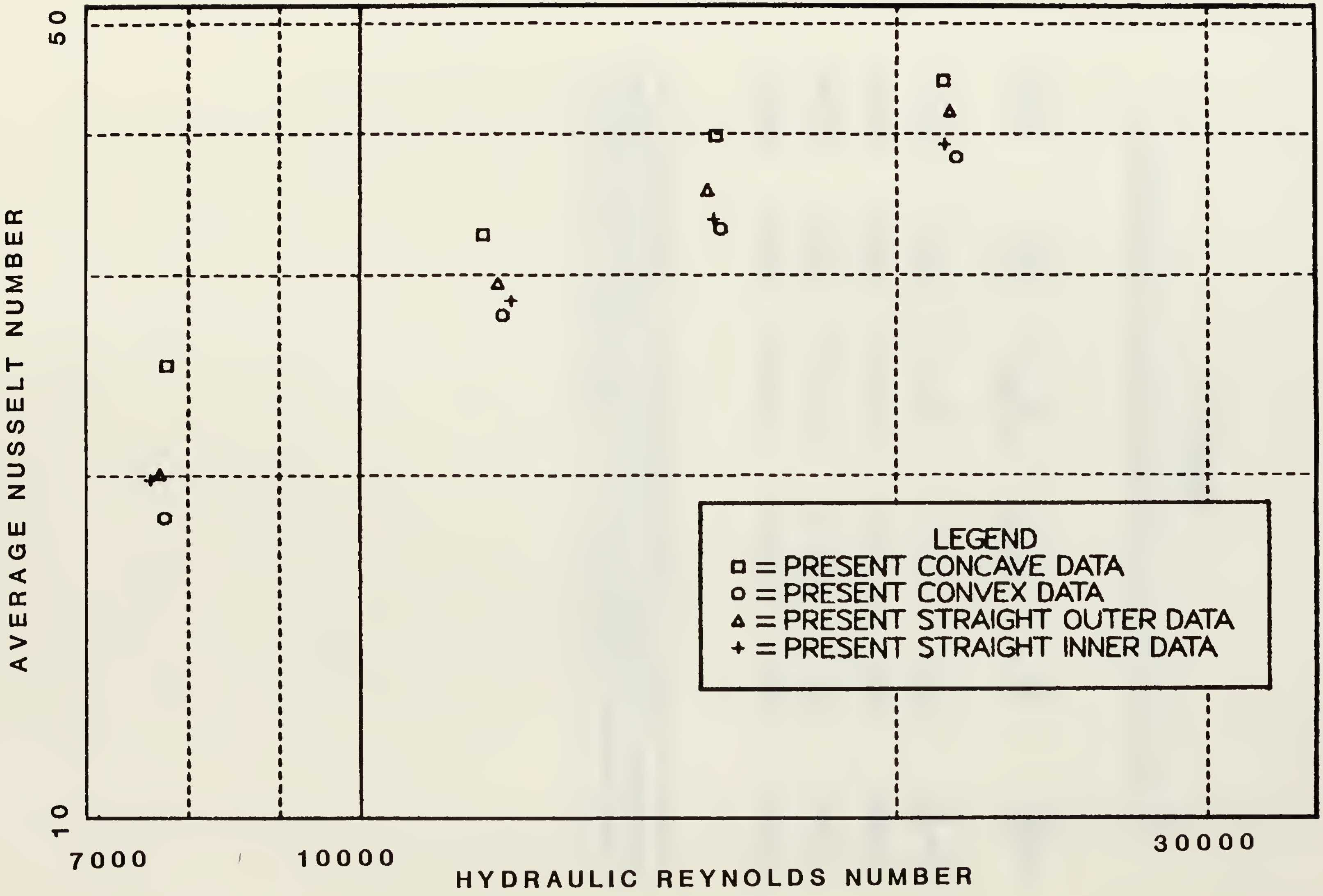

Figure 25. Present Straight vs. Curved Section Results.

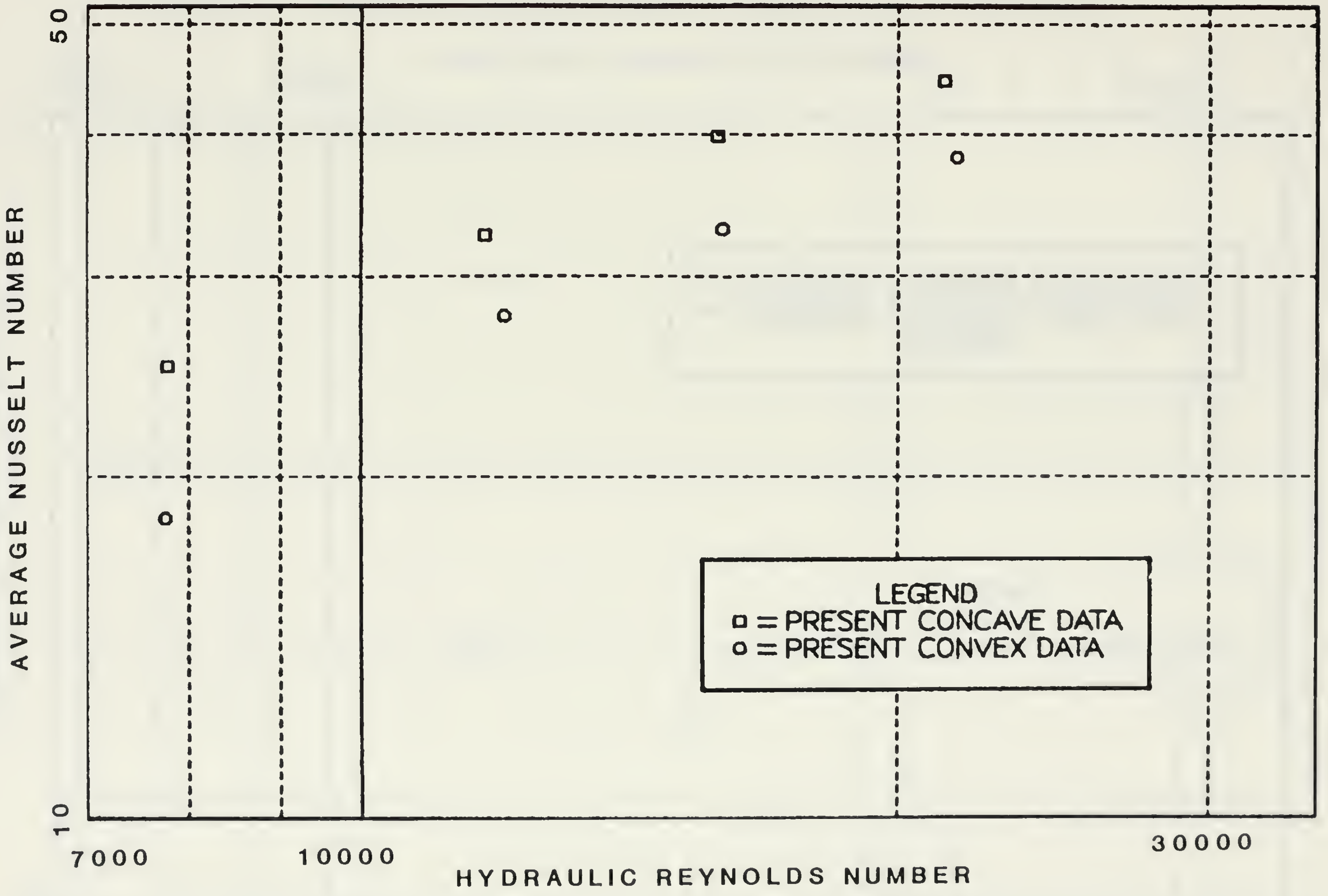

Figure 26. Present Concave vs. Convex Section Results.

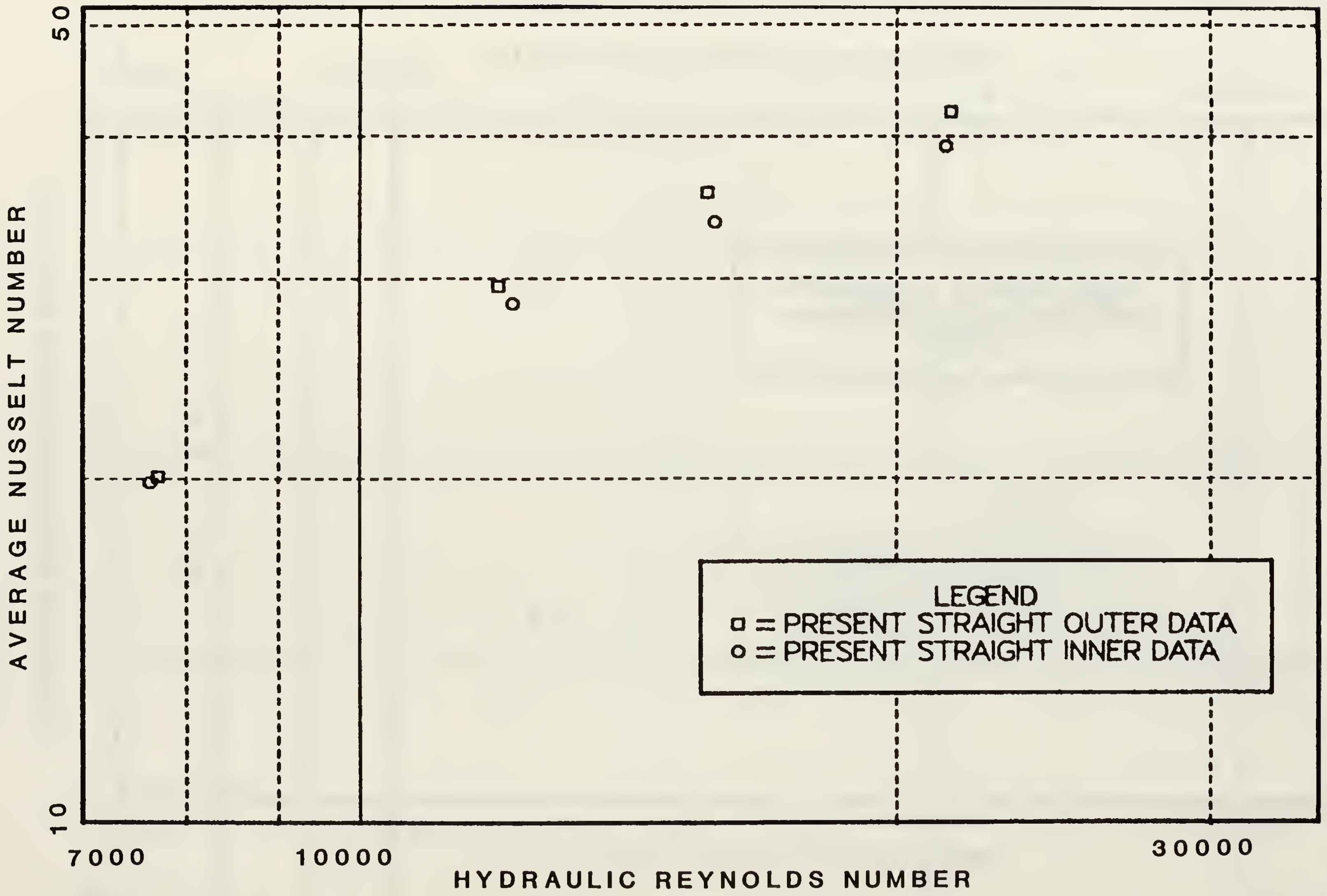

Figure 27. Present Straight Outer vs. Inner Section Results.

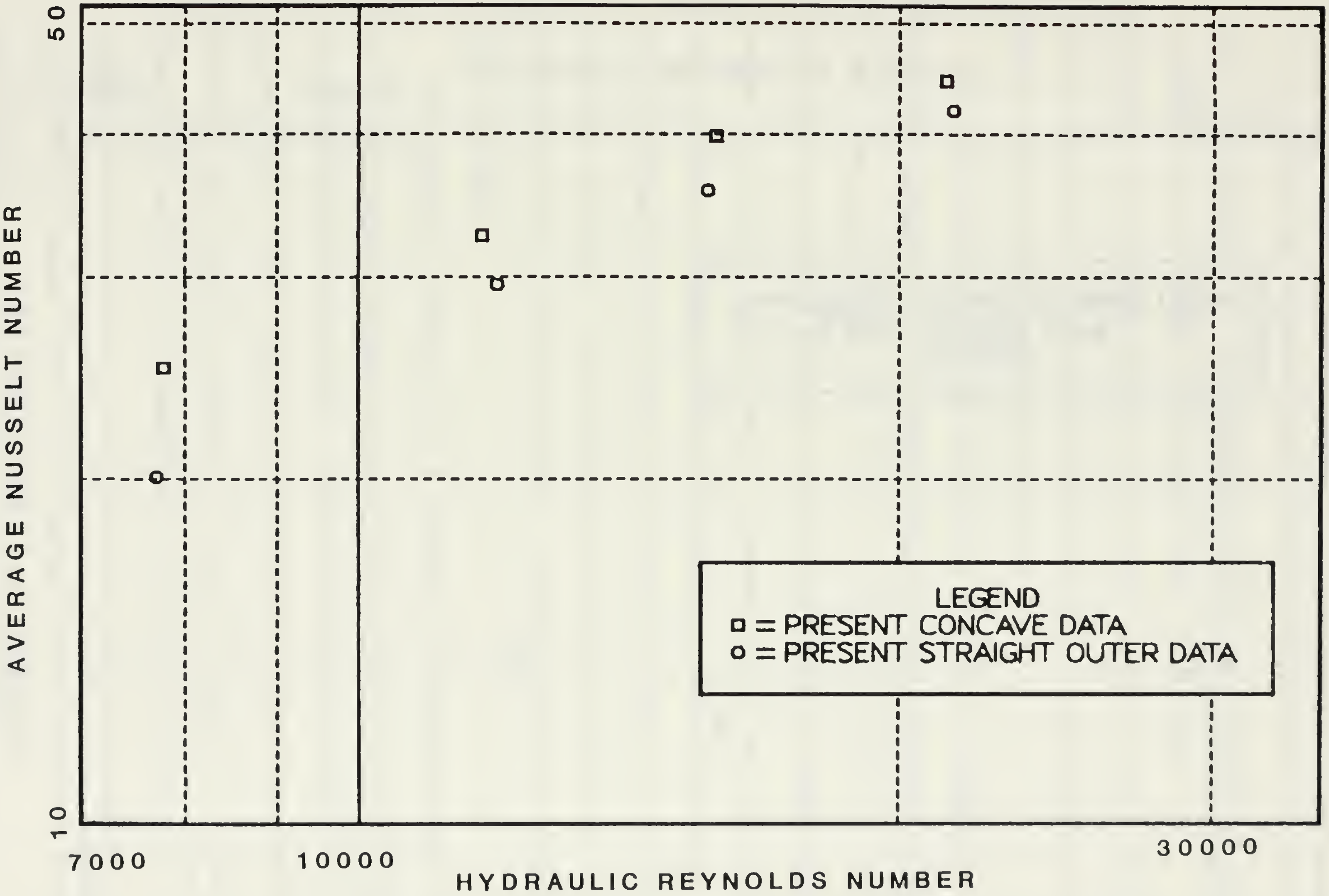

Figure 28. Present Concave vs. Straight Outer Section Results.

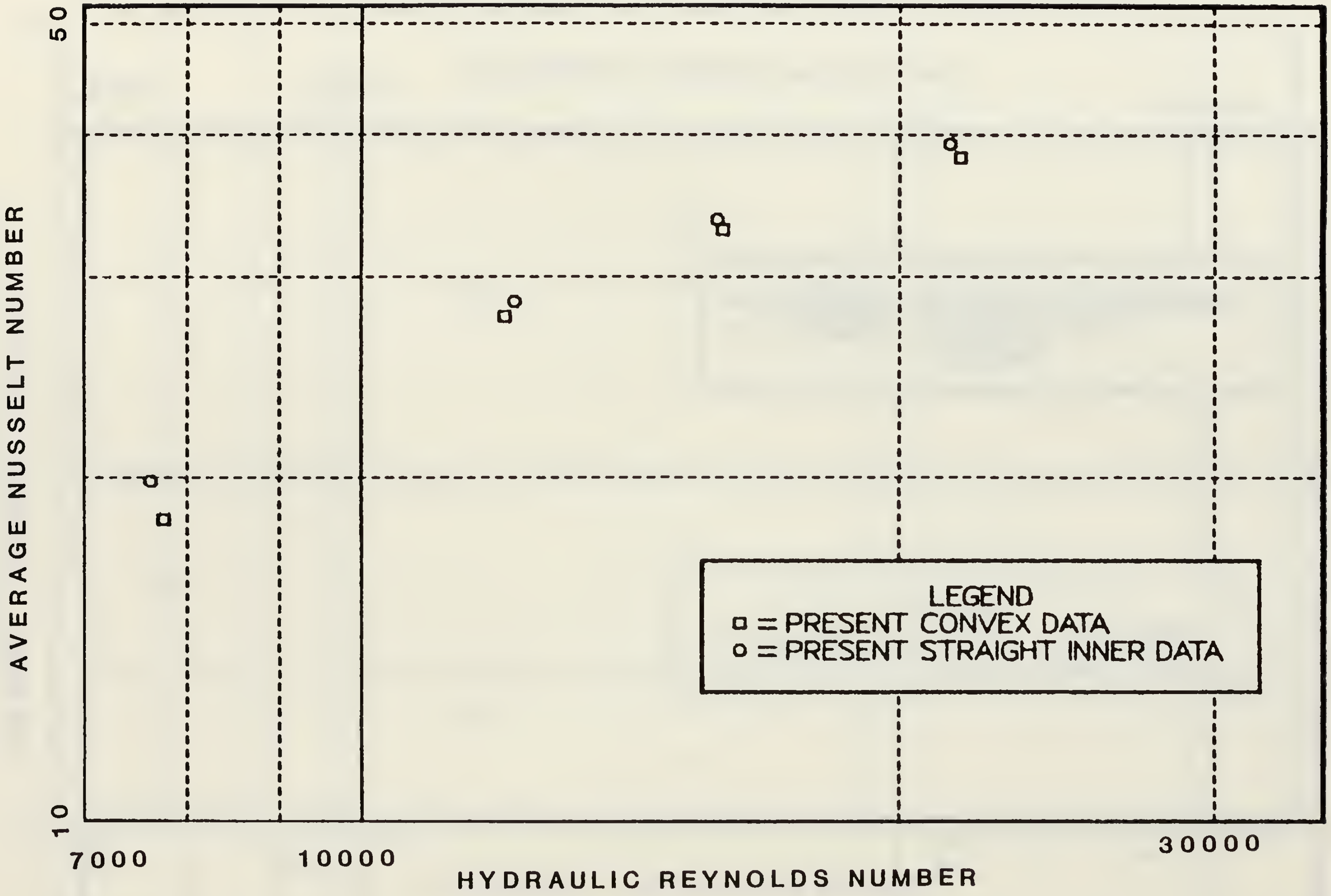

Figure 29. Present Convex vs. Straight Inner Section Results.

As would be expected the results indicate an increase in the rate of heat transfer with increasing Reynolds number for both the straight and curved test sections. In addition, the heat transfer rate was highest in the concave curved section for each Reynolds number investigated, and lowest in the convex curved section.

In the low end of the turbulent regime, at a hydraulic Reynolds number of 7780, the rate of heat transfer was about twenty-two percent higher in the concave curved section than the outer straight section. As the hydraulic Reynolds number continued to increase, between 11700 and 15800, the rate of heat transfer was approximately eleven percent higher between the concave curved section and the outer straight section. At a hydraulic Reynolds number of 21000 the difference in heat transfer rate decreased to about seven percent.

The results obtained at a hydraulic Reynolds number of 21000 have a much larger uncertainty, because the orifice air temperature was higher than the average outlet air temperature. This signifies that the air was not fully mixed at the outlet, because no heat is added to the air after the outlet air temperature is read, yet the air temperature increased. For hydraulic Reynolds numbers greater than about 17000 the channel outlet section is not long enough to allow the air to mix properly.

The values obtained for the hydraulic Reynolds number of approximately 21000 are based on the orifice air temperature vice the outlet air temperature. This resulted in a Nusselt number higher than obtained by using the the outlet air temperature, but still lower than the actual Nusselt number, because of the small heat loss between the outlet nozzle and the thermocouple at the orifice. This heat loss cannot be accounted for and the temperature used as an outlet air temperature was still lower than the actual outlet air temperature.

In comparing the concave curved wall to the convex curved wall the rate of heat transfer was about thirty-six percent higher in the concave section for a hydraulic Reynolds number of 7780. For hydraulic Reynolds numbers between 11700 and 15800 the rate of heat transfer was twenty percent higher in the concave section, and at a hydraulic Reynolds number of 21200 the rate of heat transfer was seventeen percent higher.

VI. DISCUSSION AND CONCLUSIONS

J. Wilson [Ref. 28], in his study, reported that the actual presence of Taylor-Gortler vortices were verified by the observation of the liquid crystal isotherm distribution in the curved test section. He further reported, that at low values of hydraulic Reynolds number and through most of the transition regime, liquid crystal bands were oriented in the streamwise direction. As the Reynolds number increased turbulent forces began to dominate in the curved section and less evidence could be detected for the existence of the vortices.

The high aspect ratio of the channel provided the basis for the assumption that the experimental apparatus should behave like infinite parallel plates. Holihan's data [Ref. 26] tended to verify this assumption. His experimental data in the laminar flow region, approached the theoretical limit for average Nusselt number for parallel plates with one wall heated at a constant heat flux and the opposite wall adiabatic [Ref. 32]. Based on the assumptions mentioned above, comparisons were made with other analytical and experimental results that were of the same or similar problems.

A comparison of the experimental results of this study and the experimental results of Daughety [Ref. 27] and

Wilson [Ref. 28] are shown in Figure 30 for the curved section, and Figure 31 for the straight section. The channel aspect ratio was 40 for each of these studies and the experimental procedures were similar, with the exception of a slight modification in Wilson's procedures. Wilson [Ref. 28] made a correction to determine the temperature drop across the liquid crystal sheet covering the heated wall. By applying this temperature drop to the measured temperature, the true temperature of the heated wall would be known. After reviewing Wilson's data and experimental procedure it was detected that Wilson was over estimating the temperature drop across the liquid crystal by approximately five to seven percent, and this lead to an over estimation of T of ten to twelve percent. This resulted in an over estimation of the average heat transfer coefficient and the average Nusselt number of between ten and twelve percent. When Wilson's data is lowered by ten percent, both his data and Daughety's data fall within the uncertainty bands of the present study as shown in Figures 32 and 33. Differences were attributed to the inability to acccount for all of the heat transfer processes and the limitations inherent in any experimental work.

Ballard [Ref. 25] reported an increase in the rate of heat transfer between a concave wall and a straight outer wall of eleven percent for laminar flows. Holihan [Ref. 26] reported an increase of fifteen percent for laminar flows

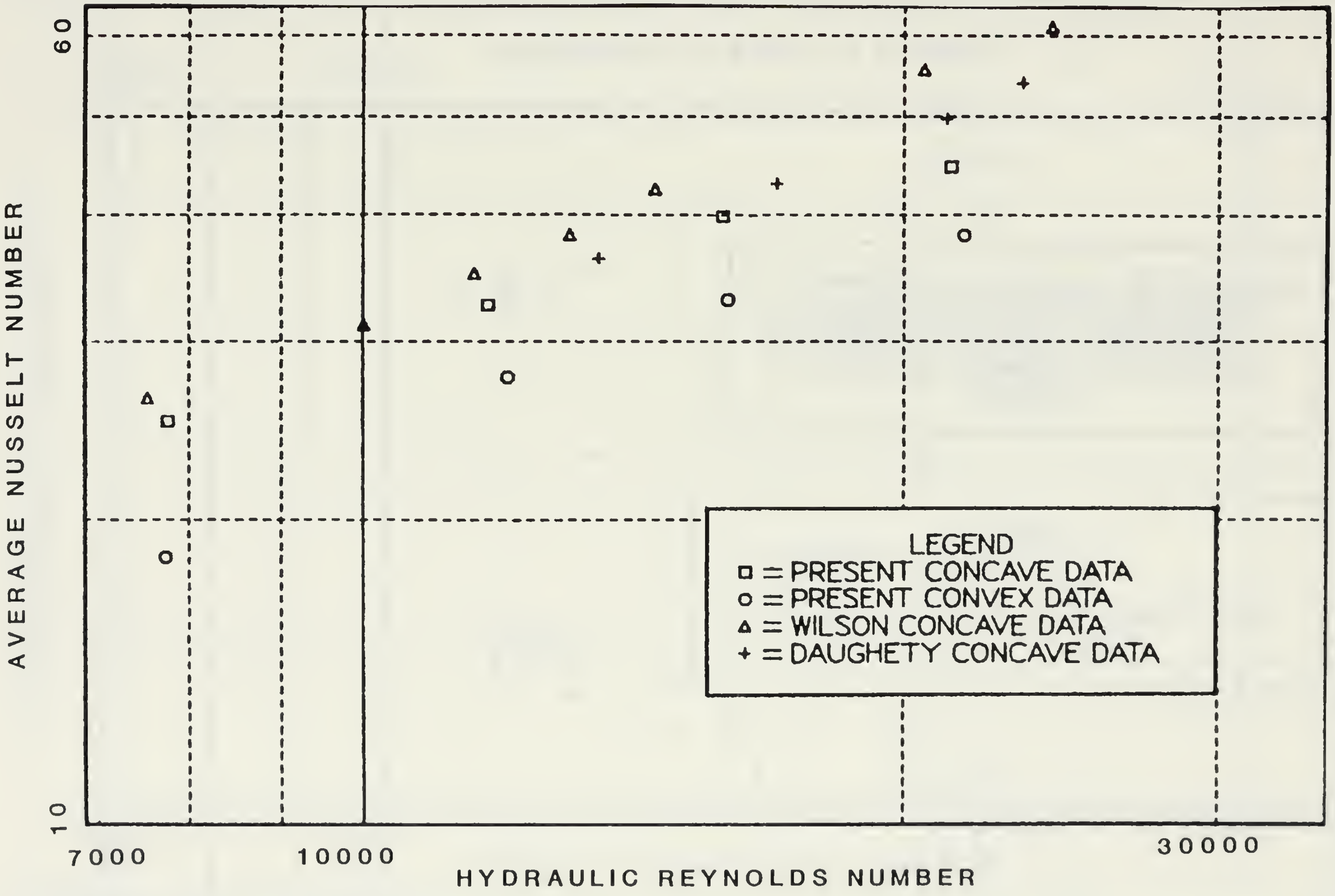

Figure 30. Comparison of Present Data with Daughety and Wilson, Curved Section.

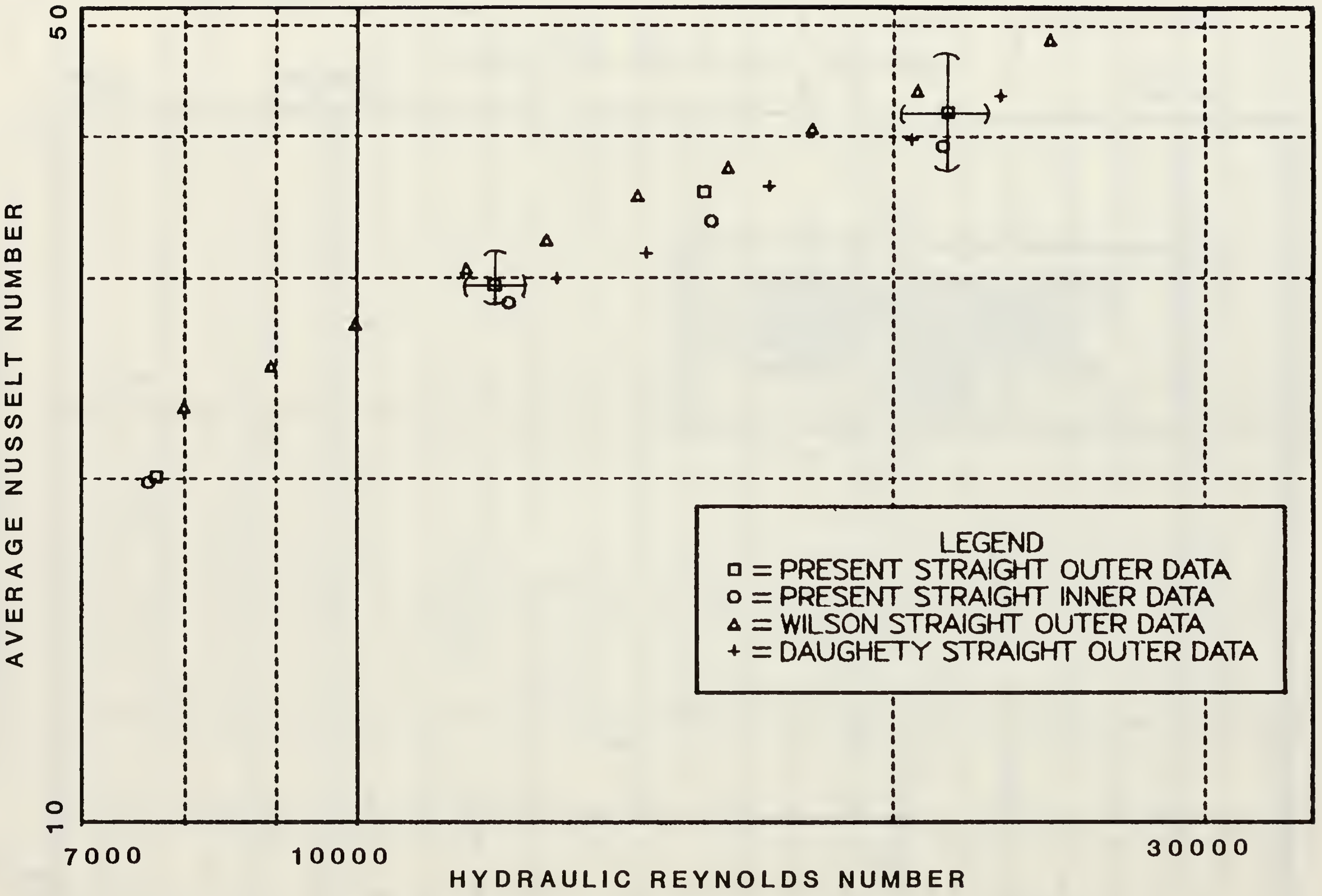

Figure 31. Comparison of Present Data with Daughety and Wilson, Straight Section.

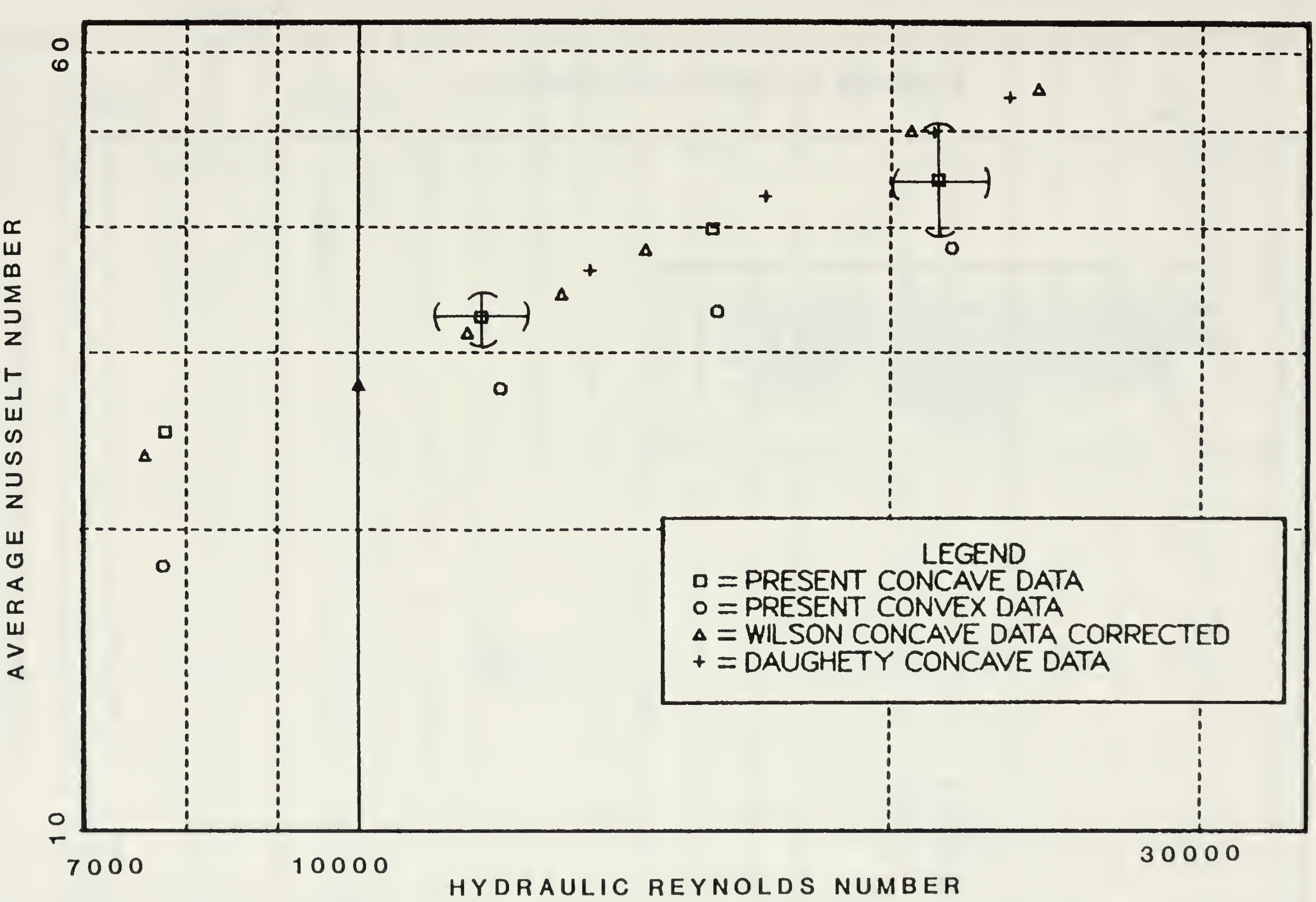

Figure 32. Comparison of Present Data with Daughety and Corrected Wilson, Curved Section.

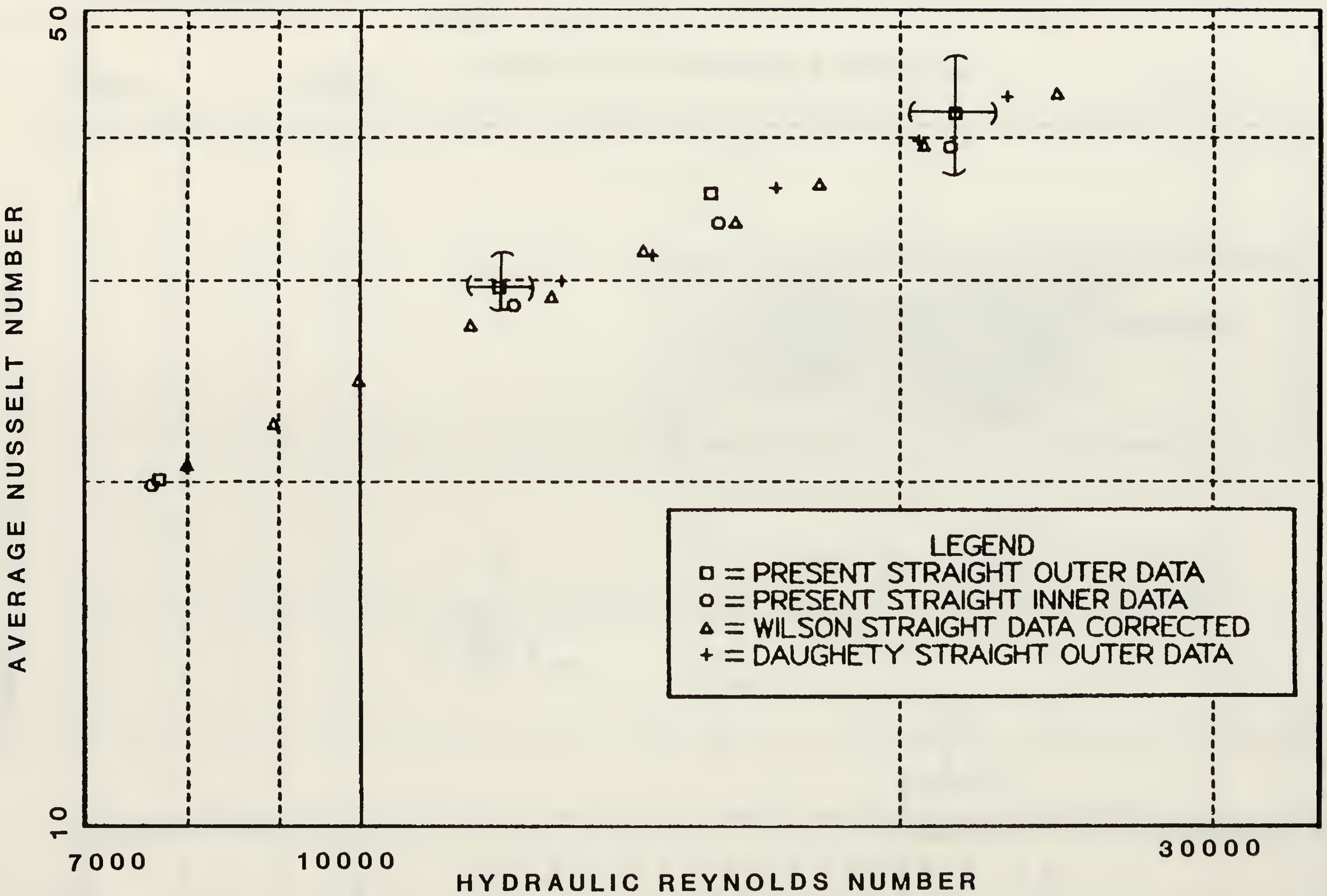

Figure 33. Comparison of Present Data with Daughety and Corrected Wilson, Straight Section.

and thirty percent for transition flows. Daughety [Ref. 27], reported an increase of twenty percent in the heat transfer rate for turbulent flows. Wilson [Ref. 28], reported an increase of forty-five percent for laminar flows, twenty percent for transition flows, thirteen percent for hydraulic Reynolds numbers between 5400 and 12000, and about twenty-six percent at a hydraulic Reynolds number of 24000. This compares very favorably with the present results, except for the data at a hydraulic Reynolds number of 21000. No conclusion can be made about the present results at a hydraulic Reynolds number of 21000 because of the high uncertainty of the data as previously mentioned. This area needs further experimentation before accurate conclusions can be made about the heat transfer rate at high hydraulic Reynolds numbers.

Kreith [Ref. 16] reported an increase in the rate of heat transfer along a concave wall as compared to a convex wall of twenty-five to sixty percent for hydraulic Reynolds numbers between 10^4 to 10^6. This also compares favorably with the present results which indicate an increase of seventeen to thirty-eight percent when comparing concave wall to convex wall.

A comparison of analytical and experimental results with those of the present study for the straight test section is shown graphically in Figure 34. The Dittus-Boelter equation

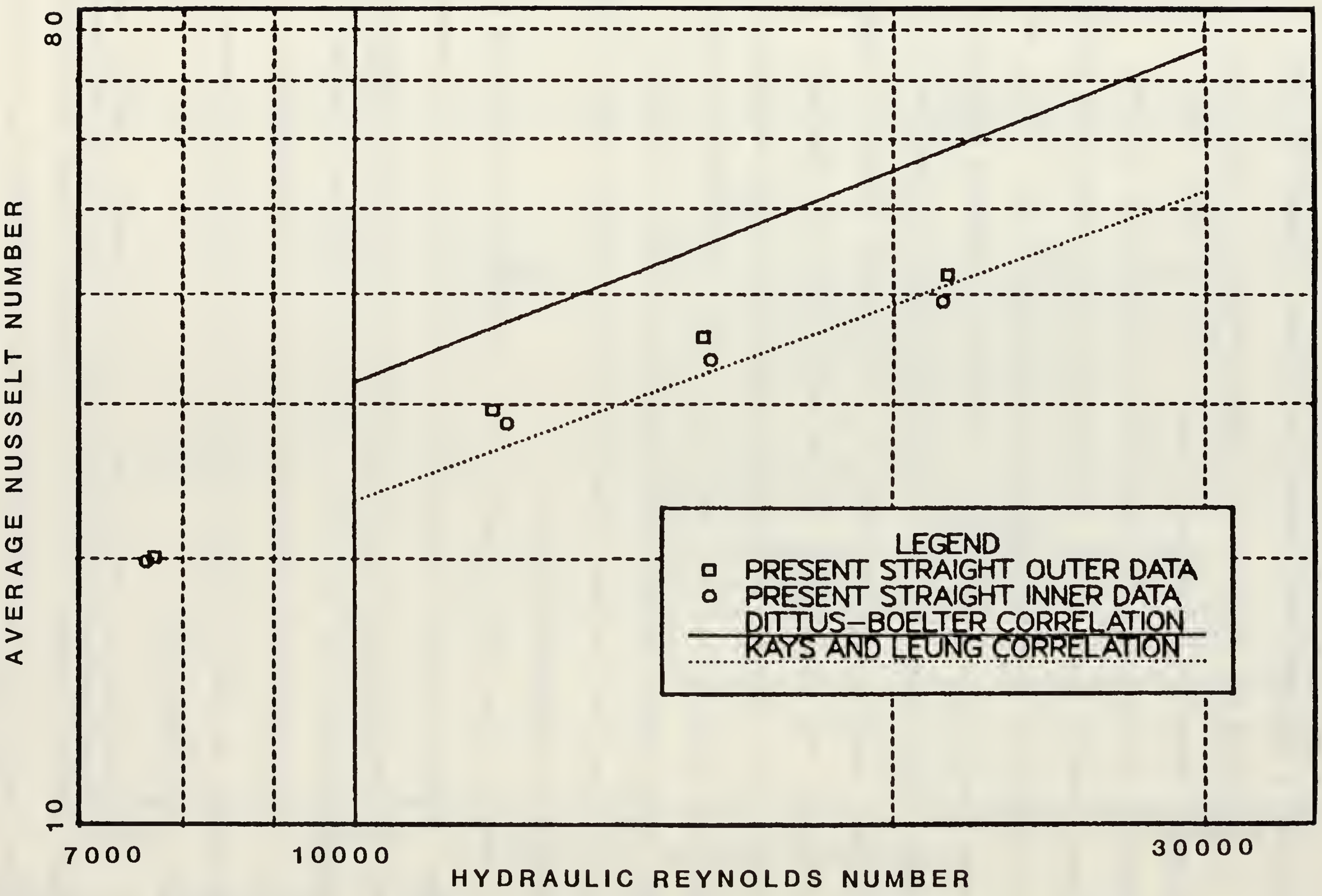

Figure 34. Comparison of Present Data with Dittus-Boelter, Kays and Leung, for Turbulent Flow, Straight Section.

[Ref. 29] for heat transfer in a straight tube for constant wall temperature is plotted from:

$$Nu = 0.02Re^{0.8}$$

For a Prandtl number equal to 0.71. Additionally, the results of Kays and Leung [Ref. 21] for heat transfer in annular passages are shown for r* = 1.0, which equates to parallel plates. When examined these results compare favorably with the present data.

The curved section data is plotted in Figure 35, and is compared to the experimental work of Brinich and Graham [Ref. 22]. The accuracy of the data points used from Brinich and Graham are subject to some error, in that the actual values are not given in their study and had to be taken from a plot of Stanton number versus Reynolds number.

After carefully examining the past and present data the trends and results are consistent. Heat transfer rates increase with increasing Reynolds numbers. Also, the concave curved section enhances the rate of heat transfer over the convex curved section and the straight test sections for laminar, transition, and turbulent flows. The presence of Taylor-Gortler vortices in the laminar and transition regime seems to be the major contributing factor to this enhancement. Whether the Taylor-Gortler vortices continue to exist in the turbulent flow regime remains to be seen.

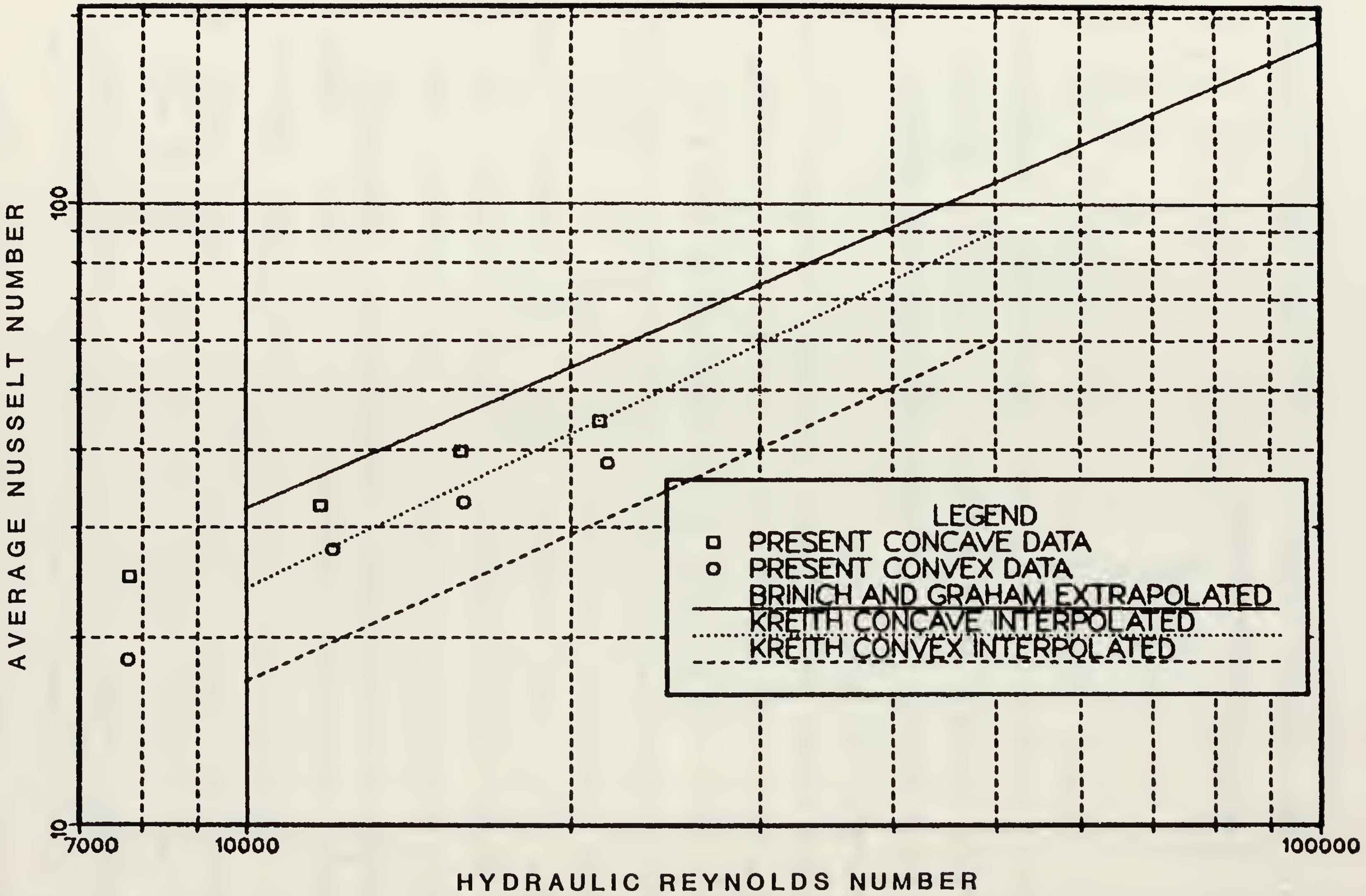

Figure 35. Comparison of Present Data with Brinich and Graham, and Kreith, for Turbulent Flow, Curved Section.

VII. RECOMMENDATIONS

The amount of experimental work remaining in the study of heat transfer in curved channels is still significant. The present experimental apparatus has been tested in the turbulent regime, and the test data proves that accurate results can be obtained for hydraulic Reynolds numbers below 17000, slightly higher when heating the straight test section. Additional experiments into the laminar, transition, and turbulent region should be conducted to better understand the heat transfer processes occurring in the straight and curved sections. By remaining below a hydraulic Reynolds number of 17000 accurate data can be obtained and significant conclusions can be drawn in the comparison of the curved sections to the straight section, and the concave curved wall to the convex curved wall.

To improve the accuracy of the data and results some slight modifications to the present channel should be done. First, the straight outlet section of the channel should be lengthened to ensure proper mixing of the heated outlet air. Second, some sort of honey combing, screening, or other type of device should be placed in the outlet section to enhance the mixing of the heated outlet air. Finally, extra thermocouples should be placed at the outlet and read more then once during a data run to decrease the uncertainty of the outlet air temperature (T_{out}) and the uncertainty of the difference between the inlet and outlet air temperature. By applying these recommendations the uncertainty of the Nusselt number can be reduced to four percent or less.

Further experiments at hydraulic Reynolds numbers greater than 17000 also need to be examined. This can be accomplished if the above recommendations are taken along with one other. The channel walls need outer support to prevent the center of the channel from collapsing at the high hydraulic Reynolds numbers. Slight collapsing was noticed at hydraulic Reynolds numbers greater than 20000. This collapsing was caused by the laminating of two 0.3175 centimeter thick walls which were not as rigid as the single 0.635 centimeter thick walls used previously. The actual hydraulic Reynolds numbers that can be attained and still yield accurate results will be limited by the power of the compressor and the rigidity of the channel's walls.

Finally, once a strong data base can be obtained for each test section further experimentation can be conducted with different boundary conditions. For example, both curved walls heated at the same constant heat flux. Once this can be done a true comparison of the heat transfer rate of the total curved test section can be compared to the total straight test section, i.e., both curved walls versus both straight walls.

APPENDIX A: COMPUTER PROGRAM

```
1000  !  FILE NAME: DRP2A
1010  !  LAST REVISION DATE:  21 OCTOBER 1985
1020  !  AUTHOR:  LT. GEORGE G. GALYO
1030!
1040  !  PROGRAM FOR GATHERING AND REDUCING DATA WHEN HEATING ONE COPPER PLATE,
1050  !  WITH 10 MINUTES BETWEEN RUNS.  PROGRAM IS MODIFIED TO ACCOUNT FOR
1060  !  BROKEN THERMOCOUPLE CHANNELS 5, 16, 21, AND 26 WHICH EFFECT OUTER
1070  !  CURVED HEATER, AND THERMOCOUPLE CHANNEL 47 WHICH EFFECTS INNER CURVED
1080  !  HEATER.
1090!
1100  COM /Co/ D(7),Aa(76,2)
1110  DIM Emf(79),T(79)
1120!
1130  !  CORRELATION FACTORS FOR EMF TO DEGREES CELSIUS FOR CU-CO T/C.
1140!
1150  DATA 0.10086091,25727.94369,-767345.8295.78025595.81
1160  DATA -9247486589,6.97688E+11,-2.66192E+13,3.94078E+14
1170  READ D(*)
1180  PRINTER IS 701
1190  BEEP
1200  INPUT "ENTER MONTH, DAY, AND TIME (MM:DD:HH:MM:SS)",Time$
1210  OUTPUT 709;"TD";Time$
1220  BEEP
1230  INPUT "ENTER INPUT MODE (0=3054A,1=FILE)",Im
1240  IF Im=1 THEN
1250  BEEP
1260  INPUT "ENTER NAME OF EXISTING DATA FILE",Oldfile$
1270  PRINT USING "20X,""These Results Are From Data File:  "",10A";Oldfile$
1280  PRINT
1290  PRINT
1300  ELSE
1310  BEEP
1320  INPUT "ENTER NAME OF NEW DATA FILE?",Newfile$
1330  PRINT USING "20X,""Data For This Run Is Stored In Data File:  "",10A";Newf
ile$
1340  PRINT
1350  PRINT
1360  END IF
1370!
1380  !  ENTER THE CHANNEL CONFIGURATION.
1390!
1400  PRINT USING "9X,""THE FOLLOWING CHANNEL CONFIGURATION WAS SELECTED:"""
1410  PRINT
1420  BEEP
1430  INPUT "SELECT HEATER TYPE (0=STRAIGHT, 1=CURVED)",Itype
1440  IF Itype=0 THEN PRINT USING "12X,""Heating STRAIGHT Test Section."""
1450  IF Itype=1 THEN PRINT USING "12X,""Heating CURVED Test Section."""
1460  BEEP
1470  INPUT "SELECT HEATER POSITION (0=OUTER, 1=INNER)",Ipos
1480  IF Ipos=0 THEN PRINT USING "12X,""Heating OUTER Plate."""
1490  IF Ipos=1 THEN PRINT USING "12X,""Heating INNER Plate."""
1500  PRINT
1510!
1520  !  ENTERS FILES WITH T/C CALIBRATION COEFFICIENTS BASED ON HEATER TYPE.
1530!
1540  IF Itype=0 THEN ASSIGN @Filec TO "STRA_COEF"
1550  IF Itype=1 THEN ASSIGN @Filec TO "CURV_COEF"
1560  FOR I=0 TO 76
1570  ENTER @Filec;Aa(I,0),Aa(I,1),Aa(I,2)
1580  NEXT I
```

```
1590  ASSIGN @Filec TO *
1600!
1610  !  INSERT DATA STORAGE DISK.
1620!
1630  BEEP
1640  INPUT "CHANGE DISK AND HIT ENTER",Ok
1650  IF Im=1 THEN ASSIGN @File TO Oldfile$
1660  IF Im=0 THEN
1670  CREATE BDAT Newfile$,40
1680  ASSIGN @File TO Newfile$
1690  END IF
1700  ENTER 709;Time$
1710  CLEAR 709
1720  PRINT USING "20X,""Month, Day, and Time: "".14A";Time$
1730  PRINT
1740!
1750  !  FOR DATA RUN READ AND STORE ALL RAW EMF VALUES.
1760!
1770  IF Im=0 THEN
1780  OUTPUT 709;"AR AF00 AL79"
1790  OUTPUT 722;"F1 R1 T1 Z1 FL1"
1800  FOR I=0 TO 79
1810  OUTPUT 709;"AS"
1820  ENTER 722;Emf(I)
1830  NEXT I
1840  OUTPUT @File;Emf(*)
1850  ELSE
1860  ENTER @File;Emf(*)
1870  END IF
1880  OUTPUT 709;"TD"
1890!
1900  !  CONVERT AND CALIBRATE ALL T/C READINGS TO DEGREES CELSIUS.
1910!
1920  PRINT USING "9X,""THE FOLLOWING DATA WERE RECORDED:"""
1930  PRINT
1940  FOR I=0 TO 79
1950  IF I=38 OR I=39 OR I=77 OR I=78 THEN
1960  IF (Ipos=0 AND I=38) OR (Ipos=1 AND I=77) THEN
1970  Iadd=0
1980  IF Ipos=1 THEN Iadd=39
1990  PRINT USING "12X,""Heater Voltage (Vh)        = "",2D.3D,"" (V)""";Emf(38+Ia
dd)
2000  PRINT USING "12X,""Resistor Voltage (Vr)      = "",2D.3D,"" (V)""";Emf(39+Ia
dd)
2010  IF Ipos=0 THEN PRINT USING "12X,""Precision Resistor (Rpr) =  2.01729 (Ohm
s)"""
2020  IF Ipos=1 THEN PRINT USING "12X,""Precision Resistor (Rpr) =  2.00839 (Ohm
s)"""
2030  PRINT
2040  END IF
2050  ELSE
2060!
2070  !  IF T/C OUT OF RANGE PRINT A QUE.
2080!
2090  Aemf=Emf(I)
2100  IF Aemf<3.E-4 OR Aemf>3.E-3 THEN
2110  T(I)=999.99
2120  ELSE
2130  CALL Tvsv(Emf(I),Tt)
2140  IF I=79 THEN
```

```
2150  T(I)=Tt
2160  GOTO 2210
2170  END IF
2180  T(I)=FNTcorr(Tt,I)
2190  END IF
2200  END IF
2210  NEXT I
2220!
2230  !  PRINT ALL T/C READINGS.
2240!
2250  PRINT USING "12X,""OUTER PLATE:"""
2260  PRINT USING "14X,""T/C Number:     1       2       3       4       5
 6"""
2270  PRINT USING "14X,""Temp (C):    "",6(3D.DD,2X)";T(0),T(1),T(2),T(3).T(4),T
(5)
2280  PRINT USING "14X,""T/C Number:     7       8       9      10      11
12"""
2290  PRINT USING "14X,""Temp (C):    "",6(3D.DD,2X)";T(6),T(7),T(8),T(9).T(10),
T(11)
2300  PRINT USING "14X,""T/C Number:    13      14      15      16      17
18"""
2310  PRINT USING "14X,""Temp (C):    "",6(3D.DD.2X)";T(12),T(13),T(14),T(15).T(
16),T(17)
2320  PRINT USING "14X,""T/C Number:    19      20      21      22      23
24"""
2330  PRINT USING "14X,""Temp (C):    "",6(3D.DD,2X)";T(18),T(19),T(20).T(21),T(
22),T(23)
2340  PRINT USING "14X,""T/C Number:    25      26      27      28      29
30"""
2350  PRINT USING "14X,""Temp (C):    "",6(3D.DD,2X)";T(24),T(25),T(26).T(27),T(
28),T(29)
2360  PRINT
2370!
2380  !  CALCULATE AVERAGE TEMPERATURE OF OUTER HEATED WALL.
2390!
2400  Sum=0.
2410  IF Itype=0 THEN
2420  FOR I=0 TO 29
2430  Sum=Sum+T(I)
2440  NEXT I
2450  Two=Sum/30
2460!
2470  !  CORRECTION FOR BROKEN T/C CHANNELS 5, 16, 21, AND 26 IN OUTER CURVED HE
ATER.
2480!
2490  ELSE
2500  FOR I=0 TO 29
2510  IF I=5 OR I=16 OR I=21 OR I=26 THEN 2530
2520  Sum=Sum+T(I)
2530  NEXT I
2540  Two=Sum/26
2550  END IF
2560  PRINT USING "12X,""OUTER INSULATION:"""
2570  PRINT USING "14X,""T/C Number:    31 (Tinso1)   32 (Tinso2)   33 (Tinso3)"
""
2580  PRINT USING "14X,""Temp (C):        "",3(3D.DD,8X)":T(30),T(31).T(32)
2590  Tinso1=T(30)
2600  Tinso2=T(31)
2610  Tinso3=T(32)
2620  PRINT
```

```
2630  PRINT USING "12X,""ORIFICE TEMP (Torf) = "",3D.DD,"" (C)""";T(33)
2640  PRINT
2650  PRINT USING "12X,""INLET TEMPERATURE:"""
2660  PRINT USING "14X,""T/C Number:    35       36       37       38"""
2670  PRINT USING "14X,""Temp (C):     "",4(3D.DD,2X)";T(34),T(35),T(36),T(37)
2680  PRINT
2690!
2700  !  CALCULATE AVERAGE INLET TEMPERATURE.
2710!
2720  Sum=0.
2730  FOR I=34 TO 37
2740  Sum=Sum+T(I)
2750  NEXT I
2760  Tin=Sum/4
2770  PRINT USING "12X,""INNER PLATE:"""
2780  PRINT USING "14X,""T/C Number:    41       42       43       44       45
46"""
2790  PRINT USING "14X,""Temp (C):     "",6(3D.DD,2X)";T(40),T(41),T(42),T(43),T(
44),T(45)
2800  PRINT USING "14X,""T/C Number:    47       48       49       50       51
52"""
2810  PRINT USING "14X,""Temp (C):     "",6(3D.DD,2X)";T(46),T(47),T(48),T(49),T(
50),T(51)
2820  PRINT USING "14X,""T/C Number:    53       54       55       56       57
58"""
2830  PRINT USING "14X,""Temp (C):     "",6(3D.DD,2X)";T(52),T(53),T(54),T(55),T(
56),T(57)
2840  PRINT USING "14X,""T/C Number:    59       60       61       62       63
64"""
2850  PRINT USING "14X,""Temp (C):     "",6(3D.DD,2X)";T(58),T(59),T(60),T(61),T(
62),T(63)
2860  PRINT USING "14X,""T/C Number:    65       66       67       68       69
70"""
2870  PRINT USING "14X,""Temp (C):     "",6(3D.DD,2X)";T(64),T(65),T(66),T(67),T(
68),T(69)
2880  PRINT
2890!
2900  !  CALCULATE AVERAGE TEMPERATURE OF INNER HEATED WALL.
2910!
2920  Sum=0.
2930  IF Itype=0 THEN
2940  FOR I=40 TO 69
2950  Sum=Sum+T(I)
2960  NEXT I
2970  Twi=Sum/30
2980!
2990  !  CORRECTION FOR BROKEN T/C CHANNEL 47 IN INNER CURVED HEATER.
3000!
3010 ELSE
3020 FOR I=40 TO 69
3030 IF I=47 THEN 3050
3040 Sum=Sum+T(I)
3050 NEXT I
3060 Twi=Sum/29
3070 END IF
3080  PRINT USING "12X,""INNER INSULATION:"""
3090  PRINT USING "14X,""T/C Number:    71 (Tinsi1)   72 (Tinsi2)   73 (Tinsi3)"
""
3100  PRINT USING "14X,""Temp (C):          "",3(3D.DD,8X)";T(70),T(71),T(72)
3110  Tinsi1=T(70)
```

```
3120  Tinsi2=T(71)
3130  Tinsi3=T(72)
3140  PRINT
3150  PRINT USING "12X,""OUTLET TEMPERATURE:"""
3160  PRINT USING "14X,""T/C Number:     74       75       76       77"""
3170  PRINT USING "14X,""Temp (C):     "",4(3D.DD,2X)";T(73),T(74),T(75),T(76)
3180  PRINT USING "@,#"
3190!
3200  !  CALCULATE AVERAGE OUTLET TEMPERATURE.
3210!
3220  Sum=0.
3230  FOR I=73 TO 76
3240  Sum=Sum+T(I)
3250  NEXT I
3260  Tout=Sum/4
3270!
3280  !  CALCULATE DIFFERENCE BETWEEN CHANNEL INLET AND OUTLET TEMPERATURES.
3290!
3300  Tdiff=Tout-Tin
3310!
3320  !  CALCULATE CHANNEL BULK TEMPERATURE.
3330!
3340  Tblk=(Tin+Tout)/2
3350!
3360  !  PRINT CALCULATED TEMPERATURES.
3370!
3380  PRINT USING "9X,""THE FOLLOWING TEMPERATURES WERE CALCULATED:"""
3390  PRINT
3400  PRINT USING "12X,""Average Outer Wall Temperature (Two)             = "",3D.
DD,"" (C)""";Two
3410  PRINT USING "12X,""Average Inner Wall Temperature (Twi)             = "",3D.
DD,"" (C)""";Twi
3420  PRINT USING "12X,""Average Outlet Temperature (Tout)                = "",3D.
DD,"" (C)""";Tout
3430  PRINT USING "12X,""Average Inlet Temperature (Tin)                  = "",3D.
DD,"" (C)""";Tin
3440  PRINT USING "12X,""Channel Inlet and Outlet Temp Diff (Tdiff)       = "",3D.
DD,"" (C)""";Tdiff
3450  PRINT USING "12X,""Average Bulk Temperature (Tblk)                  = "",3D.
DD,"" (C)""";Tblk
3460!
3470  !  CALCULATE DELTA T (Tdel) FOR USE IN CALCULATING H LATER.
3480!
3490  Tdelo=Two-Tblk
3500  Tdeli=Twi-Tblk
3510  IF Ipos=0 THEN Tdel=Tdelo
3520  IF Ipos=1 THEN Tdel=Tdeli
3530  PRINT USING "12X,""Mean Temperature Difference (Tdel)               = "",3D.
DD,"" (C)""";Tdel
3540!
3550  !  CALCULATE DIFFERENCE BETWEEN OUTER AND INNER WALL.
3560!
3570  Twdiff=ABS(Two-Twi)
3580  PRINT USING "12X,""Outer and Inner Wall Temp Difference (Twdiff)  = "",3D.
DD,"" (C)""";Twdiff
3590!
3600  !  CALCULATE LOCAL CHANNEL TEMPERATURES AT INLET, MIDDLE AND OUTLET.
3610!
3620  Tcin=Tin+(.5*Tdiff/12)
3630  Tcmid=Tin+(4.5*Tdiff/12)
```

```
3640  Tcout=Tin+(11.5*Tdiff/12)
3650  PRINT USING "12X,""Average Local Channel Temp at Inlet (Tcin)      = "",3D.
DD,"" (C)""";Tcin
3660  PRINT USING "12X,""Average Local Channel Temp at Middle (Tcmid)    = "",3D.
DD,"" (C)""";Tcmid
3670  PRINT USING "12X,""Average Local Channel Temp at Outlet (Tcout)    = "",3D.
DD,"" (C)""";Tcout
3680!
3690  !  CALCULATE AVERAGE LOCAL HEATED WALL TEMPERATURE AT INLET.
3700!
3710  Sum=0.
3720  Iadd=0
3730  IF Ipos=1 THEN Iadd=40
3740!
3750  !  CORRECTION FOR BROKEN T/C CHANNELS 5, AND 47 CURVED HEATER ONLY.
3760!
3770  IF Itype=1 THEN
3780  FOR I=0 TO 6
3790  IF (Ipos=0 AND I=5) OR (Ipos=1 AND I=6) THEN 3810
3800  Sum=Sum+T(I+Iadd)
3810  NEXT I
3820  Twin=Sum/6
3830  ELSE
3840  FOR I=0 TO 7
3850  IF (Ipos=0 AND I=7) OR (Ipos=1 AND I=6) THEN 3870
3860  Sum=Sum+T(I+Iadd)
3870  NEXT I
3880  Twin=Sum/7
3890  END IF
3900  PRINT USING "12X,""Avg Local Heated Wall Temp at Inlet (Twin)      = "",3D.
DD,"" (C)""";Twin
3910!
3920  !  CALCULATE AVERAGE LOCAL HEATED WALL TEMPERATURE NEAR MIDDLE.
3930!
3940  Sum=0.
3950!
3960  !  CORRECTION FOR BROKEN T/C CHANNEL 16 CURVED HEATER ONLY.
3970!
3980  IF Itype=1 AND Ipos=0 THEN
3990  FOR I=9 TO 15
4000  IF I=10 THEN 4020
4010  Sum=Sum+T(I)
4020  NEXT I
4030  Twmid=Sum/6
4040  ELSE
4050  FOR I=9 TO 16
4060  IF (Ipos=0 AND I=10) OR (Ipos=1 AND I=9) THEN 4080
4070  Sum=Sum+T(I+Iadd)
4080  NEXT I
4090  Twmid=Sum/7
4100  END IF
4110  PRINT USING "12X,""Avg Local Heated Wall Temp Near Middle (Twmid) = "",3D.
DD,"" (C)""";Twmid
4120!
4130  !  CALCULATE AVERAGE LOCAL HEATED WALL TEMPERATURE AT OUTLET.
4140!
4150  Sum=0.
4160!
4170  !  CORRECTION FOR BROKEN T/C CHANNEL 26 CURVED HEATER ONLY.
4180!
```

```
4190  IF Itype=1 AND Ipos=0 THEN
4200  FOR I=23 TO 29
4210  IF I=26 THEN 4230
4220  Sum=Sum+T(I)
4230  NEXT I
4240  Twout=Sum/6
4250  ELSE
4260  FOR I=23 TO 29
4270  Sum=Sum+T(I+Iadd)
4280  NEXT I
4290  Twout=Sum/7
4300  END IF
4310  PRINT USING "12X,""Avg Local Heated Wall Temp at Outlet (Twout)   = "",3D.
DD,"" (C)""";Twout
4320  PRINT
4330  PRINT
4340!
4350  !  ENTER ORIFICE PRESSURE DATA.
4360!
4370  BEEP
4380  INPUT "ENTER PATM (inHg), DPM(inH20), P1M(inH20), RE1".Patm.Dpm.P1m.Re1
4390  PRINT USING "9X,""THE FOLLOWING ORIFICE DATA WERE ENTERED:"""
4400  PRINT
4410  PRINT USING "12X,""Patm(inHg)     DPM(inH20)     P1M(inH20)      RE1"""
4420  PRINT USING "14X,2(2D.DD,10X),(2D.DD,7X),5D.D";Patm,Dpm,P1m,Re1
4430  PRINT
4440!
4450  !  CONVERT PRESSURE READINGS TO SI UNITS AND P1M TO ABSOLUTE.
4460!
4470  Patm=Patm*3376.8
4480  Pdel=Dpm*248.84
4490  P1=Patm-(P1m*248.84)
4500  Torf=T(33)
4510!
4520  !  PHYSICAL PROPERTIES AND CONSTANTS.
4530!
4540  R=286.987 !FOR AIR.
4550  Rho=P1/(R*(Torf+273.15)) !DENSITY OF AIR AT ORIF PLATE.
4560  Gamma=1.40 !FOR AIR.
4570  Cp=1006 !Cp GOOD FOR Tblk BETWEEN 12 AND 33 (DEG C).
4580  Gc=1.0
4590  Sigma=5.669E-8
4600  Ecu=.12  !EMISSIVITY OF COPPER.
4610!
4620  !  DIMENSIONS OF CHANNEL.
4630!
4640  Dc=.006350
4650  Wid=.2540
4660  Ri=.297
4670  Pwet=2*(Dc+Wid)
4680  Ac=Dc*Wid
4690  Dhd=4*Ac/Pwet
4700  Apl=.0774192
4710!
4720  !  PROPERTIES OF INSULATION.
4730!
4740  Xins=.0127
4750  Kins=3.8E-2
4760!
4770  !  ENTER ORIFICE CONFIGURATION.
```

```
4780!
4790  BEEP
4800  INPUT "SELECT DIAMETER OF ORIFICE (0=.5334, 1=1.0755 (inches))",Size
4810  IF Size=0 THEN Dorf=.013548
4820  IF Size=1 THEN Dorf=.027318
4830!
4840  !  DIMENSIONS OF PIPE AND ORIFICE PLATE.
4850!
4860  A=(PI*Dorf^2)/4
4870  Dpipe=.051772
4880  Apipe=PI*Dpipe^2/4
4890  Beta=Dorf/Dpipe
4900  PRINT USING "12X,""Dorf(m)         A(m^2)          Beta"""
4910  PRINT USING "12X,(Z.6D,6X),(Z.3DE,6X),Z.4D";Dorf,A,Beta
4920  PRINT
4930  PRINT
4940!
4950  !  CORRELATION FOR EXPANSION FACTOR BASED ON 1D AND 1/2D TAPS.
4960!
4970  Y=1-(.41+.35*Beta^4)*(Pdel/(Gamma*P1))
4980!
4990  !  CALCULATION OF FLOW COEFFICIENT (K) IN SI UNITS.
5000!
5010  B=.0002+2.794E-5/Dpipe+(.0038+1.016E-5/Dpipe)*(Beta^2+(16.5+1.968504E+2*Dp
ipe)*Beta^16)
5020!
5030  !  K1 AND K2 ARE DUMMY VARIABLES TO CALCULATE Ko.
5040!
5050  K1=.6014-5.3974064E-3/Dpipe^.25
5060  K2=(.376+2.8971138E-2/Dpipe^.25)*(1.6129E-7/(Dpipe^2*Beta^2+6.35E-5*Dpipe)
+Beta^4+1.5*Beta^16)
5070  Ko=K1+K2
5080  K=Ko+1000*B/Re1^.5
5090!
5100  !  Mu CORRELATION GOOD FOR Torf BETWEEN 17 AND 41 DEGREES CELSIUS.
5110!
5120  Mu=4.6971429E-8*Torf+1.7194722E-5
5130!
5140  !  CALCULATE Mdot AND REpipe AND COMPARE TO PREDICTED RE1.
5150!
5160  Mdot=K*A*Y*(2*Gc*Rho*Pdel)^.5
5170  Repipe=(Mdot*Dpipe)/(Mu*Apipe)
5180  Diff=(ABS(Re1-Repipe)/Re1)*100
5190  Re1=Repipe
5200  IF Diff>.001 THEN 5080
5210  PRINT USING "9X,""THE FOLLOWING DATA WERE CALCULATED:"""
5220  PRINT
5230  PRINT USING "12X,""Orifice Expansion Factor (Y)     =  "",Z.4D,";Y
5240  PRINT USING "12X,""Orifice Flow Coefficient (K)     =  "",Z.4D,";K
5250  PRINT USING "12X,""Density Based on Torf (Rho)      =  "",Z.4D,""     (kg/m^
3)""";Rho
5260  PRINT USING "12X,""Viscosity Based on Torf (Mu)     = "".2Z.3DE,"" (kg/m.s)
""";Mu
5270!
5280  !  Mu CORRELATION GOOD FOR Tblk BETWEEN 17 AND 41 DEGREES CELSIUS.
5290!
5300  Mu=4.6971429E-8*Tblk+1.7194722E-5
5310  Red=(Mdot*Dc)/(Mu*Ac)
5320  Rehd=(Mdot*Dhd)/(Mu*Ac)
5330!
```

```
5340  !  CALCULATION OF POWER INTO HEATER PLATE.
5350!
5360  Iadd=0
5370  IF Ipos=1 THEN Iadd=39
5380  IF Ipos=0 THEN Rpr=2.01729
5390  IF Ipos=1 THEN Rpr=2.00839
5400  Qp=(Emf(38+Iadd)*Emf(39+Iadd))/Rpr
5410!
5420  !  CALCULATION OF HEAT INPUT TO AIR.
5430!
5440  Qair=Mdot*Cp*(Tout-Tin)
5450!
5460  !  CALCULATE LOCAL HEAT TRANSFER COEF. AND NUSSELT NUMBER.
5470!
5480  Kair=7.7257143E-5*Tcin+.024165836
5490  Hin=Qair/(Apl*(Twin-Tcin))
5500  Nuin=(Hin*Dhd)/Kair
5510  Kair=7.7257143E-5*Tcmid+.024165836
5520  Hmid=Qair/(Apl*(Twmid-Tcmid))
5530  Numid=(Hmid*Dhd)/Kair
5540  Kair=7.7257143E-5*Tcout+.024165836
5550  Hout=Qair/(Apl*(Twout-Tcout))
5560  Nuout=(Hout*Dhd)/Kair
5570!
5580  !  Kair CORRELATION GOOD FOR Tblk BETWEEN 17 AND 41 DEGREES CELSIUS.
5590!
5600  Kair=7.7257143E-5*Tblk+.024165836
5610!
5620  !  CALCULATE AVERAGE HEAT TRANSFER COEF. AND NUSSELT NUMBER.
5630!
5640  Havg=Qair/(Apl*Tdel)
5650  Nuavg=(Havg*Dhd)/Kair
5660!
5670  !  CALCULATE HEAT LOSSES.
5680!
5690  Qlo1=(Kins*Apl*(Tinso1-Tinso2))/Xins
5700  Qlo2=(Kins*Apl*(Tinso2-Tinso3))/Xins
5710  Qlo=(Qlo1+Qlo2)/2
5720  Qli1=(Kins*Apl*(Tinsi1-Tinsi2))/Xins
5730  Qli2=(Kins*Apl*(Tinsi2-Tinsi3))/Xins
5740  Qli=(Qli1+Qli2)/2
5750  Rr=2.0*((1-Ecu)/(Apl*Ecu))+(1.0/Apl)
5760  Qr=(Sigma*(ABS((Two+273.15)^4-(Twi+273.15)^4)))/Rr
5770  Qdel=Qp-Qair-Qlo1-Qr-Qli1
5780!
5790  !  CALCULATE DEAN NUMBER.
5800!
5810  De=.5*Red*((Dc/2)/Ri)^.5
5820  PRINT USING "12X,""Viscosity Based on Tblk (Mu)     = "",2Z.3DE,"" (kg/m.s)
""";Mu
5830  PRINT USING "12X,""Therm Cond Based on Tblk (Kair) =  "",Z.3DE,"" (W/m.K)"
"";Kair
5840  PRINT
5850  PRINT USING "12X,""Patm   = "",6D.DD,"" (N/m^2)""";Patm
5860  PRINT USING "12X,""Pdel   =    "",4D.DD,"" (N/m^2)""";Pdel
5870  PRINT USING "12X,""P1     = "",6D.DD,"" (N/m^2)""";P1
5880  PRINT USING "12X,""Mdot   =     "",Z.4D,"" (kg/s)""";Mdot
5890  PRINT USING "12X,""Repipe = "",6D.D";Repipe
5900  PRINT USING "12X,""Red    = "",6D.D";Red
5910  PRINT USING "12X,""Rehd   = "",6D.D";Rehd
```

```
5920!
5930  !  ONLY PRINT DEAN NUMBER WHEN HEATING CURVED SECTION.
5940!
5950  IF Itype=1 THEN PRINT USING "12X,""De     =    "",4D.D";De
5960  PRINT
5970  PRINT USING "12X,""Qp   = "",3D.3D,"" (Watts)"",7X,""Qair = "",3D.3D,"" (W
atts)""";Qp,Qair
5980  PRINT USING "12X,""Qlo1 =  "",2D.3D,"" (Watts)"",7X,""Qli1 =  "",2D.3D,""
(Watts)""";Qlo1,Qli1
5990  PRINT USING "12X,""Qlo2 =  "",2D.3D,"" (Watts)"",7X,""Qli2 =  "",2D.3D,""
(Watts)""";Qlo2,Qli2
6000  PRINT USING "12X,""Qlo  =  "",2D.3D,"" (Watts)"",7X,""Qli  =  "",2D.3D,""
(Watts)""";Qlo,Qli
6010  PRINT USING "12X,""Qr   =  "",2D.3D,"" (Watts)"",7X,""Qdel =  "",2D.3D,""
(Watts)""";Qr,Qdel
6020  PRINT
6030  PRINT USING "12X,""Hin  = "",3D.DD,"" (W/m^2C)"",7X,""Nuin  = "",3D.DD,";H
in,Nuin
6040  PRINT USING "12X,""Hmid = "",3D.DD,"" (W/m^2C)"",7X,""Numid = "",3D.DD,";H
mid,Numid
6050  PRINT USING "12X,""Hout = "",3D.DD,"" (W/m^2C)"",7X,""Nuout = "",3D.DD,";H
out,Nuout
6060  PRINT USING "12X,""Havg = "",3D.DD,"" (W/m^2C)"",7X,""Nuavg = "",3D.DD,";H
avg,Nuavg
6070  PRINT
6080  PRINT
6090  BEEP
6100  INPUT "WILL THERE BE ANOTHER RUN? (1=Y,0=N)",Go_on
6110  IF Go_on<>0 THEN
6120  PRINT USING "@,#"
6130  IF Im=0 THEN WAIT 600
6140  GOTO 1700
6150  END IF
6160  PRINT USING "8X,""END OF RUN"""
6170  PRINT USING "@,#"
6180  PRINTER IS 1
6190  ASSIGN @File TO *
6200  END
6210!
6220  !  CONVERTS EMF TO DEGREES CELSIUS.
6230!
6240  SUB Tvsv(V,T)
6250  COM /Co/ D(7),Aa(76,2)
6260  Sum=0
6270  FOR I=0 TO 7
6280  Sum=Sum+D(I)*V^I
6290  NEXT I
6300  T=Sum
6310  SUBEND
6320!
6330  !  CALIBRATES T/C READINGS.
6340!
6350  DEF FNTcorr(T,I)
6360  COM /Co/ D(7),Aa(76,2)
6370  Tc=Aa(I,0)
6380  FOR J=1 TO 2
6390  Tc=Tc+Aa(I,J)*T^J
6400  NEXT J
6410  RETURN Tc
6420  FNEND
```

APPENDIX B: SAMPLE CALCULATIONS

Figure 36 below, shows the major heat transfer components for each of the test sections. The sample calculations that follow, demonstrate the methods used by the computer to calculate these components as well as the Reynolds number, average heat transfer coefficient, and average Nusselt number for each set of data. Part A of Appendix B contains a sample printout of a data run, followed by a summation of the data. The sample calculations are for the concave curved section, but those for the straight section are similar.

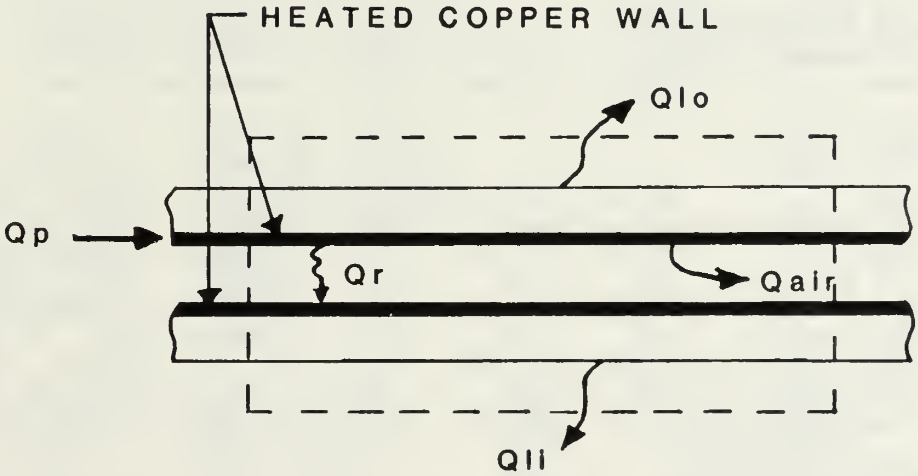

Figure 36. Energy Balance in Test Section.

1. SAMPLE CALCULATION DATA

```
THE FOLLOWING CHANNEL CONFIGURATION WAS SELECTED:

   Heating CURVED Test Section.
   Heating OUTER Plate.

           Month, Day, and Time: 10:17:13:47:11

THE FOLLOWING DATA WERE RECORDED:

   Heater Voltage (Vh)       = 61.337 (V)
   Resistor Voltage (Vr)     =  5.195 (V)
   Precision Resistor (Rpr)  =  2.01729 (Ohms)

   OUTER PLATE:
     T/C Number:      1       2       3       4       5       6
     Temp (C):      42.75   41.57   44.39   41.23   44.55   40.59
     T/C Number:      7       8       9      10      11      12
     Temp (C):      46.54   42.61   43.51   43.47   44.77   43.86
     T/C Number:     13      14      15      16      17      18
     Temp (C):      43.40   44.18   44.10   41.97   38.06   45.73
     T/C Number:     19      20      21      22      23      24
     Temp (C):      45.79   48.45   49.18   33.83   45.32   45.51
     T/C Number:     25      26      27      28      29      30
     Temp (C):      45.30   46.47   30.31   45.80   45.98   47.28

   OUTER INSULATION:
     T/C Number:     31 (Tinso1)   32 (Tinso2)   33 (Tinso3)
     Temp (C):          49.58         37.29         29.36

   ORIFICE TEMP (Torf) =  24.16 (C)

   INLET TEMPERATURE:
     T/C Number:     35      36      37      38
     Temp (C):      20.55   20.48   20.47   20.43

   INNER PLATE:
     T/C Number:     41      42      43      44      45      46
     Temp (C):      21.43   21.31   21.16   21.14   21.05   21.92
     T/C Number:     47      48      49      50      51      52
     Temp (C):      21.03   22.39   21.10   21.05   21.38   21.46
     T/C Number:     53      54      55      56      57      58
     Temp (C):      21.23   21.27   21.17   21.19   21.15   21.35
     T/C Number:     59      60      61      62      63      64
     Temp (C):      21.25   21.56   21.47   21.74   21.66   22.18
     T/C Number:     65      66      67      68      69      70
     Temp (C):      22.05   21.91   21.85   21.78   21.74   21.73

   INNER INSULATION:
     T/C Number:     71 (Tinsi1)   72 (Tinsi2)   73 (Tinsi3)
     Temp (C):          21.53         21.49         21.32

   OUTLET TEMPERATURE:
     T/C Number:     74      75      76      77
     Temp (C):      24.29   24.38   24.38   24.25
```

```
THE FOLLOWING TEMPERATURES WERE CALCULATED:

   Average Outer Wall Temperature (Two)                 =  44.76 (C)
   Average Inner Wall Temperature (Twi)                 =  21.46 (C)
   Average Outlet Temperature (Tout)                    =  24.32 (C)
   Average Inlet Temperature (Tin)                      =  20.48 (C)
   Channel Inlet and Outlet Temp Diff (Tdiff)           =   3.84 (C)
   Average Bulk Temperature (Tblk)                      =  22.40 (C)
   Mean Temperature Difference (Tdel)                   =  22.36 (C)
   Outer and Inner Wall Temp Difference (Twdiff)        =  23.30 (C)
   Average Local Channel Temp at Inlet (Tcin)           =  20.64 (C)
   Average Local Channel Temp at Middle (Tcmid)         =  21.92 (C)
   Average Local Channel Temp at Outlet (Tcout)         =  24.16 (C)
   Avg Local Heated Wall Temp at Inlet (Twin)           =  43.51 (C)
   Avg Local Heated Wall Temp Near Middle (Twmid)       =  43.50 (C)
   Avg Local Heated Wall Temp at Outlet (Twout)         =  46.06 (C)

THE FOLLOWING ORIFICE DATA WERE ENTERED:

   Patm(inHg)      DPM(inH2O)      P1M(inH2O)       RE1
     29.79           18.58           12.55        15500.0

   Dorf(m)          A(m^2)          Beta
   0.027318       5.861E-04       0.5277

THE FOLLOWING DATA WERE CALCULATED:

   Orifice Expansion Factor (Y)     =  0.9852
   Orifice Flow Coefficient (K)     =  0.6323
   Density Based on Torf (Rho)      =  1.1424     (kg/m^3)
   Viscosity Based on Torf (Mu)     = 18.330E-06 (kg/m.s)
   Viscosity Based on Tblk (Mu)     = 18.247E-06 (kg/m.s)
   Therm Cond Based on Tblk (Kair)  =  2.590E-02 (W/m.K)

   Patm    = 100594.87 (N/m^2)
   Pdel    =   4623.45 (N/m^2)
   P1      =  97471.93 (N/m^2)
   Mdot    =     0.0375 (kg/s)
   Repipe  =  50352.2
   Red     =   8097.1
   Rehd    =  15799.1
   De      =    418.6

   Qp    = 157.971 (Watts)        Qair = 144.950 (Watts)
   Qlo1  =   2.847 (Watts)        Qli1 =     .009 (Watts)
   Qlo2  =   1.838 (Watts)        Qli2 =     .038 (Watts)
   Qlo   =   2.342 (Watts)        Qli  =     .023 (Watts)
   Qr    =    .751 (Watts)        Qdel =   9.415 (Watts)

   Hin  =  81.90 (W/m^2C)         Nuin   =  39.39
   Hmid =  86.78 (W/m^2C)         Numid  =  41.58
   Hout =  85.51 (W/m^2C)         Nuout  =  40.70
   Havg =  83.75 (W/m^2C)         Nuavg  =  40.07
```

V_H = 61.337 V

V_{PR} = 5.195 V

R_{PR} = 2.0173 Ω

P_{atm} = 29.79 in. Hg

ΔP = 18.58 in. H_2O

P_1 = 12.55 in. H_2O

T_{in} = 20.48 C

T_{out} = 24.32 C

T_{wo} = 44.76 C

T_{wi} = 21.49 C

$T_{ins,i1}$ = 21.53 C

$T_{ins,i2}$ = 21.49 C

$T_{ins,01}$ = 49.58 C

$T_{ins,02}$ = 37.29 C

T_{orf} = 24.16

K_{air} = 25.90×10^{-3} W/mC

C_{pair} = 1006 J/Kg K

μ_{air} = $4.6971 \times 10^{-8} \times T_{air} + 1.71947 \times 10^{-5}$

K_{ins} 3.80×10^{-2} W/mC

ΔX_{ins} = 0.0127 m

ε_{cu} = 0.12

σ = 5.669×10^{-8} W/m^2K^4

β = .5277

γ = 1.40

g_c = 1 Kg m/Ns^2

R = 286.98 Nm/Kg K

F_{wo-wi} = 1.0

A_{PL} = .07742 m^2

A_c = .0016 m^2

A_{pipe} = .00211 m^2

D_c = .00635 m

D_{pipe} = .0518 m

D_{orf} = .027318 m

P_{wet} = .5207 m

Ri = .297 m

2. TEMPERATURE CALCULATIONS

a. Bulk Temperature (T_{blk})

$$T_{blk} = \frac{T_{in} + T_{out}}{2} = \frac{20.48 + 24.32}{2} = 22.40 \text{ C}$$

b. Mean Temperature Difference (ΔT)

$$\Delta T = T_{wo} - T_{blk} = 44.76 - 22.40 = 22.36$$

c. Temperature Difference Between Outer and Inner Wall (T_{wdiff})

$$T_{wdiff} = T_{wo} - T_{wi} = 44.76 - 21.49 = 23.27 \text{ C}$$

3. POWER CALCULATIONS

a. Power Supplied (Q_p)

$$Q_p = \frac{V_H \; V_{PR}}{R_{PR}} = \frac{(61.337)(5.195)}{(2.0173)} = 157.97 \text{ W}$$

b. Heat Lost Through the Back of the Outer Plate (Q_{lo})

$$Q_{lo} = \frac{T_{ins,o1} - T_{ins,o2}}{(\Delta X_{ins})/(K_{ins})(A_{PL})} = \frac{(49.58 - 37.29)}{(0.0127)/(3.80\text{x}10^{-2})(.07742)}$$

$$= 2.85 \text{ W}$$

c. Heat Lost Through the Back of the Inner Plate (Q_i)

$$Q_{li} = \frac{T_{ins,i1} - T_{ins,i2}}{(\Delta X_{ins})/(K_{ins})(A_{PL})} = \frac{(21.53 - 21.49)}{(0.0127)/(3.80\text{x}10^{-2})(.07742)}$$

$$= .01 \text{ W}$$

d. Heat Radiated (Q_r)

(1) Radiation Resistance (R_R)

$$R_R = 2 \text{ x } \left(\frac{1 - \varepsilon_{cu}}{A_{PL} \; \varepsilon_{cu}}\right) + \frac{1}{A_{PL} \; F_{wo-wi}}$$

$$= \frac{1}{A_{PL}} \left[\frac{2}{\varepsilon_{cu}} - 1\right] = \frac{1}{0.07742} \left[\frac{2}{.12} - 1\right] = 202.36 \text{ m}^{-2}$$

(2) Heat Radiated (Q_r)

$$Q_r = \frac{\sigma(T_{wo}^4 - T_{wi}^4)}{R_R} \qquad T\ [=]\ K$$

$$= \frac{(5.669\times10^{-8})[(44.76+273)^4 - (21.49+273)^4]}{202.36}$$

$$= 0.75\ W$$

4. MASS FLOW RATE CALCULATIONS

a. Pressure Conversions

(1) $P_{atm} = 29.79$ in Hg x 3376.8 = 100594.87 N/m^2

(2) ΔP = 18.58 in H_2O x 248.84 = 4623.5 N/m^2

(3) P_1 = (12.55 in H_2O x 248.84) - 100594.87

= 97471.93 N/m^2

b. Density of Air (ρ_{air})

$$\rho_{air} = \frac{P_1}{R\ T_{orf}} = \frac{(97471.93)}{(286.98)(24.16 + 273)} = 1.1424\ Kg/m^3$$

c. Expansion Factor (Y)

$$Y = 1 - [.41 + .35\beta^4]\ \frac{\Delta P}{\gamma P_1}$$

$$= 1 - [.41 + .35(.5277)^4]\ \frac{4623.5}{(1.40)(97471.93)}$$

$$= .9852$$

d. Area of Orifice (A)

$$A = \frac{\pi (D_{orf})^2}{4} = \frac{\pi(.027318)^2}{4} = .005861 \text{ m}^2$$

e. Mass Flow Rate ($\dot{m}$)

$$\dot{m} = YKA \quad 2g_c \, \rho_{air} \, \Delta P = (.9852)K(.0005861)$$

$$\times \quad 2(1)(1.1424)(4623.5)$$

$$\dot{m} = .05935 \text{ K}$$

Iterating:

Assume a Pipe Reynolds number = 50000

Obtain a value for K, the flow coefficient, from reference 30. K = .6325

Solve for $\dot{m}$. $\dot{m}$ = .0375 Kg/s

Solve for new $Re_{pipe} = \dfrac{\dot{m} \, D_{pipe}}{A_{pipe}\mu_{air}} = \dfrac{(.0375)(.0518)}{(.00211)(18.33 \times 10^{-6})}$

Re_{pipe} = 550225

Check convergence and repeat process if necessary.

(Convergence if difference less than .001)

$\dot{m}$ = .0375 Kg/s

5. REYNOLDS NUMBER CALCULATIONS

a. $$Re_{pipe} = \frac{\dot{m}\ D_{pipe}}{A_{pipe}\mu_{air}} = \frac{(.0375)(.0518)}{(.00211)(18.33\text{x}10^{-6})} = 50225$$

b. $$Re_d = \frac{\dot{m}\ D_c}{A_c\ \mu_{air}} = \frac{(.0375)(.00635)}{(.0016)(18.25\text{x}10^{-6})} = 8097.1$$

c. $$Re_{hd} = \frac{\dot{m}\ D_{hd}}{A_c\ \mu_{air}}$$

(1) $$D_{hd} = \frac{4\ \text{x}\ A_c}{P_{wet}} = \frac{(4)(.0016)}{.5207} = .01229\ \text{m}$$

$$Re_{hd} = \frac{\dot{m}\ D_{hd}}{A_c\mu_{air}} = \frac{(.0375)(.01229)}{(.0016)(18.25\text{x}10^{-6})} = 15799.1$$

6. HEAT CONVECTED TO AIR CALCULATION

a. $$Q_{air} = \dot{m}C_p(T_{out}-T_{in}) = (.0375)(1006)(24.32-20.48) = 144.95\ \text{W}$$

7. AVERAGE HEAT TRANSFER COEFFICIENT CALCULATION

$$\bar{h} = \frac{Q_{air}}{A_{PL}\ \Delta T} = \frac{144.95}{(.07742)(22.36)} = 83.72\ \text{W/m}^2\text{C}$$

8. AVERAGE NUSSELT NUMBER CALCULATION

$$\overline{Nu}_{hd} = \frac{\bar{h}\ D_{hd}}{K_{air}} = \frac{(83.73)(.01229)}{25.90\ \text{x}\ 10^{-3}} = 39.73$$

9. DEAN NUMBER CALCULATION

$$De = \frac{Re_d}{2}\sqrt{\frac{Dc/2}{Ri}} = \frac{8097.1}{2}\sqrt{\frac{.00635/2}{.297}} = 418.6$$

APPENDIX C: EXPERIMENTAL UNCERTAINTY

The uncertainties for the major variable in the experiments, were calculated in accordance with the method described by S. Kline and F. McClintoch [Ref. 33]. The estimates of the uncertainty in the measured quantities were made conservatively. As a result, there is considerable confidence in the uncertainties as calculated.

The following equations were used to calculate the uncertainties:

$$(1) \quad \frac{d\rho}{\rho} = \left(\left(\frac{dR}{R}\right)^2 + \left(\frac{dP_1}{P_1}\right)^2 + \left(\frac{dT_{orf}}{T_{orf}}\right)^2 \right)^{1/2}$$

$$(2) \quad \frac{d\dot{m}}{\dot{m}} = \left[\left(\left(\frac{dY}{Y}\right)^2 + \left(\frac{dK}{K}\right)^2 + \left(\frac{dA}{A}\right)^2 \right) + \left(1/4 \left(\left(\frac{d\rho_{air}}{\rho_{air}}\right)^2 + \left(\frac{d\Delta P}{\Delta P}\right)^2 \right)\right) \right]^{1/2}$$

$$(3) \quad \frac{dQ_{air}}{Q_{air}} = \left(\left(\frac{d\dot{m}}{\dot{m}}\right)^2 + \left(\frac{d\,C_{pair}}{C_{pair}}\right)^2 + \left(\frac{d(T_{out}-T_{in})}{T_{out}-T_{in}}\right)^2 \right)^{1/2}$$

$$(4) \quad \frac{d\bar{h}}{\bar{h}} = \left(\left(\frac{dQ_{air}}{Q_{air}}\right)^2 + \left(\frac{dA_{PL}}{A_{PL}}\right)^2 + \left(\frac{d\Delta T}{\Delta T}\right)^2 \right)^{1/2}$$

$$(5) \quad \frac{d\overline{Nu}_{hd}}{\overline{Nu}_{hd}} = \left(\left(\frac{d\bar{h}}{\bar{h}}\right)^2 + \left(\frac{dD_{hd}}{D_{hd}}\right)^2 + \left(\frac{dK_{air}}{K_{air}}\right)^2 \right)^{1/2}$$

$$(6) \quad \frac{dRe_{hd}}{Re_{hd}} = \left(\left(\frac{d\dot{m}}{\dot{m}}\right)^2 + \left(\frac{dD_{hd}}{D_{hd}}\right)^2 + \left(\frac{d\mu_{air}}{\mu_{air}}\right)^2 + \left(\frac{dA_c}{A_c}\right)^2 \right)^{1/2}$$

The following quantities had their uncertainty calculated by dividing the estimated error in the quantity by the value of the quantity, and these uncertainties are considered constant for the range of values in this experiment:

Quantity	Uncertainty
A	.0093
A_c	.0408
A_{PL}	.0080
C_{pair}	.0020
Dc	.0400
D_{hd}	.0396
K	.0030
K_{air}	.0038
P_{atm}	.0010
R	.0003
W_{id}	.0080
Y	.0020
μ_{air}	.0054

The following quantities had the worst case error for hydraulic Reynolds numbers below 17000:

Quantity	Error
T_{blk}	$\pm .1^\circ C$
T_{in}	$\pm .1^\circ C$
T_{orf}	$\pm .1^\circ C$
T_{out}	$\pm .1^\circ C$
T_{wo}	$\pm .1^\circ C$
$T_{out}-T_{in}$	$\pm .2^\circ C$
ΔT	$\pm .2^\circ C$

For hydraulic Reynolds numbers greater than 17000 the error in the outlet temperature was much higher, as mentioned previously, and the following errors apply:

Quantity	Error
T_{blk}	$\pm .2^\circ C$
T_{in}	$\pm .1^\circ C$
T_{orf}	$\pm .1^\circ C$
T_{out}	$\pm .3^\circ C$
T_{wo}	$\pm .1^\circ C$
$T_{out}-T_{in}$	$\pm .4^\circ C$
ΔT	$\pm .3^\circ C$

The uncertainties for the following quantities were calculated using the sample data for the outer curved test section at a hydraulic Reynolds number of 15800:

Quantity	Uncertainty
P_1	.0159
ΔP	.0108
T_{orf}	.0003
$T_{out}-T_{in}$	.0521
ΔT	.0089
ρ_{air}	.0159
$\dot{m}$	.0139
Q_{air}	.0540
h	.0553
Nu_{hd}	.0681
Re_{hd}	.0588

The uncertainty for the following quantities were calculated for the outer curved test section at a hydraulic Reynolds number of 21200:

Quantity	Uncertainty
P_1	.0043
ΔP	.0053
T_{orf}	.0003
$T_{out}-T_{in}$	.1039
ΔT	.0111
ρ_{air}	.0043
$\dot{m}$	.0105
Q_{air}	.1044

$\overline{h}$	.1053
$\overline{Nu}_{hd}$	.1126
Re_{hd}	.0581

By multiplying the quantity by its uncertainty the possible error can be calculated. The previous uncertainty calculations for a hydraulic Reynolds number of 15800 yielded $\overline{Nu}_{hd} = 40.07 \pm 2.73$ and a $Re_{hd} = 15800 \pm 928$. For the run at a hydraulic Reynolds number of 21200 the $\overline{Nu}_{hd} = 44.71 + 5.03$ and a $Re_{hd} = 21200 \pm 1232$.

The major source of uncertainty in the average Nusselt number is the uncertainty in the difference between the outlet and inlet air temperature. If this uncertainty can be brought below four percent, then the uncertainty of the average Nusselt number will be dictated by the uncertainty of the measured dimensions of the channel. In particular, the channel height (D_c) which has an uncertainty $dD_c/D_c = .0400$. The uncertainty of the channel height can only be reduced by increasing the channel height, and/or using materials with better tolerances.

LIST OF REFERENCES

1. Taylor, G. I., "Stability of a Viscous Liquid Contained Between Two Rotating Cylinders," Philosophical Transactions of the Royal Society of London, series A, V. 233, pp. 289-343, 1923.

2. National Advisory Committee for Aeronautics, Technical Memorandum 1375, On the Three Dimensional Instability of Laminar Boundary Layers on Concave Walls, by H. Gortler, 1942.

3. Smith, A. M. O., "On the Growth of Taylor-Gortler Vortices Along Highly Concave Walls," Quarterly of Applied Mathematics, V. 8, pp. 233-263, November 1955.

4. Dement'eva, K. V. and Aronov, I. Z., "Hydrodynamics and Heat Transfer in Curvelinear Channels of Rectangular Cross Section," Journal of Engineering Physics, V. 34, No. 6, pp. 666-671, 1978.

5. Mayle, R. E., Kopper, F. C., Blair, M. F., and Bailey, D. A., "Effect of Streamline Curvature on Film Cooling," Journal of Engineering for Power, Trans. ASME, V. 99, Series A, No. 1, pp. 77-82, January 1977.

6. Nicolas, J. and LeMeur, A., "Curvature Effects on a Turbine Blade Cooling Film," ASME Paper No. 74-GT-156, 1974.

7. Folayan, C. O. and Whitelaw, J. H., "The Effectiveness of Two-Dimensional Film-Cooling Over Curved Surfaces," ASME Paper No. 76-HT-31, 1976.

8. Lord Rayleigh, "On the Dynamics of Revolving Fluids," Proceedings of The Royal Society of London, Series A, V. 93, pp. 148-154, 1916. Reprints in Scientific Papers, V. 6, pp. 447-453.

9. Taylor, G. I., "Distribution of Velocity and Temperature Between Concentric Rotating Cylinders," Proceedings of the Royal Society of London, Series A, V. 151, pp. 494-512, 1935.

10. Dean, W. R., "Fluid Motion in a Curved Channel," Proceedings of the Royal Society of London, Series A, V. 121, pp. 402-420, 1928.

11. Reid, W. H., "On the Stability of Viscous Flow in a Curved Channel," Proceedings of the Royal Society of London, Series A, V. 244, pp. 186-198, 1958.

12. Schlichting, H., Boundary Layer Theory, 7th Ed., pp. 529-536, McGraw-Hill, 1979.

13. Kelleher, M. D., Flentie, D. L., and McKee, R. J., "An Experimental Study of the Secondary Flow in a Curved Rectangular Channel," Journal of Fluids Engineering, V. 102, pp. 92-96, March 1980.

14. Winoto, S. H., Durao, D. F. G., and Crane, R. I., "Measurement within Gortler Vortices," Journal of Fluids Engineering, V. 101, pp. 517-520, December 1979.

15. Aihara, Y., "Nonlinear Analysis of Gortler Vortices," The Physics of Fluids, V. 19, pp. 1655-1660, November 1976.

16. Kreith, F., "The Influence of Curvature on Heat Transfer to Incompressible Fluids," Trans. ASME, V. 77, pp. 1247-1256, 1955.

17. Aerospace Research Laboratories Reprt ARL 65-68, A Simplified Approach to the Influence of Gortler-Type Vortices on the Heat-Transfer from a Wall, by Leif N. Persen, May 1965.

18. Cheng, K. C., and Akiyama, M., "Laminar Forced Convection Heat Transfer in Curved Rectangular Channels," International Journal of Heat and Mass Transfer, V. 13, pp. 471-490, 1970.

19. Shibani, A. A., and Ozisik, M. N., "A Solution to Heat Transfer in Turbulent Flow Between Parallel Plates," International Journal of Heat and Mass Transfer, V. 20, pp. 65-573, 1977.

20. Mori, Y., Uchida, Y., and Ukon, T., "Forced Convective Heat Transfer in a Curved Channel with a Square Cross Section," International Journal of Heat and Mass Transfer, V. 14, pp. 1787-1805, 1971.

21. Kays, W. M. and Leung, E. Y., "Heat Transfer in Annular Passages - Hydrodynamically Developed Turbulent Flow with Arbitrarily Prescribed Heat Flux," International Journal of Heat and Mass Transfer, V. 6, pp. 507-557, 1963.

22. Brinich, P. F. and Graham, R. W., "Flow and Heat Transfer in a Curved Channel," NASA Technical Note No. TN-D-8464, 1977.

23. McKee, R. J., An Experimental Study of Taylor-Gortler Vortices in a Rectangular Channel, Eng. Thesis, Naval Postgraduate School, Monterey, California, 1973.

24. Durao, M. do Carmo, Investigation of Heat Transfer in Straight and Curved Rectangular Ducts Using Liquid Crystal Thermography, Eng. Thesis, Naval Postgraduate School, Monterey, California, 1977.

25. Ballard, J. C. III, Investigation of Heat Transfer in Straight and Curved Rectangular Ducts, Master's Thesis, Naval Postgraduate School, Monterey, California, 1980.

26. Holihan, R. G., Jr., Investigation of Heat Transfer in Straight and Curved Rectangular Ducts for Laminar and Transition Flows, Master's Thesis, Naval Postgraduate School, Monterey, California, 1981.

27. Daughety, S. F., Experimental Investigation of Turbulent Heat Transfer in Straight and Curved Rectangular Ducts, Master's Thesis, Naval Postgraduate School, Monterey, California, 1983.

28. Wilson, J. L., Experimental Investigation of Turbulent Heat Transfer in Straight and Curved Rectanglar Ducts, Master's Thesis, Naval Postgraduate School, Monterey, California, 1984.

29. Gebhart, B., Heat Transfer, 2nd Edition, p. 260, McGraw-Hill, New York, 1971.

30. The American Society of Mechanical Engineers, Supplement to ASME Power Test Codes, Chapter 4, Flow Measurement, p. 25, 1959.

31. Benedict, R. P., Fundamentals of Temperature, Pressure, and Flow Measurements, 2nd Edition, pp. 443-447, John Wiley and Sons, 1969.

32. Shah, R. K. and London, A. L., Laminar Flow Forced Convection in Ducts, Supplement 1, pp. 305-312, Academic Press, 1978.

33. Kline, S. J., and McClintock, F. A., "Describing Uncertainties in Single-Sample Experiments," Mechanical Engineering, V. 75, pp. 3-8, January 1953.

INITIAL DISTRIBUTION LIST

		No. Copies
1.	Defense Technical Information Center Cameron Station Alexandria, Virginia 22304-6145	2
2.	Library, Code 0142 Naval Postgraduate School Monterey, California 93943-5100	2
3.	Department Chairman, Code 69 Department of Mechanical Engineering Naval Postgraduate School Monterey, California 93943-5100	1
4.	Professor M. D. Kelleher, Code 69Kk Department of Mechanical Engineering Naval Postgraduate School Monterey, California 93943-5100	3
5.	Lieutenant George G. Galyo 724 Charette Road Philadelphia, Pennsylvania 19115	2

062-1917

216453

Thesis
G1422 Galyo
c.1 Experimental investigation of turbulent heat transfer in straight and curved rectangular ducts.

216453

Thesis
G1422 Galyo
c.1 Experimental investigation of turbulent heat transfer in straight and curved rectangular ducts.

thesG1422
Experimental investigation of turbulent
3 2768 000 65141 8
DUDLEY KNOX LIBRARY